The Catalytic Role of Iron Species in the Chlorination of Cassiterite.

A thesis submitted for the Degree of

Doctor of Philosophy

of the

University of London

by

Rodney Graham Lythe.

Department of Mining and Mineral Technology,
Royal School of Mines,
Imperial College of Science and Technology,
University of London.

February, 1969.

1. Abstract.

Various samples of synthetic and natural cassiterite have been reacted in H_2/HCl and CO/HCl mixtures in the range 500 - 700°C; the reactions occurring have been studied using a variety of techniques. Cassiterite undergoes two reactions in each of these mixtures, one to produce $SnCl_2$ and the other to produce $SnCl_4$. Grains of natural cassiterite reacted preferentially in those regions containing iron-bearing inclusions. Addition of 4.39% Fe_2O_3 to synthetic cassiterite caused increases in the rate of reaction in H_2/HCl of approximately 100% at 600°C; the presence of Fe_2O_3 also catalysed the reaction of synthetic cassiterite in CO/HCl mixtures. The presence of Nb_2O_5 and WO_3, two common impurities, retarded the reaction in H_2/HCl. The presence of Fe_2O_3 represses the reaction to produce $SnCl_4$ by relieving the high energy sites at which this reaction occurs. Catalysis of the reactions, which produce $SnCl_2$, occurs via chemisorption of the reductant on iron metal produced by reduction of Fe_2O_3.

Acknowledgements.

This work was carried out in the Department of Mining and Mineral Technology at the Imperial College of Science and Technology under the general direction of Professor M.G. Fleming, whom the author wishes to thank for the provision of research facilities. Thanks are also due to Imperial Chemical Industries Ltd. for financial support provided during the period of this research work.

The author is much indebted to his supervisor, Doctor A.P. Prosser, for his continued interest, advice and guidance. The help of Drs. E.A.D. White, T.I. Barry and J. Gavrilovič, by their performance of the crystal growth experiments, e.s.r. study and electron microprobe analysis respectively, is gratefully acknowledged.

Thanks are also extended to the technical staff of the Mineral Technology Department for the maintenance of the research facilities and for assistance with the photography.

The author also wishes to acknowledge the help of the typist, Mrs. O. Hodgins, and of Mr. R. Puddy in the presentation of diagrams.

Contents. Page

2. Introduction

2.1. Occurrence of tin.

The principal mineral of tin is the dioxide · cassiterite, and it is found in many localities throughout the world. Cassiterite occurs as veins in hard rock, primary cassiterite, and in alluvial deposits where particles of the mineral have been liberated from the rock matrix by weathering. The percentage tin contents of these two types of ore bodies are approximately 2 and 0.1 respectively.

2.2. Classical methods of treatment of alluvial and lode deposits.

In alluvial deposits the cassiterite occurs as discrete particles of up to 3 cm diameter and no grinding process is required to liberate it from the other, valueless minerals (gangue). The high specific gravity of cassiterite (6.95) as compared to the gangue (2.7) is used to separate the cassiterite from the other minerals in machines that have been developed over many centuries. The high grade tin concentrate so produced contains 80-90% SnO_2; the chief impurities are the oxides of Si, Fe, Nb, Ta, Ti, W and Mn while spectrographic analysis has shown that traces of Ge, Sc, Zr, Ga, Be, Hf, In and V also occur[1]. This material is subjected to carbothermic reduction to produce metallic tin. The crude tin is further refined by partial melting, poling or by blowing air through the melt.

Cassiterite occurring in vein deposits is still firmly embedded in a rock matrix from which it is released by the expensive processes of crushing and grinding or comminution. Comminution of the ore results in heavy losses of tin in the separation stages owing to the formation of particles too small to be amenable to existing gravity separation techniques. In Bolivia, for instance, only 50% of the total tin content is recovered[2]. The tailings from such a process usually contain more tin than most commercially viable alluvial deposits; it is the particle size of the cassiterite which determines the success of the process. The concentrate resulting from this treatment is treated in the same way as that obtained from an alluvial deposit.

2.3. Chemical methods of treatment of cassiterite.

The failure of current physical processes to separate fine-grain cassiterite from relatively rich vein deposits, of which there are an appreciable number[3], has led to the consideration of chemical methods of treatment for low-grade tin concentrates (i.e. less than 50% Sn). These methods may have one of two purposes, either to increase the SnO_2 content of the material for eventual smelting or to bypass the smelter and form metallic tin by some other means.

Selective leaching of the SnO_2 using some aqueous reagent has been considered a possibility but is not viable commercially owing to the very slow rate of dissolution of

the cassiterite. Owing to the refractory nature of the mineral it is necessary to use a higher temperature than that possible with aqueous systems and various processes requiring heat treatment are described in the following paragraphs.

The reaction of SnO_2 with elemental sulphur or locally occurring pyrite both with and without addition of carbon has been investigated by numerous research workers[2,4-7]. Although high yields of SnS were obtained, the severalfold excess of sulphur and the high temperatures (up to 1300°C), required rendered the process uneconomic.

Studies have also been made by Decroly et al[8,9] on the possibility of volatilising SnO from low-grade tin concentrates by autoreduction under vacuum at 1150°C. The process, however, is too slow, requiring residence times of more than three hours, even in the presence of metallic iron as reductant.

A number of procedures involving the conversion of cassiterite to tin chlorides have been proposed and investigated; they have certain advantages over the previously mentioned treatments in that the reaction is fast below 1000°C, the reagents may be selective and also that the resultant chlorides may be easily converted into SnO_2 by hydrolysis or directly to metal by electrolysis. These processes are discussed in more detail in section 2.5.

2.4. Chloride metallurgy in current processes.

Treatment of mineral ores by chlorination is a well-established unit process of extractive metallurgy. In the following consideration of some of these processes certain general aspects are apparent which are also pertinent to any chemical treatment of cassiterite involving the production of tin chlorides. Most of the metals realised by chlorination procedures are present as multiple oxides (e.g. W from $CaWO_4$ and Nb and Ta from $(Fe, Mn)((Nb,Ta)O_3)_2$) which are not amenable to processing by conventional hydrometallurgical or smelting techniques. Their increasing usage and rarity provides economic justification for this comparatively expensive treatment. The basic requirements are first, a high degree of selectivity, preferably in the formation of the chloride but possibly in the volatility or solubility of two or more chlorides formed by the reaction. The second requirement is a method of converting the chloride into a useful form of the metal.

The best known process of this type is the Kroll process for the production of Ti and Zr from rutile and zirconia respectively. The metal oxide is briquetted with carbon and reacted with chlorine at red heat to produce the volatile tetrachloride which may then be fractionally distilled to free it from impurities such as ferric chloride. The tetrachloride is reduced to metal with molten magnesium or sodium at approximately 800°C in an argon atmosphere. The metal may

be freed from magnesium and mcgnesium chloride by volatilisation of these impurities at 1000°C.

Ferrovanadium, which is produced by smelting, is used as the source material in the commercial production of vanadium metal by a modification of the above process. In this case the alloy is chlorinated to VCl_4 and subsequently reduced to metal by molten magnesium.

Niobium and tantalum occur as mixed pentoxides, these are reacted with chlorine to produce the volatile pentachlorides, which are subjected to reduction by hydrogen at 500 - 550°C; at this temperature only the $NbCl_5$ is converted to solid, non-volatile $NbCl_3$, leaving $TaCl_5$ in the vapour phase. Niobium metal is produced by further reduction.

Another treatment which is being developed for commercial use is the TORCO process for the segregation of metallic copper from refractory copper ores.[10,11] In this case the finely ground ore (less than 5% Cu present as mixed oxide/sulphide) is mixed with 1 - 1.5% carbon and 0.3 - 1% sodium chloride and heated to 700 - 800°C. It is believed that HCl, formed from hydrous silicates in the ore and the sodium chloride, reacts with the copper minerals to form cuprous chloride vapour; the latter is reduced by hydrogen at the surface of the carbon particles regenerating HCl. Metallic copper, in the form of larger grains than the original minerals, is the end product.

Many chemically feasible chlorination processes for the production of the chlorides of Ta, Cu, Pb, Ag, Mn, Mo, W, Th, Ge and Si,[12-21] have been investigated by various workers but none, so far, has been developed to a commercial scale of operation.

The principal disadvantages of chlorination are the chemical engineering difficulties of dealing with highly corrosive reagents at elevated temperatures and the problems involved in the recovery of volatile chlorides. The higher chlorides are susceptible to hydrolysis and difficult to collect in a condenser. Also, where fluidised beds have been tested, abrasion by the hard mineral particles is a serious problem. The chlorination of cassiterite, as a viable commercial process, would also be subject to these difficulties and in addition, where a low-grade concentrate is used, the large amount of heat required would present a further economic problem.

2.5. Chloride metallurgy of tin.

Tin forms two chlorides, $SnCl_4$ and $SnCl_2$, either of which may be prepared using a variety of chlorinating agents; $SnCl_2$ is formed only when a reductant is present. Table 1 shows the standard free energy change on converting one mole of SnO_2 to $SnCl_4$ using a number of common metallic chlorides, HCl and Cl_2. [The thermodynamic data given in this thesis are taken from Bulletin 605 of the U.S. Bureau of Mines by C.E. Wicks and F.E. Block (1963) and from 'Metallurgical

Thermochemistry' by O. Kubaschewski, E.Ll. Evans and C.B.Alcock, 4 edn., Pergamon, London (1967).]

Table 1.

Free energies of reaction of SnO_2 to $SnCl_4$ using different chlorinating agents. (kcal per mole of SnO_2)

Temperature(^oK)	NaCl	KCl	$MgCl_2$	$CaCl_2$	$FeCl_3$	HCl	Cl_2
800	183.1	233.9	3.7	66.1	-1.0	4.2	5.5
900	179.3	231.1	-0.7	62.1	1.1	5.1	3.1
1000	176.3	228.3	-3.1	59.7	5.0	8.1	2.7
1100	174.7	226.9	-4.2	57.6	7.0	9.4	1.4

This table shows that both NaCl and KCl would be poor chlorinating agents; the reactions involving $MgCl_2$ and $CaCl_2$ may be made more favourable by the addition of silica, which is usually present in gangue material, to convert oxide products to silicates. Under these conditions, any mildly unfavourable free energy changes would be offset by the removal of the volatile $SnCl_4$ so that the reaction would go to completion. The use of $FeCl_3$ presents a difficulty in that it would condense with the $SnCl_4$ and a considerable refining operation would be necessary. The presence of carbon in the reaction with Cl_2 would render it even more favourable by removing oxygen as CO_2 ($\Delta G^o_{1000^oK} = -97.6$ kcal).

The production of $SnCl_4$ instead of $SnCl_2$ presents a number of technical difficulties and economic problems.

The formation of $SnCl_4$ requires more chlorinating agent unless the process can be cyclised and at these temperatures the best chlorinating agent, viz. chlorine, is unselective so that iron oxides are also converted to the volatile trichloride. Also if $SnCl_4$ is to be condensed then large losses would be incurred as the vapour pressure is still appreciable at the lowest practicable industrial temperatures (7mm at 10°C). As has been mentioned previously, air must be excluded to prevent the back reaction:

$$SnCl_4(g) + O_2(g) \longrightarrow SnO_2(c) + 2Cl_2(g), \quad \Delta G^{o}_{1000^{o}K} = -2.7\text{kcal.}$$

and the hydrolysis:

$$SnCl_4(g) + 2H_2O(g) \longrightarrow SnO_2(c) + 4HCl(g), \quad \Delta G^{o}_{1000^{o}K} = -8.1\text{kcal.}$$

Owing to these difficulties, the production of $SnCl_4$ has not been considered as a viable large scale commercial process in the extraction of tin and most research work has been carried out on the formation of $SnCl_2$ by reaction of cassiterite with a chlorinating agent in the presence of a reductant. The formation of $SnCl_2$ has a number of advantages in that less chlorinating agent is used, incondensible losses are decreased as the boiling point is 925°K, and less refining is needed as other gaseous impurity chlorides, e.g. $FeCl_3$, remain volatile at that temperature. Non-volatile chlorides, e.g. NaCl, would remain with the gangue material.

Stannous chloride may be produced from cassiterite using a variety of reductants and chlorinating agents. A number of processes using the following reagents have been investigated:

$C/NaCl$;[22] $C/CaCl_2$;[23-25] $C/ZnCl_2$;[26,27] $C/FeCl_2$;[26-28] $C/MgCl_2$;[25,29] CO/Cl_2;[30] CO/HCl;[31] H_2/HCl.[32-37] Reaction in the first five systems may be represented as follows:

$$SnO_2(c) + C(c) + MCl_2\ (c,l) = SnCl_2(g,l) + CO(g) + MO(c)$$

The temperatures at which $\Delta G^o = 0$, above which the reaction is favoured, are given below:

M :	2Na	Ca	Zn	Fe	Mg
T(°C):	>1500	930	630	650	530

These figures may be regarded as a rough guide only as the activities of the chlorides may be reduced by mutual solution, while the presence of silica will in some cases decrease the temperature required by converting oxide products to silicates.

Reaction in CO/Cl_2 occurs according to the following operation:

$$SnO_2(c) + 2CO(g) + Cl_2(g) = SnCl_2(g,l) + 2CO_2(g)$$

$$\Delta G^o_T = -54,600 - 3.9T$$

The reaction is thermodynamically feasible at all sensible temperatures.

SnO_2 reacts in CO/HCl and H_2/HCl as follows:

$$SnO_2(c) + CO(g) + 2HCl(g) = SnCl_2(g,l) + CO_2(g) + H_2O(g)$$

and

$$SnO_2(c) + H_2(g) + 2HCl(g) = SnCl_2(g,l) + 2H_2O(g)$$

for which the respective standard free energy changes are:

$6,730 + 5.06T \log T + 2.22 \times 10^{-3}T^2 - 33.30T$ and

$15,330 + 5.06T \log T + 2.22 \times 10^{-3}T^2 - 44.14T$. The reactions

are thermodynamically favourable above approximately 650 and 550°K respectively.

The use of solid chlorides causes melting phenomena in the charge resulting in lower conversion yields while gaseous chlorine is unselective so that HCl appears to be the best available chlorinating agent. The use of $FeCl_2$ is further ruled out as iron is usually regarded as a troublesome impurity during smelting and efforts have been made in the past to remove it from the gangue material by acid leaching; however, when the tin content of the ore is low, this process becomes inhibitively expensive. Paradoxically, in two of the treatments mentioned above viz. the Ashcroft-Elmore process [28], and Chizikov's work, [30] $FeCl_3$ and Fe_2O_3 are added respectively, in the one case to effect the chlorination itself and in the other to increase the rate of chlorination. Chizikov found that the presence of approximately 20% Fe_2O_3 achieved a 40% increase in the volatilisation of $SnCl_2$ from the reaction of SnO_2 in CO/Cl_2.

In the majority of cases, the research work done on the above processes has consisted of feasibility studies using various samples of low-grade tin concentrates. Nieuwenhuis, [31] Prosser and Romero [35] and, to some extent, others of the U.S. Bureau of Mines [32-34], however, have examined the kinetics of reaction of cassiterite in CO/HCl and H_2/HCl mixtures. Nieuwenhuis used a synthetic concentrate containing 5% Sn,

1.25% Fe and 68% SiO_2 and studied the reaction in a fluidised bed at 700-800°C. The gas mixture he used was equivalent to CO/HCl, being formed from partially burned oil and Cl_2. He found that $SnCl_2$ was the major product and that the rate of volatilisation was proportional to the hydrogen chloride concentration. The rate increased with decreasing $CO:CO_2$ ratio above the minimum required for conversion and P_{CO} and the P_{HCl}: P_{CO} ratio did not affect the rate; he calculated the activation energy as 28 Kcal $mole^{-1}$. In order to obtain stannous chloride, as the major product, he found it was necessary to rapidly cool the exit gases to prevent the following oxidation reaction:

$$2SnCl_2(g) + 2CO_2(g) \rightleftharpoons SnCl_4(g) + SnO_2(c) + 2CO(g)$$

$$\Delta G^{o}_{T} = -18,570 - 3.46T \log T - 3.26 \times 10^{-3}T^2 + 58.45\ T.$$

This reaction is increasingly favoured as the temperature is lowered.

The reaction between a rich tin concentrate (~77% SnO_2) of an alluvial Nigerian cassiterite and H_2/HCl mixtures has been studied by Prosser and Romero[35]. Using the technique of thermogravimetry and carrying out the reaction in the region of 600°C, two types of rate curve were found: in one case, at high pressures of hydrogen and low hydrogen chloride pressures, the reaction started immediately and proceeded steadily; increasing the proportion of hydrogen chloride had the effect of causing initial rapid reaction of

approximately 5% of the cassiterite in thirty minutes, which was followed by an induction period of several hours. For steady reaction at 610°C, they found the data fitted the rate law:

$$R/p = 1.1 \times 10^{-4}$$

where R is the % cassiterite volatilised per second and p is the partial pressure of hydrogen in cm Hg. No correlation was found between the reaction rate and the pressure of hydrogen chloride.

The presence of an induction period would indicate the build-up of a reaction intermediate and examination of particles, during the early period of reaction, showed that they begin to react in regions of crystal imperfection. Some residues showed the presence of particles varying in the extent of reaction, while microscopic examination of polished sections of the original material showed the existence of bands of iron oxide inclusions, each band varying in the size and density of these inclusions.[35]

Coupled with the evidence produced by Chizikov[30], it may be inferred that these inclusions have a possible catalytic role, either in the solid state or as gaseous intermediates e.g. $FeCl_3$.

2.6. Description of project.

Hydrogen and hydrogen chloride at low pressures are considered to be easily produced in situ by electrolysis in a

country where hydro-electric power is cheaply available; this would be the case if the mountainous region of Bolivia were developed. The principal factors militating against the use of such a process involving H_2/HCl mixtures are the large amount of external heating required and corrosion, thus any decrease in the reaction temperature would make this treatment economically more feasible. This investigation, therefore, deals with the possible catalytic function of iron-bearing materials in such a system, which would effectively lower the required temperature for a given yield. As any examination of the catalytic role of these inclusions requires the prior study of the reaction in the absence of impurities, the preliminary work of Prosser and Romero[35] is extended using a variety of pure SnO_2 specimens. Attempts are made to determine the effects of impurities and also the mechanism by which they produce these effects. To determine the kinetics and mechanism of the reaction certain variables are taken into account:

1. Temperature.
2. State of the stannic oxide-particle size, bed-depth.
3. Gas composition and total gas pressure.
4. Gas-flow rate.
5. Pretreatment of the stannic oxide - stoichiometry.
6. Influence of products.
7. Amount and physical state of the impurities.

Where appropriate, the effects of these variables are studied using both macro- and micro-techniques.

3. Experimental procedure.

The reaction of cassiterite in H_2/HCl and CO/HCl has been investigated using a number of techniques; these may be broadly divided into macroscopic and microscopic methods. Macroscopic techniques have been used to determine the effects of variables, such as gas pressure and temperature, on the rate of reaction of a comparatively large sample consisting of small particles of cassiterite. This will be referred to as bulk chlorination. Other methods employed have shown the course of reaction on the surfaces of single grains or crystals of cassiterite.

3.1. Thermogravimetry.

The extent of bulk chlorination was followed using a thermogravimetric method. The sample was suspended by a Pyrex spring, the extension of which was measured by a cathetometer. The apparatus for preparing and circulating the gas mixtures is shown in Figure 1.

The sample to be chlorinated, usually about 0.1 g, was weighed into the alumina bucket, O, and the whole apparatus evacuated. The sample was heated to the required temperature (500 - 700°C) with the vacuum pump still operating. The reactor tube, V, and the circulatory apparatus, K, were isolated from the rest of the apparatus and the requisite quantities of gases were admitted to the reservoir C. When the sample had reached the required temperature the gas mixture was expanded into the reaction tube and the circulating

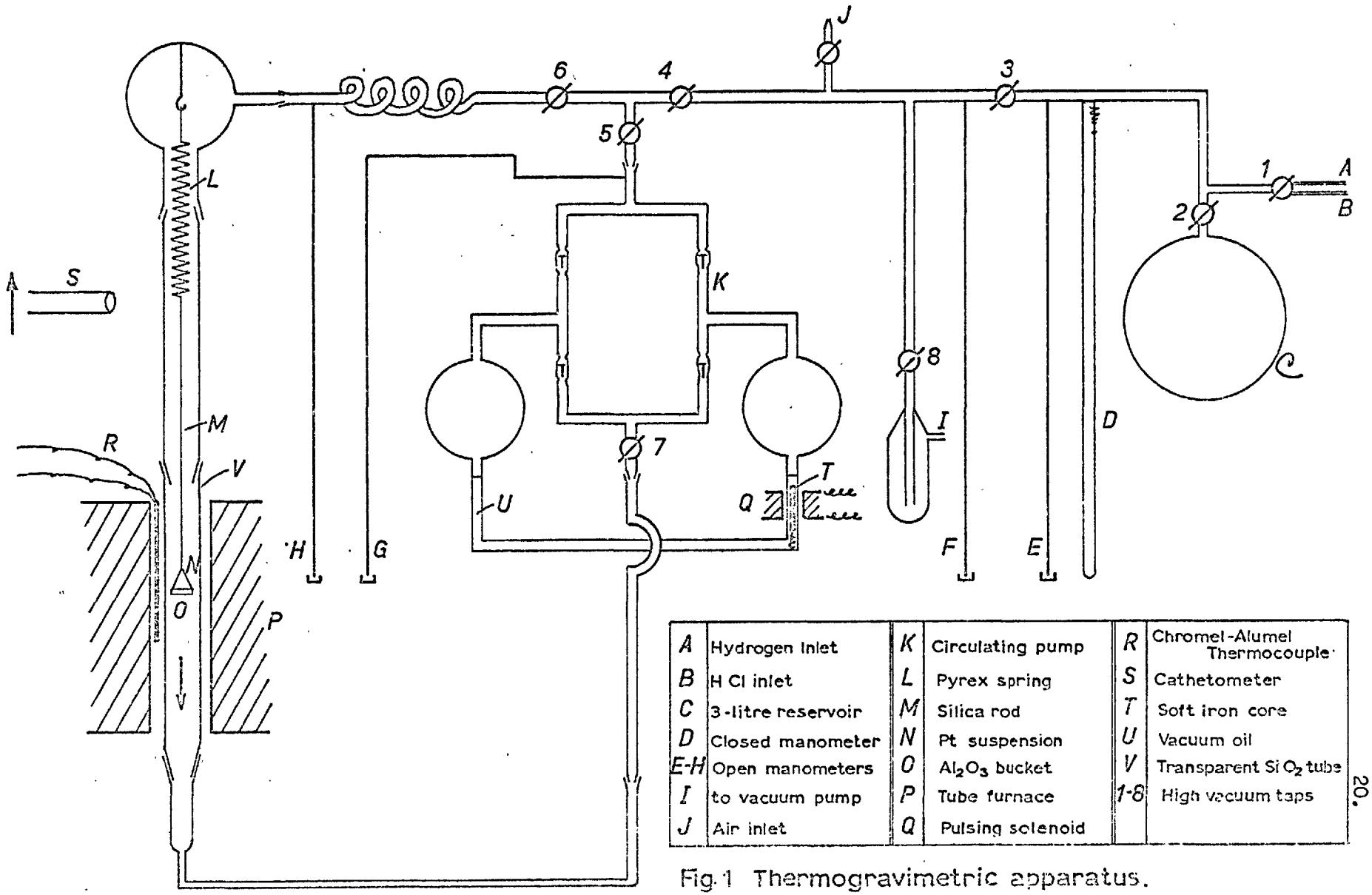

A	Hydrogen inlet	*K*	Circulating pump	*R*	Chromel-Alumel Thermocouple
B	H Cl inlet	*L*	Pyrex spring	*S*	Cathetometer
C	3-litre reservoir	*M*	Silica rod	*T*	Soft iron core
D	Closed manometer	*N*	Pt suspension	*U*	Vacuum oil
E-H	Open manometers	*O*	Al_2O_3 bucket	*V*	Transparent SiO_2 tube
I	to vacuum pump	*P*	Tube furnace	*1-8*	High vacuum taps
J	Air inlet	*Q*	Pulsing solenoid		

Fig. 1 Thermogravimetric apparatus.

pump started. This pump drove the gas mixture round the apparatus so that the reaction products were swept down the furnace tube and did not condense on the suspension system. The impeller of the pump consisted of a soft iron rod under oil which was made to oscillate by a pulsed solenoid, thus driving the gas through the ground-glass valve system shown.

Initially the temperature was maintained by small adjustments of the controlling auto-transformer; later it was controlled to within 1°C using an Ether Mini Temperature Regulator. The temperature was measured using a potentiometer and a chromel-alumel thermocouple in a porcelain sheath placed between the silica tube and the furnace tube. In a preliminary experiment, the internal and external temperatures were compared while the tube was in the furnace with both ends tightly corked; the temperature difference was not more than 1°C.

3.1.1. Separation of additives and SnO_2.

In order to determine whether the preferential reaction observed in the presence of certain solid impurities involved the formation of gaseous intermediates, experiments were performed with the solid additive out of contact with the SnO_2. A cross-section of the sample holder used in these experiments is shown in Figure 2. It can be seen that, with a downward flow of gas, any gaseous compound formed by reaction with the additive has good opportunity of contact with the tin oxide.

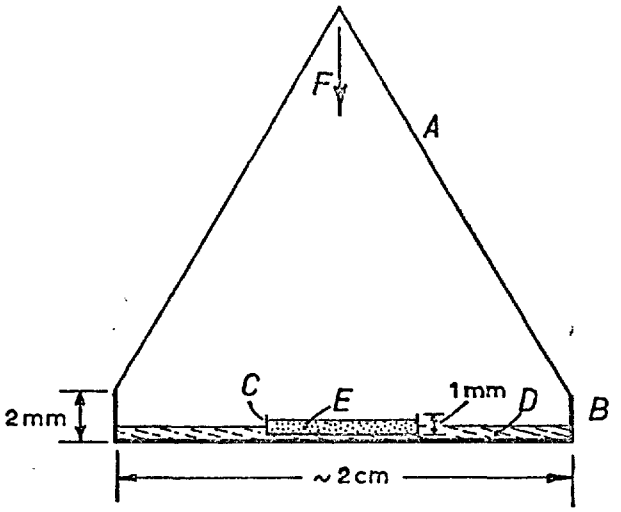

A Platinum suspension B Alumina bucket C Pyrex dish

D $Sn O_2$ E $Fe_2 O_3$ F Direction of gas flow

Fig. 2 Sample holder for keeping solid catalyst out of contact with $Sn O_2$.

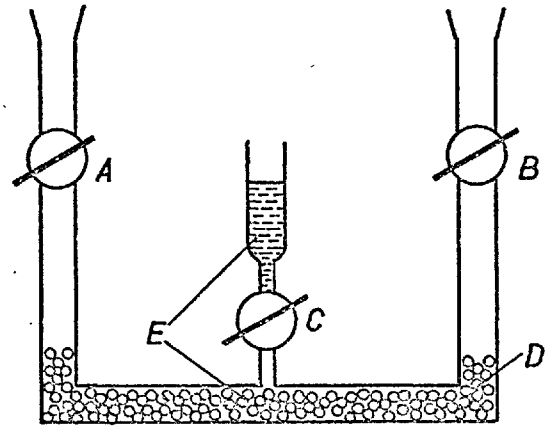

A-C Taps D 5mm dia. glass spheres E Saturated HCl solution

Fig. 3 Apparatus for introduction of water vapour (Inserted in gas circulating line).

3.1.2. Addition of products of reaction.

The effect of the presence of reaction products in the $SnO_2/H_2/HCl$ reaction was investigated by the introduction of water vapour into the gas mixture. Figure 3 is a diagram of the apparatus inserted into the circulating system. 10M HCl was admitted to the glass spheres after this section was evacuated and isolated from the remainder. Once the H_2/HCl mixture had been admitted to the sample, the taps A and B were opened and the circulating pump started. The gas stream was soon saturated with water vapour at approximately 2mm Hg[39].

3.2. Microscopic examination.

3.2.1. Visual microscopy.

Attempts were made to correlate visible features in polished sections of individual grains of cassiterite with reactivity. To do this it was necessary to find a mounting material inert to H_2/HCl at about 600°C. After some preliminary experiments involving platinum and pressed alumina discs the grains were eventually mounted by mixing them with powdered Pyrex glass, pressing the mixture into a disc and heating it to 700°C. A higher temperature was considered undesirable as some modification to the cassiterite might have occurred[40]. The disc was polished using successively smaller diamonds; the size of the diamonds in the final stage was approximately 1μm.

The sectioned grains of cassiterite were photographed at magnifications up to X 2500 using a Zeiss Ultraphot photo-microscope. Many of the grains contained inclusions and some exhibited considerable complexity as to the distribution of the former; others, however, had small inclusions (approx. 1 μm) occurring in well-defined areas. A detailed description of the types of grains encountered is given in section 4.1.

The sectioned grains were reacted in H_2/HCl under similar conditions to those used in the bulk chlorination experiments. After a period of up to 1.8 ks, the reaction was quenched by switching off and lowering the furnace and at the same time subjecting the silica tube to a blast of cold air. The grains were once again photographed and the process repeated, increasing the temperature or reaction time as necessary, until a complete photographic record of reaction up to approximately 10% was obtained. The degrees of reaction of different areas of grains were correlated with visible features present in the unreacted sections.

3.2.2. Electron-probe microanalysis.

In order to determine the effect of composition on the rate of reaction some grains which contained colour-zones and inclusions in distinct areas were subjected to electron-probe microanalysis before reaction. The sectioned grains and Pyrex mounts were first coated with carbon using an Edwards vacuum coating unit, to render the surface of the disc conducting.

The electron-probe microanalysis was kindly carried out by Dr. J. Gavrilovič of the Dept. of Mining and Mineral Technology using a Cambridge 'Geoscan' instrument. The distributions of Sn, Fe, Nb, Ta, Ti, Mn were determined. The carbon coating was removed by light polishing before the sectioned grains were reacted as described in section 3.2.1. Again, a correlation between composition and reactivity variations was detected.

3.3. Preparation of synthetic SnO_2 samples.

3.3.1. SnO_2 powder.

Reagent grade stannic oxide powder, as received from Fison's Scientific Ltd., was used in the preliminary experiments. The surface area of this sample was determined using krypton adsorption and the B.E.T. method; it was found to be $3.2 \pm 0.3\ m^2g^{-1}$, corresponding to an average crystal size of approximately 0.3 μm.

3.3.2. SnO_2 crystals.

Stannic oxide crystals were grown by the cuprous oxide flux method[41]. SnO_2 powder was prepared by reaction of tin and nitric acid, both of A.R. grade, to give metastannic acid which was dehydrated at 900°C. The SnO_2 was mixed with twice its volume of Cu_2O in a 50 cm^3 platinum crucible and this was heated in air to 1250°C, the temperature of the rim of the crucible being approximately 1150°C. This temperature was maintained for one week and the furnace was allowed to cool to

25°C over a period of three days. The crystals were separated from the solid slug with HCl. The actual crystal growth was performed by Dr. E.A.D. White of the Materials Science Crystal Growth Laboratory.

In appearance, the crystals were slightly buff-coloured and varied in habit from rods to platelets; the colour was presumed to be owing to a degree of non-stoichiometry. The size-fraction chosen for experimental work was 75 - 105 μm. The specific surface area was determined by the B.E.T. method using krypton and was found to be 3×10^{-3} m^2g^{-1} indicating a true particle size of 150 ± 50 μm, i.e. the particles were single crystals with few cracks or holes.

3.3.3. Annealed SnO_2 crystals.

The crystals obtained by the Cu_2O flux method described in section 3.3.2. were further heat-treated in air in either platinum or alumina crucibles according to the following programme: 1265°C for 24h; cooled to 1000°C over 4h; maintained at 1000°C for 20h; cooled to 400°C over 3h and removed. As a result of this treatment the colour had changed from buff to mauve and this was attributed to a change in non-stoichiometry. The temperature of 1265°C was chosen as being near the sintering temperature (approximately half the absolute melting point) and the slow cooling rate was to prevent dislocations and cracks induced by thermal shock.

3.3.4. Iron-doped SnO_2 crystals.

Various attempts were made to 'dope' SnO_2 crystals with iron. The first method tried was addition of Fe_2O_3 to the cuprous oxide flux; e.s.r analysis showed that this sample contained approximately 100 p.p.m. Fe (cf. section 4.2.3.). In the second method, the SnO_2 crystals were mixed with Fe_2O_3 and heated in air in a molybdenum tube-furnace to temperatures up to 1450°C and for times up to 24h; the mixture was thereafter slowly cooled. Electron-probe micro-analysis showed that there was less than 0.1% Fe present in any of these batches. Also, the 'doped' crystals reacted in the same way as undoped crystals.

3.4. Preparation of SnO_2 - additive mixtures.

3.4.1. SnO_2 - metal oxides.

The additives used and their origins were:-

TiO_2 - spectrographically pure; Johnson Matthey Ltd.

NiO - spectrographically pure; Johnson Matthey Ltd.

Pt black - Hopkin and Williams.

CuO - A.R. Grade; Hopkin and Williams.

Ta_2O_5 - 3N grade; Koch Light Labs. Ltd.

Nb_2O_5 - 3N grade; Koch Light Labs. Ltd.

Co_3O_4 - ignition of A.R. grade $Co(NO_3)_2$ (Hopkin and Williams) in air at 700°C.

PbO - ignition of A.R. grade $Pb(CH_3COO)_4$ (Hopkin and Williams) in air at 500°C.

Ag_2O - precipitation from solutions of A.R. grade $AgNO_3$ and NaOH (Hopkin and Williams) with subsequent washing with water and drying at 120°C.

Fe_2O_3 - ignition of A.R. grade $Fe(NH_4)_2(SO_4)_2\ 6H_2O$ (Hopkin and Williams) in air at 700°C.

MoO_3 - A.R. grade; Hopkin and Williams.

Bi_2O_3 - ignition of A.R. grade $Bi(NO_3)_3$ (Hopkin and Williams) in air at 700°C.

WO_3 - precipitation from boiling acidified solution of re-crystallised sodium tungstate (Hopkin and Williams) followed by washing and ignition of the product at 700°C.

V_2O_5 - ignition in oxygen at 500°C of A.R. grade ammonium metavanadate (Hopkin and Williams).

The particle size in all cases was less than 37 μm and was probably of the order of 1 μm.

The mixtures of annealed SnO_2 crystals (75-105 μm) (cf. section 3.3.3.) and the synthetic additives were made up by a simple wet mix of the required amounts followed by drying at 120°C.

3.4.2. SnO_2 - iron-bearing minerals.

The minerals used were:- hematite, magnetite, columbite pyrite, ilmenite and biotite. They were in the size-range 75 - 150 μm and the mixtures were made up by wet-mixing as described in section 3.4.1.

4. Results.

This chapter is divided into three sections; the first deals with the results obtained from the microscopic examinations and mostly with the natural cassiterite. The second section deals with the results obtained by the bulk chlorination method (section 3.1.) and applies mainly to synthetic crystals. The third section deals with the analysis of products of reaction. The results are presented together with some deductions which are readily made from each group of results. The relations between the results are discussed in the next chapter.

4.1. Microscopic examination of samples of natural cassiterite

4.1.1. An alluvial Nigerian cassiterite.

This cassiterite from Jos in Nigeria had already been studied by Prosser and Romero[35] and their results have been outlined in section 2.5. Subsequent to extensive reaction in H_2/HCl, they observed particles with a distinct banded effect (see Plate 1). The bands corresponded to dark, unreacted cassiterite and a white, powdery material. In one case, even after 48 hr. in an atmosphere of H_2/HCl, the centre of a particular grain was found by electron-probe microanalysis to consist of almost pure stannic oxide. It was decided to investigate these effects by reacting mounted grains as described in section 3.2. and correlating centres of reaction with previously observed features. The concentrate was assayed by the Analytical Services Laboratory using x-ray

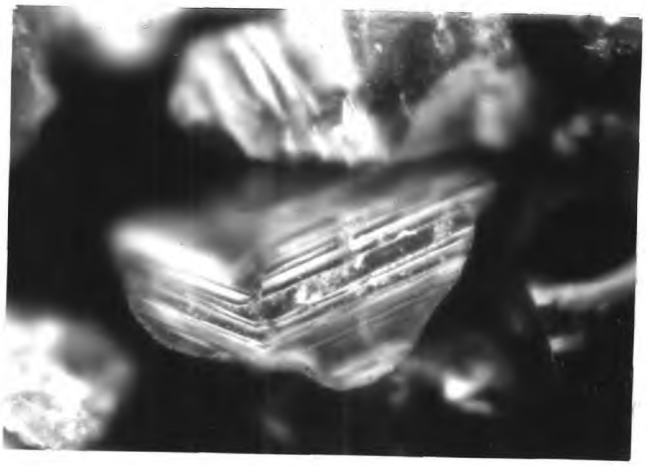

Plate 1. A banded particle of cassiterite after extensive reaction in H_2/HCl at 567°C. (X 200 before reproduction). (Photograph by courtesy of Dr. A.P. Prosser).

fluorescence and found to consist approximately of 50% Sn, 5% Fe, 5% Nb, 3% Ti, 2% Ta and 4% Si. Plates 2 and 3 illustrate the complexity of some of the particles encountered; these grains contained columbite-tantalite, silica, ilmenite and hematite. In such a grain, the distribution of inclusions was thought to be too complex to allow definitive correlation with centres of reaction.

Twelve particles on the first disc were studied and photographed at approximately X800 and X2500 magnification. As it was unreasonable to examine all of these grains with the electron-probe microanalyser and as no basis for selection was known, this latter technique was not used at this stage.

Various regions of the cassiterite grains were classified in terms of their inclusions as follows:

(i) areas with no inclusions

(ii) areas with inclusions which could be at least partly resolved by the 'Ultraphot' microscope

(iii) areas which appeared to be 'fogged' at the highest magnification. (Presumably these areas contained inclusions that were smaller than about 0.1 μm.)

Three particles exhibited these areas in an ordered pattern. Also there were many larger inclusions randomly distributed through most of the grains.

These sectioned particles were reacted at 567°C for approximately 2.3ks in P_{H_2} = 25 cm Hg and P_{HCl} = 20 cm Hg.

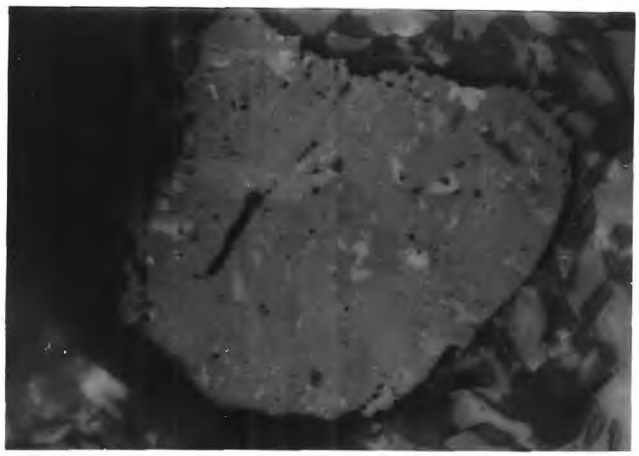

Plate 2. Section of a particle of cassiterite which has complex distribution of inclusions (X 800 before reproduction).

Plate 3. Detail of section shown in Plate 2. (X 2500 before reproduction).

Subsequent microscopic examination of the grains showed that they had all reacted to some extent; unfortunately, with most of them, it was not possible to correlate the extent of reaction with previously observed features. However, in the three grains which had shown a pattern to their inclusions, differences in the degree of reaction were remarkably clear. In these particles reaction had taken place in areas where there had been very small inclusions (type iii) leaving adjacent areas almost unreacted; (cf Plates 4 - 6); in two cases this gave rise to alternate parallel regions of reacted and unreacted material. The reacted specimens were then lightly polished to facilitate electron-probe microanalysis.

This analysis, carried out by Dr. J. Gavrilović, showed that while the tin content remained constant over the surface of the particles, the iron content was high in the areas where the three grains had reacted while the Ta and Nb content was relatively high in the regions that had not reacted. No other metallic elements were present in quantities greater than 0.1%. As the iron may have been present as the residue of inclusions, interpretation of these results was difficult without compositional data on the particles prior to reaction. The only conclusion which may be drawn from this study is that the rate of reaction is increased in those areas of very small inclusions but whether this is due to a size or composition factor cannot be inferred.

Plate 4. Section of particle of cassiterite before reaction in H_2/HCl (X 800 before reproduction).

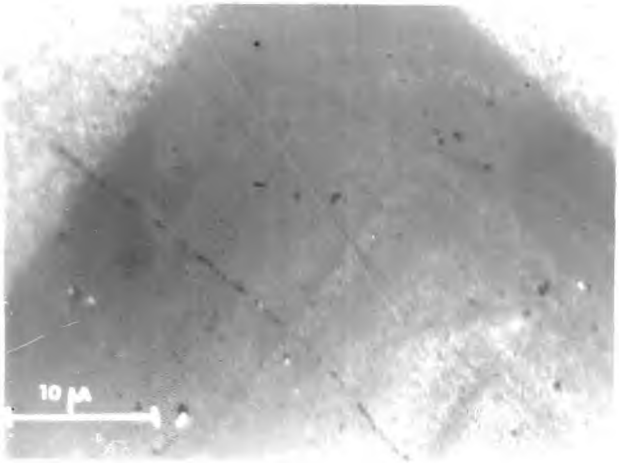

Plate 5. Detail of central area of section shown in Plate 4. This section shows distinct bands of inclusions (X 2500 before reproduction).

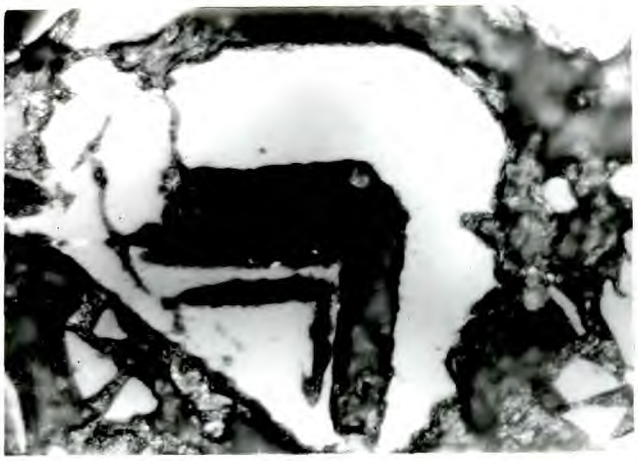

Plate 6. Section of particle shown in Plate 4, after partial reaction in H_2/HCl at 567°C and light polishing. The central area, which contained the finest inclusions, has reacted (X 800 before reproduction).

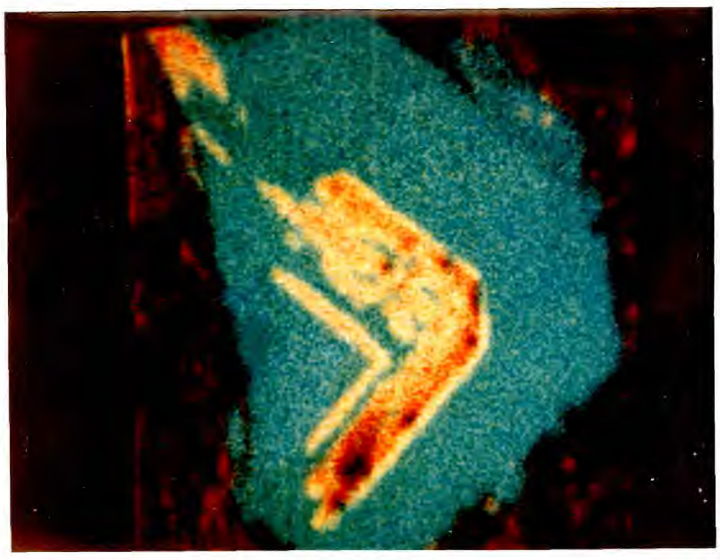

Plate 7. Electron-probe photomicrograph of section shown in Plate 6 (after reaction). The distribution of Sn, Fe and Ta is shown (X 468).
Sn = green; Fe = red; Ta = blue.
The reacted region is the one of higher iron content.

Within the almost unreacted zones there was a variation in tantalum content; there appeared to be a correlation between high Ta content and low reactivity within these zones. (cf. Plate 7).

A second batch of these grains was mounted, polished and reacted under identical conditions; in this case, electron-probe microanalysis was carried out before reaction on those grains which had comparatively simple inclusion patterns.

In a few grains, the degree of reaction could not be correlated with surface features or composition, however, in most cases it was apparent that reaction had occurred in areas of high iron content. Thus the presence of small iron-bearing inclusions catalyses the reaction in the immediate vicinity.

4.1.2. Cassiterite from Rayfield-Gona granite - a primary Nigerian cassiterite.

Grains of this cassiterite were treated in the manner previously outlined in section 3.2. The particles were optically homogeneous and exhibited no detectable compositional variation. After its reaction in P_{H_2} = 15 cm Hg and P_{HCl} = 15 cm Hg for a total of 16h at 550°C, a nearly white residue was left. This contained only tin of elements with atomic numbers greater than 10 and was quite friable. It also retained the same shape and optical properties as the original grain. The intermediate stages were not clear and the specimen was less reactive than the alluvial cassiterite described in

section 4.2.2. The residue was examined by x-ray diffraction and found to be cassiterite.

Interpretation of these data is difficult as there was no obvious change in visible properties at intermediate stages of reaction. However, it seems that at least part of the cassiterite matrix had reacted leaving behind a porous residue which still retained the same unit cell as the original.

4.1.3. A primary 'zoned' cassiterite from Nigeria. Sara Hill.

Grains of this cassiterite were examined and reacted according to the treatment process described in section 3.2; the conditions were 580°C in $P_{H_2} = P_{HCl} = 20$ cm Hg.

This specimen exhibited colour-zoning, varying sometimes in single grains from dark brown to colourless. No inclusions were found and the chemical composition was constant according to electron-probe microanalysis, corresponding to SnO_2 with approximately 1% of iron. This colour-zoning has been explained recently by Grubb et al[40,42] as being due to the presence of different iron valence states; the greater the Fe^{2+} : Fe^{3+} ratio, the darker the colour. Examination of the grains after reaction showed no preferential attack and no correlation was found either with colour-zoning or with the crystal planes exposed; this latter fact is consistent with data described in section 4.2.1. The absence of any connection between colour-zoning and reactivity indicates that the iron, present in solid solution in the cassiterite lattice,

has an effect independent of its valence state.

4.1.4. A primary Bolivian cassiterite.

This specimen was treated under the same conditions as the Nigerian 'zoned' cassiterite described in the previous section.

It also showed colour 'zoning' but was generally optically more homogeneous, again containing approximately 1% iron. No correlation was found between reaction and visible surface features.

4.2. Rates of reaction by macroscopic methods.

In order to determine the kinetics of the reactions involved and to quantify the effects of impurities, bulk chlorinations were carried out using the thermogravimetric technique described in section 3.1.

4.2.1. An alluvial Nigerian cassiterite.

Bulk chlorinations were performed using an alluvial magnetic cassiterite from Nigeria; a description of this cassiterite has been given in section 4.1.1. The grains, in the size-range 105 - 150 μm, were reacted in various H_2/HCl mixtures. The results are shown in Figure 4. They corroborate work done by Prosser and Romero[35], whose results using a static gas system are described in section 2.5. These include the presence of induction periods and a rate dependence on P_{H_2}.

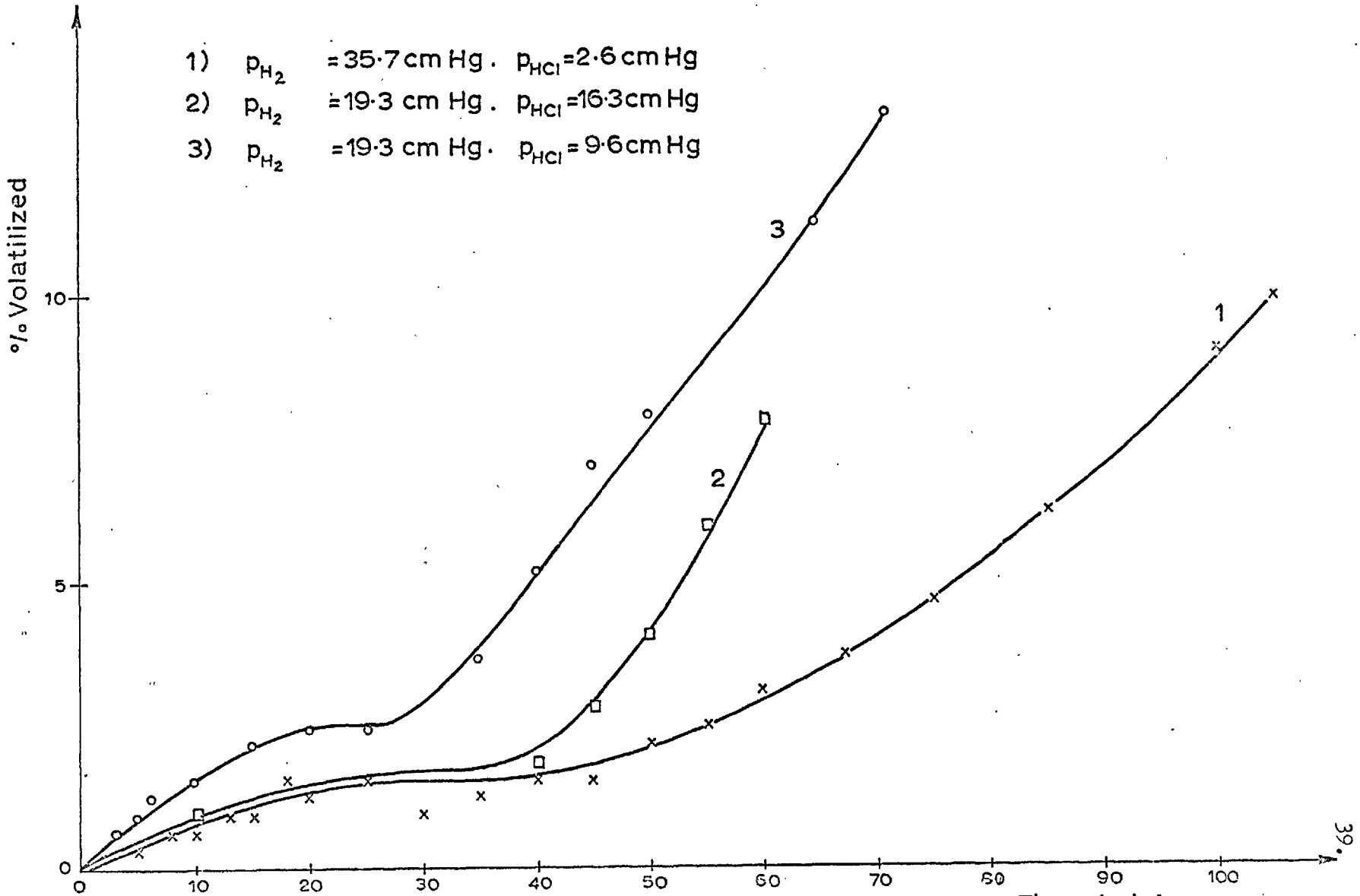

Fig. 4 Reaction of an alluvial Nigerian cassiterite. 610°C.

4.2.2. Stannic oxide crystals.

Samples of naturally occurring cassiterite contain impurities in varying quantities both as inclusions and in solid solution; they also display different surface textures, porosities, dislocation densities etc. owing to their different geological origins and environments. All of these factors could influence the reactivity of cassiterite and indeed the preferential reaction in the vicinity of iron-bearing inclusions has already been noted in section 4.1. Thus it would be difficult to deduce quantitatively the effect of any one factor from a study of the rates of reaction of various natural cassiterite samples alone. Therefore it was decided to use reproducible specimens of synthetic stannic oxide of known thermal history and to control the impurity levels by addition in a defined manner.

4.2.2.1. Effects of quantity of solid and size of crystals.

Initially, experiments were performed on the stannic oxide powder described in section 3.3.1. This powder reacted at a much faster rate than the natural cassiterite and as the rate of reaction depended on the depth of the powder layer (see Figure 5) it was deduced that the reaction was controlled by diffusion within the bed.

Thus it was considered necessary to have larger crystals to decrease the rate of reaction until it was not diffusion-controlled. These were grown using the cuprous

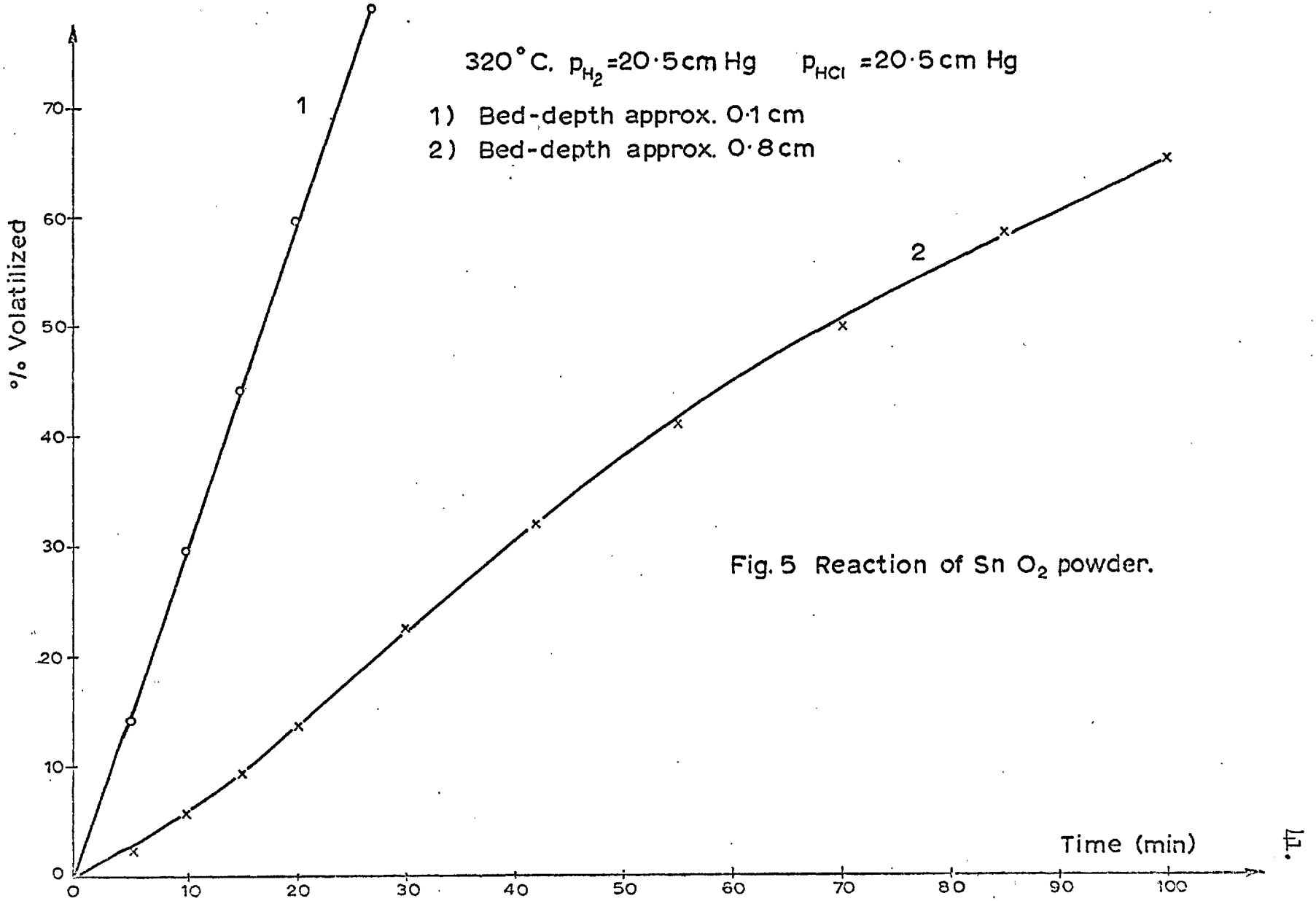

Fig. 5 Reaction of Sn O_2 powder.

oxide flux method[41] described in section 3.3.2. The results of experiments when the bed-depth of these crystals (75 - 105 μm) was varied, showed that the reaction was no longer controlled by diffusion within the bed (cf. Figure 6).

In other experiments, crystals were reacted at 550°C in $P_{H_2} = P_{HCl} = 15$ cm Hg with two widely different gas circulation rates. The results in Figure 7 show that the reaction was not controlled by diffusion from the bed of the SnO_2 crystals.

4.2.2.2. Effect of gas pressures.

Stannic oxide crystals were reacted at 500°C at various H_2 and HCl pressures. Rate curves were of the type shown in Figure 7. Owing to the difficulty of drawing tangents to these curves, the rates of reaction, in % min^{-1}, were taken as forty times the reciprocal of time at 40% reacted as interpolated from the smooth curve drawn through the experimental data. The results are shown in Figures 8 (curves 1 and 3) and 9 (curve 1).

Inspection of these curves and especially comparison of curves 1 and 3 in Figure 8, which are almost parallel, suggests that two reactions are occurring simultaneously in H_2/HCl; one involving only HCl and the other involving both of the gaseous reactants. In addition a third reaction takes place in H_2 only (cf. curve 1, Figure 8 at $P_{HCl} = 0$). The reaction in HCl only is first order with respect to HCl; the

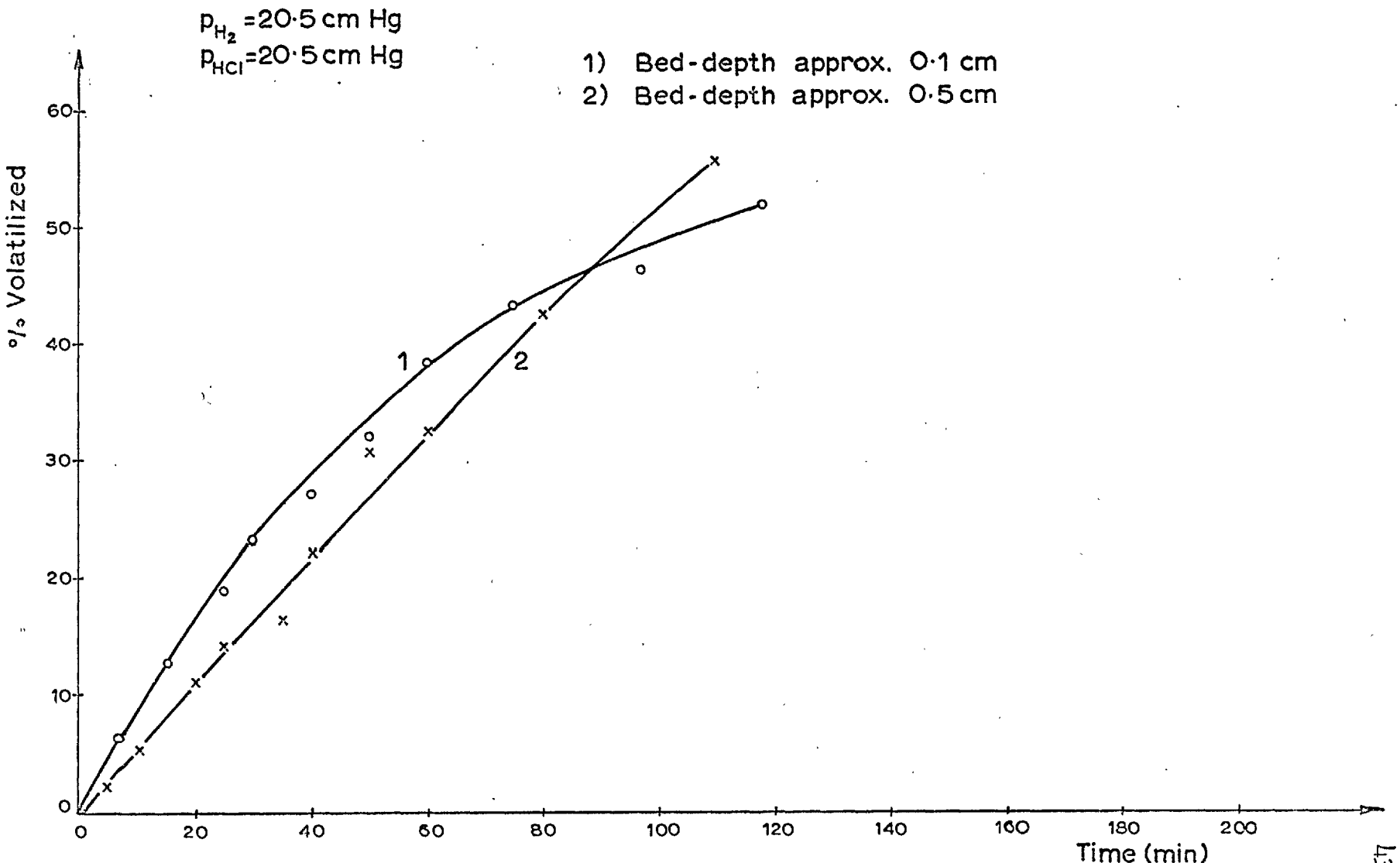

Fig. 6 $Sn O_2$ crystals. Diffusion control experiments.

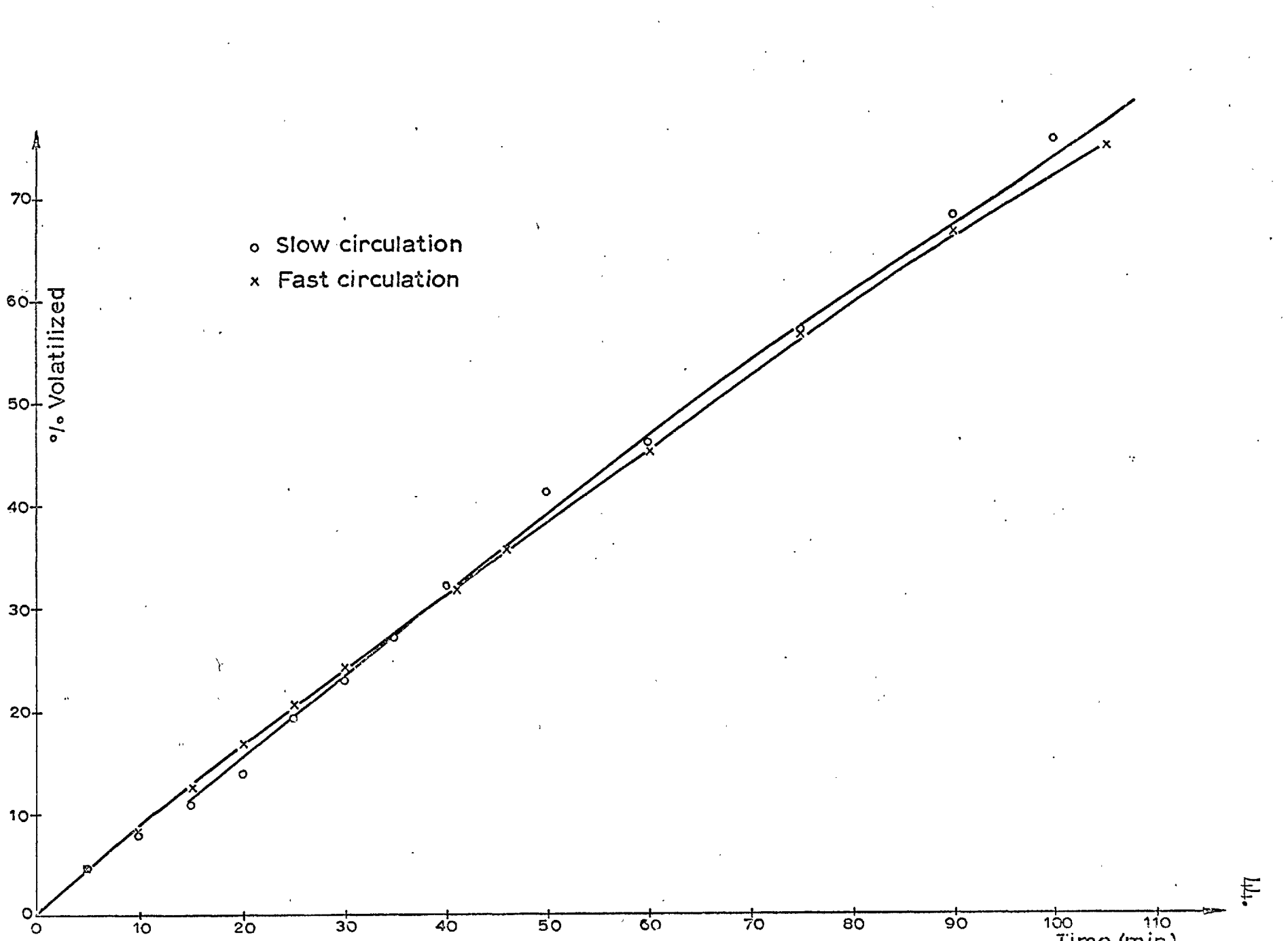

Fig. 7 Diffusion control experiments.

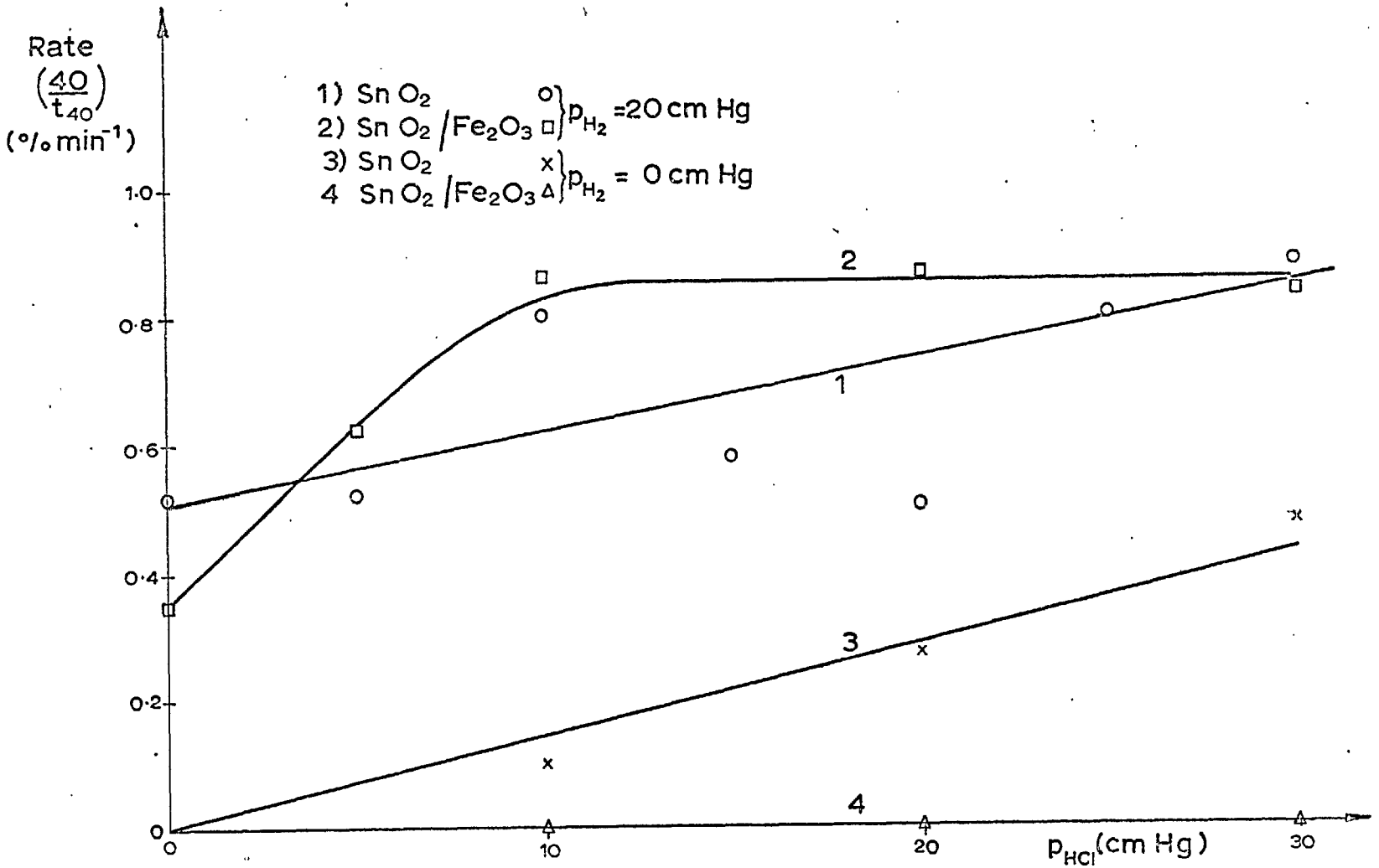

Fig. 8 Effect of Fe_2O_3 and p_{HCl} on the H_2 / H Cl reaction. 500°C.

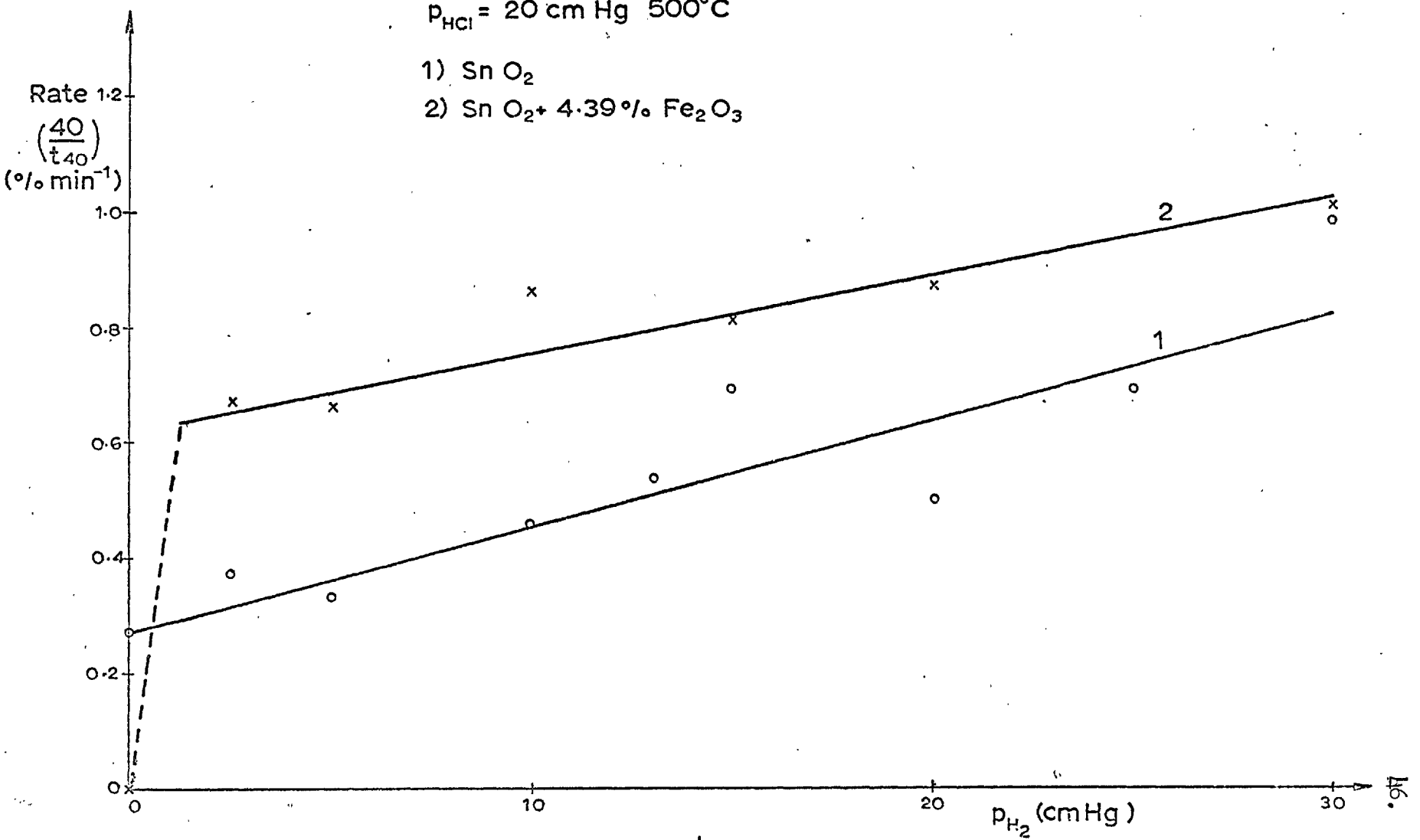

Fig. 9 Effect of Fe_2O_3 and p_{H_2} on the H_2 / H Cl reaction.

rate constant being approximately 2.4×10^{-4}% $sec^{-1}(cm\ Hg)^{-1}$. Examination of curve 1, Figure 9, shows that the rate increases linearly with increasing P_{H_2}:

$$dR/dP_{H_2} = 2.83 \times 10^{-4}\ sec^{-1}\ cm^{-1}$$

$$R = 40/t_{40}\quad (\%\ sec^{-1})$$

Thus the rate-controlling step of the reaction which occurs in H_2/HCl is one of reduction by H_2.

4.2.2.3. The effect of Fe_2O_3 on non-annealed crystals.

Iron oxide is a common impurity in cassiterite; it is present either in discrete inclusions or in solid solution. It has been shown in section 4.1. that the presence of iron compounds within a particular grain of cassiterite causes marked catalysis of the reaction of H_2/HCl within the region in which they are distributed. Therefore it was decided to investigate the effect of Fe_2O_3 on the rate of reaction of synthetic SnO_2 crystals. The crystals were mixed with 4.39% Fe_2O_3 in the manner outlined in section 3.4.1. and were reacted in H_2/HCl at 500°C with various H_2 and HCl pressures.

All the rate curves so obtained were sigmoidal unlike those found in the absence of Fe_2O_3 (cf. Figure 7). Three typical curves are shown in Figure 10. The rate of reaction was measured along the rectilinear portions of the curves. Similar experiments, performed on Fe_2O_3 alone at 500 - 600°C, showed that it remained almost constant in weight (Appendix p158) and thus the reaction rate for the given SnO_2/Fe_2O_3 mixture is 100/(100-4.39) times the rate of change of weight

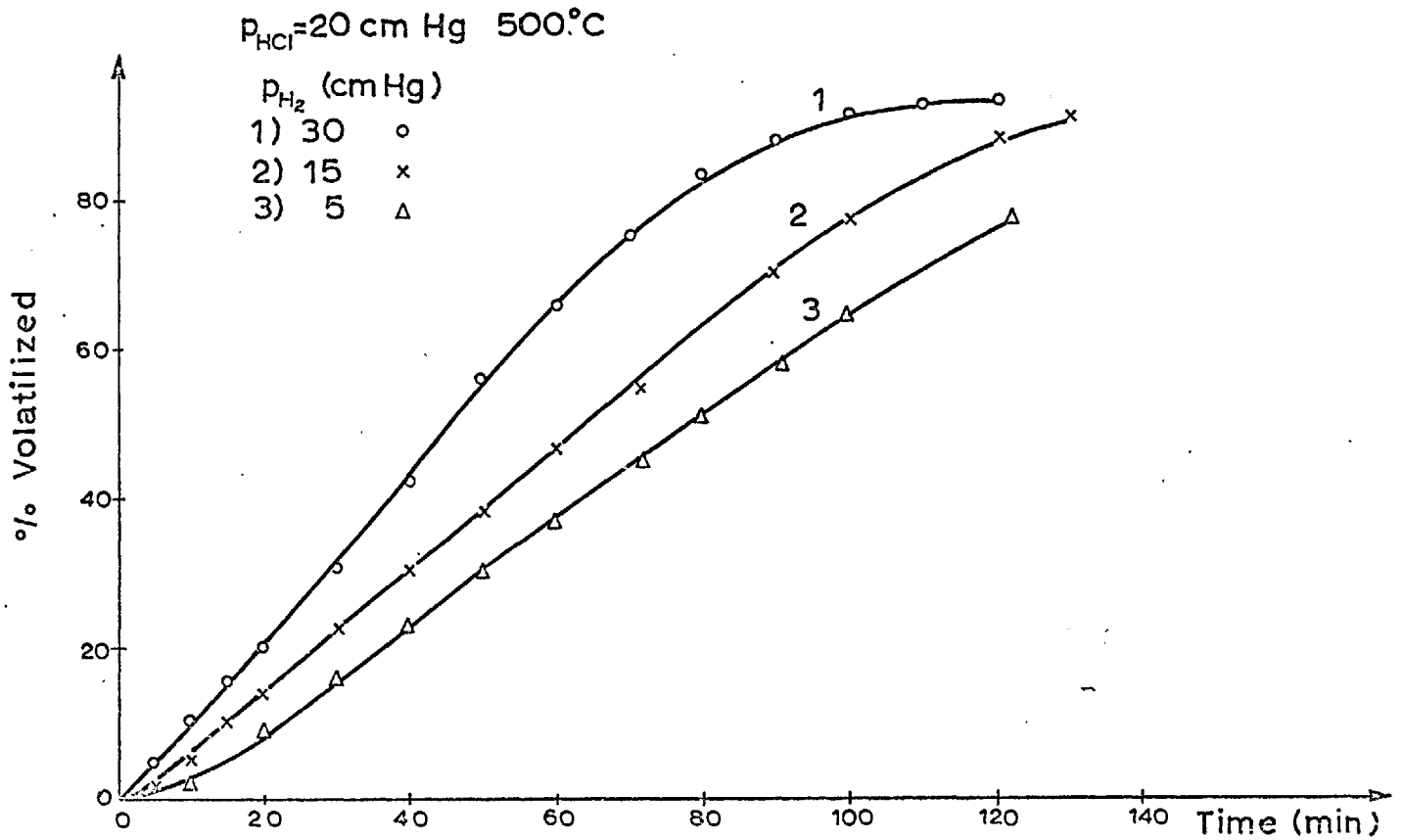

Fig. 10 Effect of Fe_2O_3 on the H_2 / HCl reaction.

of the mixture. The corrected results are depicted in curves 2 and 4 of Figure 8, and curve 2 of Figure 9.

Inspection of curves 2 and 4 of Figure 8 indicates that the presence of Fe_2O_3 inhibits reaction in HCl only but probably accelerates it slightly in the presence of H_2. The effect on the rate of varying the pressure of H_2 at constant P_{HCl}, both with and without Fe_2O_3, is shown in Figure 9, and it is apparent that Fe_2O_3 catalyses the reaction. Curves 1 and 2 of Figure 8 at $P_{HCl} = 0$ indicate a slight decrease in the rate of reduction of the crystals in the presence of Fe_2O_3, though, on the basis of two points only, this may be spurious.

The reaction in HCl only is anomalous in that it is inhibited in the presence of Fe_2O_3; the reaction presumably occurs according to the following equation:

$$SnO_2(c) + 4HCl(g) = SnCl_4(g) + 2H_2O(g)$$

for which the change in standard free energy at 500°C is 3.5kcal. The equilibrium partial pressure of $SnCl_4$ may be estimated as 0.5 atmos and thus the reaction is quite possible (cf. section 5.2). As Fe_2O_3 inhibits this reaction but catalyses that in H_2/HCl, it probably has two different functions and further clarification of these is necessary. A possible mechanism of inhibition may be found by postulating that HCl reacts predominantly with high energy sites and Fe_2O_3 either relieves or denies these sites quickly as new surfaces are exposed. In this context, epitactic growth of Fe_2O_3 on SnO_2 by HCl transport has been demonstrated by Noack[43]. The

mechanism by which Fe_2O_3 catalyses the H_2/HCl reaction is as yet unknown but again requires a rapid influence on new surfaces. The question arises, therefore, whether Fe_2O_3 or its products is active for both reactions at all stages of chlorination of a crystal.

In order to determine this point with respect to the HCl only reaction the following sequence of experiments was devised and carried out: a mixture of SnO_2 and Fe_2O_3 was reacted in HCl only at 500°C until all the iron that would volatilise had done so. The SnO_2 crystals remaining from this reaction were cooled and then reacted in H_2/HCl to approximately 20%. The reaction rate was comparable to that for pure SnO_2. The residue from this last reaction did not react in HCl only. The results are shown in Figure 11.

As the continued passivation of the crystals may have been due to repeated heating and cooling, the sequence of experiments was done again, evacuating the gas and admitting the next gas at the reaction temperature with the minimum time interval between the separate parts of the experiments. In this case the intermediate curve was sigmoidal and the SnO_2 residue reacted to approximately 12% in 95 min in the third part of the experiment in HCl only. The complete results are shown in Figure 12.

The sigmoidal shape of the intermediate curve in Figure 12 shows that some Fe_2O_3 was present in the surface of

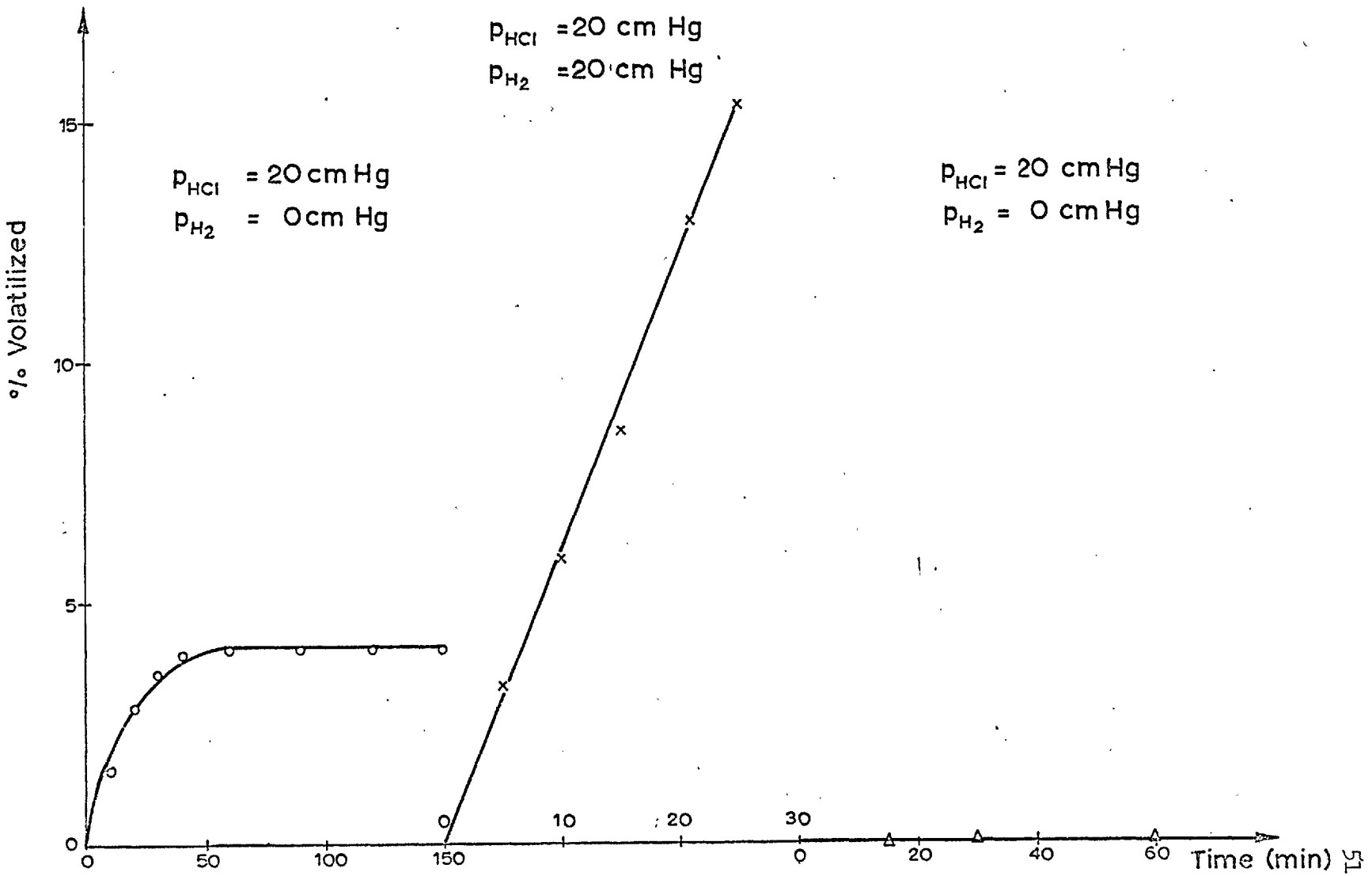

Fig. 11 Effect of Fe_2O_3 on successive HCl only and H_2/HCl reactions.
Non-annealed crystals 500°C. Cooling and reheating between each reaction.

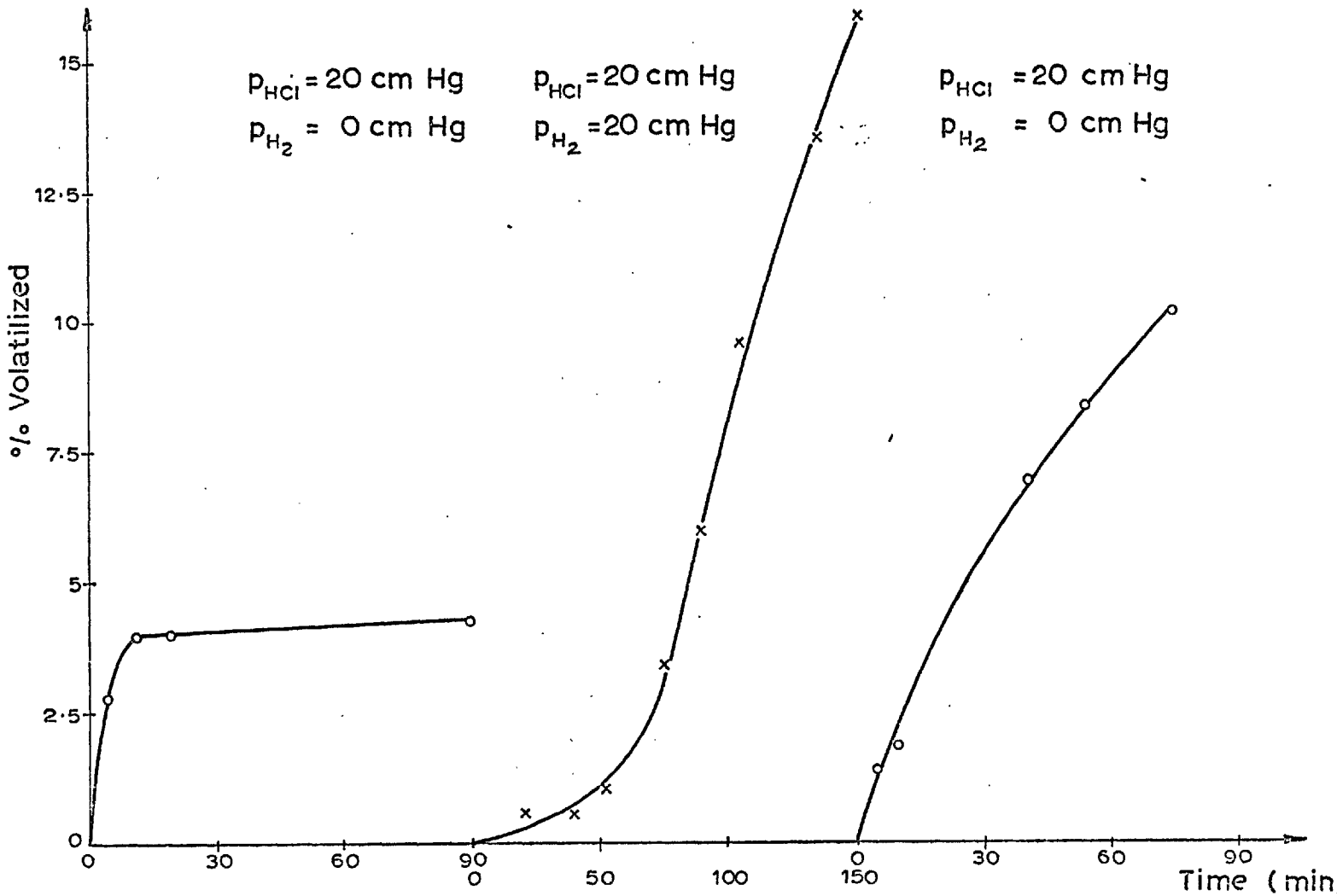

Fig. 12 Effect of Fe_2O_3 on successive H Cl only and H_2/H Cl reactions. Non-annealed crystals. 500°C. Sample maintained at the reaction temperature throughout the sequence.

the crystals even though the reaction was not markedly accelerated. Comparison of Figures 11 and 12 indicates that the residual Fe_2O_3 was more effective at catalysing the reaction in H_2/HCl. As the SnO_2 residue reacted in HCl only immediately after the H_2/HCl reaction, this shows that the residual Fe_2O_3 was not effective in inhibiting this reaction over all the crystal surface.

4.2.2.4. Microscopic examination of non-annealed crystals.

It has been demonstrated in the two preceding sections that these crystals undergo two different reactions in H_2/HCl mixtures viz. one with HCl and one with H_2/HCl. It has also been shown that removal of crystal imperfections inhibits the HCl only reaction. As it is improbable that these tetragonal crystals have the same imperfection density over all crystal faces, it should be possible by microscopic means to detect differences in the points of attack of the two reactions.

Plate 8 shows the regularity of the unreacted crystals used in these experiments. Crystals from reaction in HCl only had reacted preferentially at edges and corners i.e. high energy sites, with the result that attack was severe on the pyramidal sections comprising high index faces while only light attack was apparent on the {100}, producing rectangular etch pits on the latter (cf. Plate 9). Study of crystals reacted in H_2/HCl has shown that reaction occurs more generally over all the crystal faces.

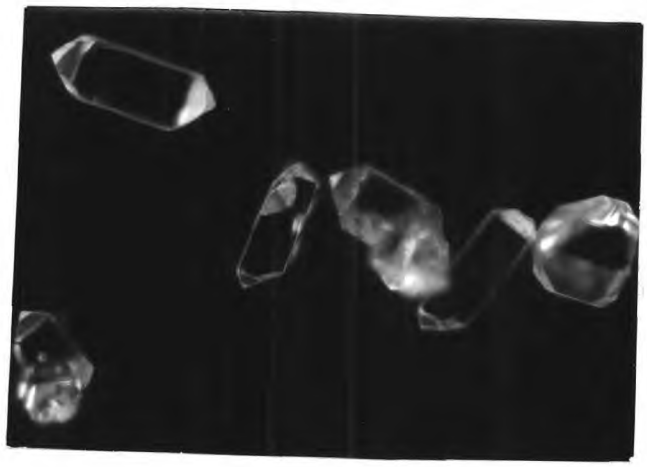

Plate 8. SnO_2 crystals produced by the cuprous oxide flux method.[41] (X 250 before reproduction).

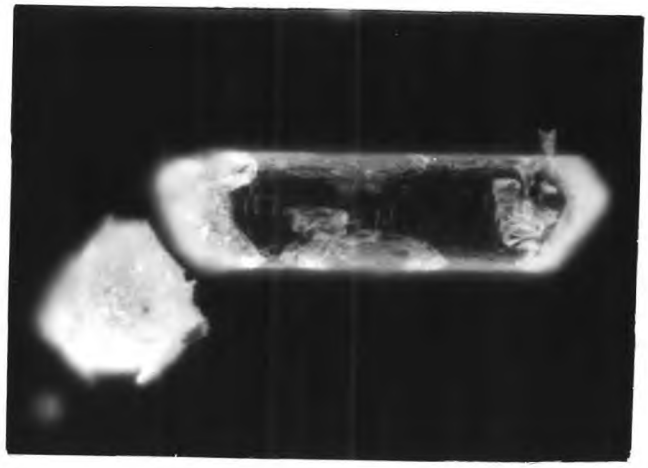

Plate 9. SnO_2 crystals after partial reaction in HCl only at 500°C. Rectangular etch-pits are visible on the {100} faces. (X 800 before reproduction).

These results were further corroborated by reacting crystals mounted and polished as described in section 3.2.1. Two specimens were reacted for 2 min at 500°C, one in P_{H_2} = 10 cm Hg and P_{HCl} = 20 cm Hg, and the other in HCl only (P_{HCl} = 20 cm Hg). The specimen reacted in HCl alone showed preferential attack on particles exposing the basal plane while the other had reacted more uniformly over all particles.

It was suggested in section 4.2.2.3. that Fe_2O_3 quenches reaction in HCl only by annealing the crystal surface in some way such as by dissolution of the Fe_2O_3 in the SnO_2 crystal. There is a possibility that Fe_2O_3, etc. may catalyse or, conversely, inhibit reaction in H_2/HCl on different crystal faces.

Crystals mixed with Fe_2O_3 were examined after reaction in H_2/HCl, as also were crystals coated with iron and subsequently oxidised before reaction. There was no apparent preference for reaction on particular faces.

4.2.3. Annealed SnO_2 crystals.

As the previous experimental results indicated that the quenching of the reaction in HCl only by Fe_2O_3 was due to the relief of crystal imperfections it was decided to anneal a batch of SnO_2 crystals by heat-treatment and to compare the reactivity before and after annealing. The annealing process was carried out as described in section 3.3.3. The annealed crystals were expected to correspond more closely to naturally

occurring cassiterite as the latter has had a much longer time in which to relieve imperfections.

4.2.3.1. Kinetics of reaction of annealed crystals alone.

Annealed SnO_2 crystals were reacted in H_2/HCl in the range 500-600°C. The variation in the rate of reaction with P_{H_2} is shown in Figures 13 (curve 1), 14 (curve 1) and 15 (curve 1).

At 500°C the reaction is first order with respect to P_{H_2} throughout the range of P_{H_2} but at higher temperatures and high P_{H_2}, the order with respect to H_2 decreases. Inspection of curve 1 of Figure 15 shows that annealing of the crystals has caused inhibition of the reaction in HCl only at 600°C and its elimination at 500 and 550°C (cf. curves 1, Figures 13 and 14). Again this evidence indicates that crystal imperfections activate the HCl only reaction.

4.2.3.2. Activation Energy.

An Arrhenius plot of the results is shown in Figure 16. Each point is based on at least three determinations of the rate constant which were in good agreement. The lack of linearity indicates that perhaps the reaction takes place by two different mechanisms at the higher and lower temperatures used or that a different step in the same reaction mechanism ... rate-controlling. The activation energies for the high and low temperature mechanisms are 14 and 52 kcal respectively.

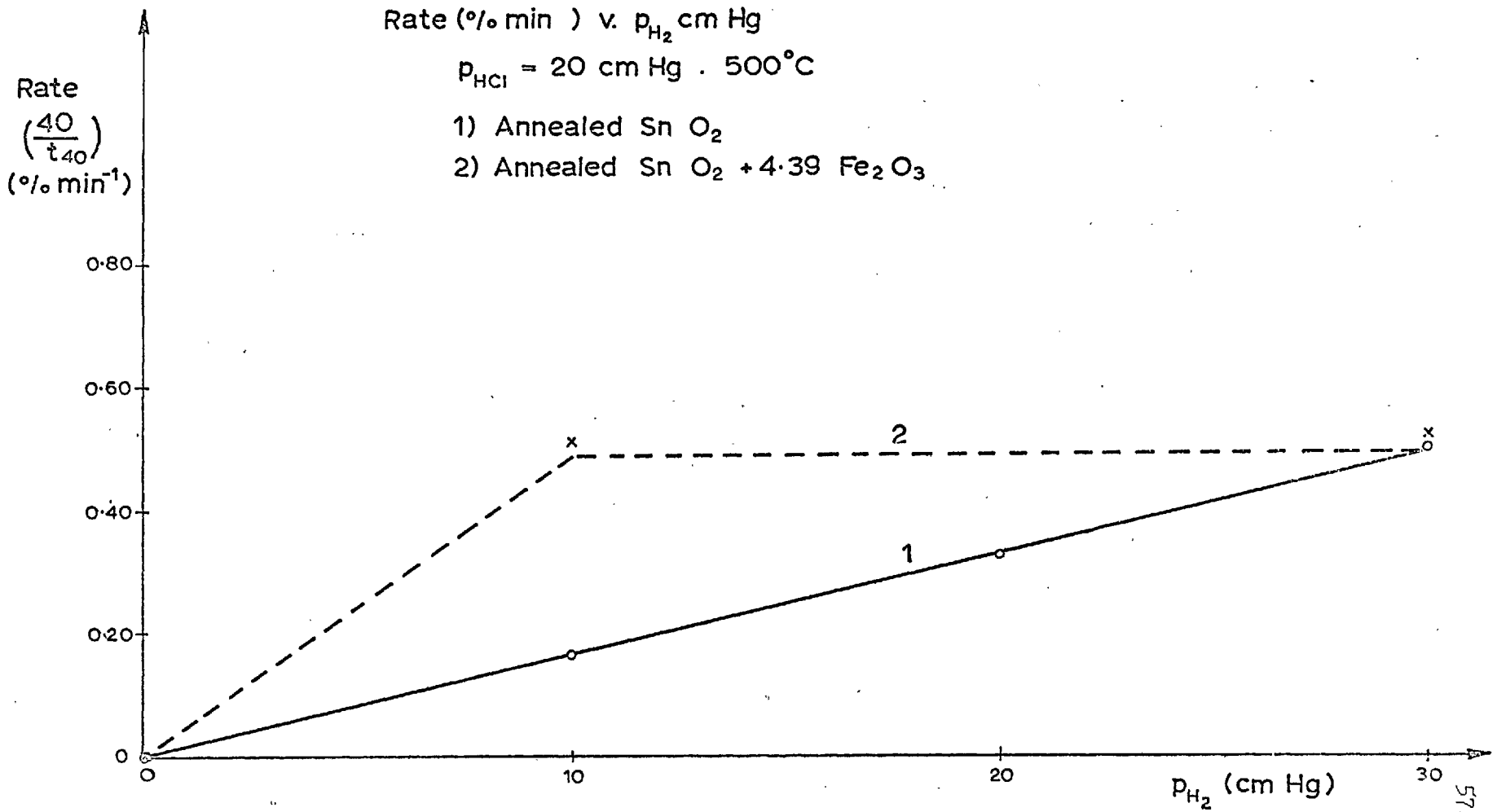

Fig. 13 Effect of varying p_{H_2}. 500°C. annealed crystals ± Fe_2O_3.

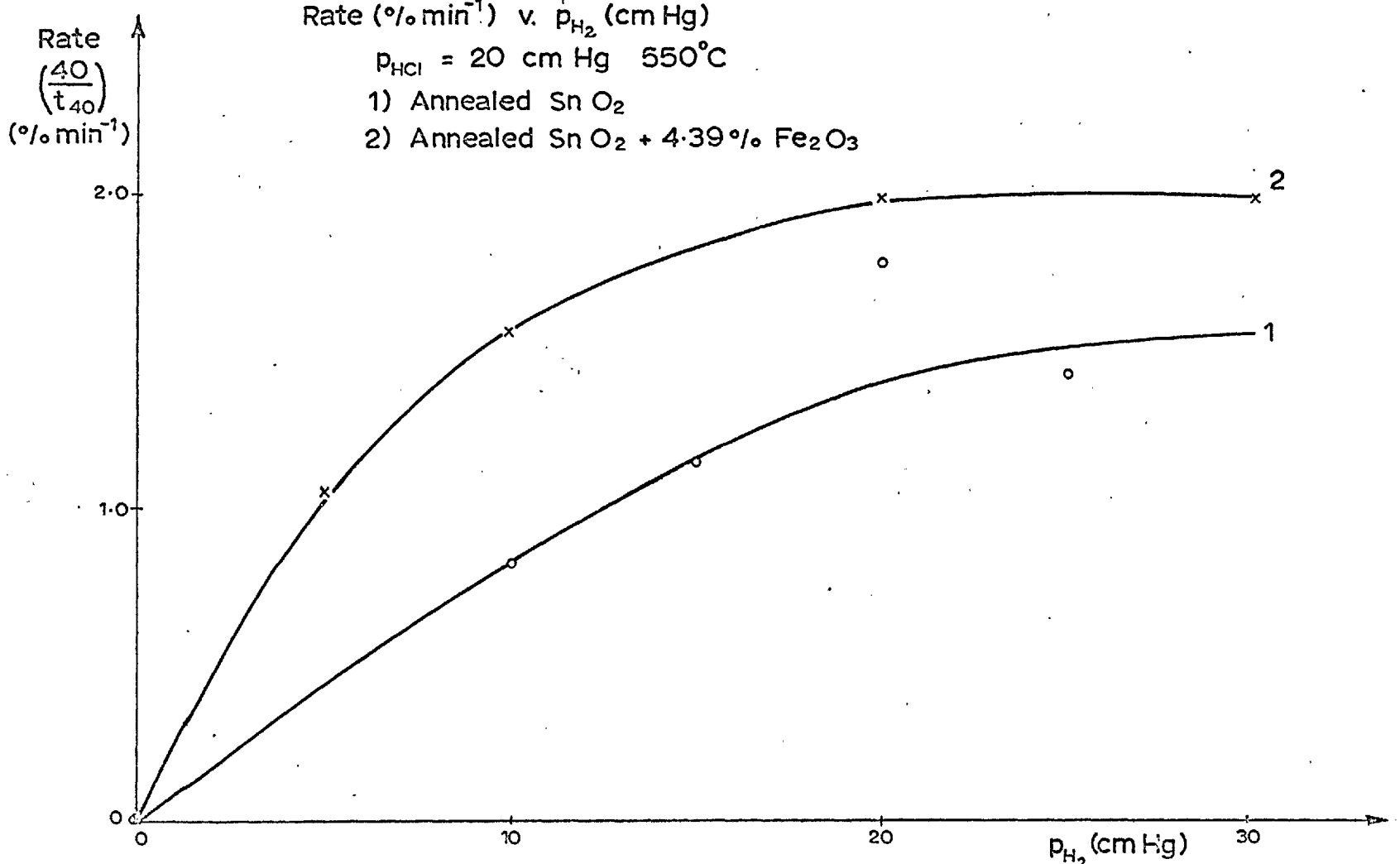

Fig. 14 Effect of varying p_H . Annealed crystals ± Fe_2O_3. 550°C.

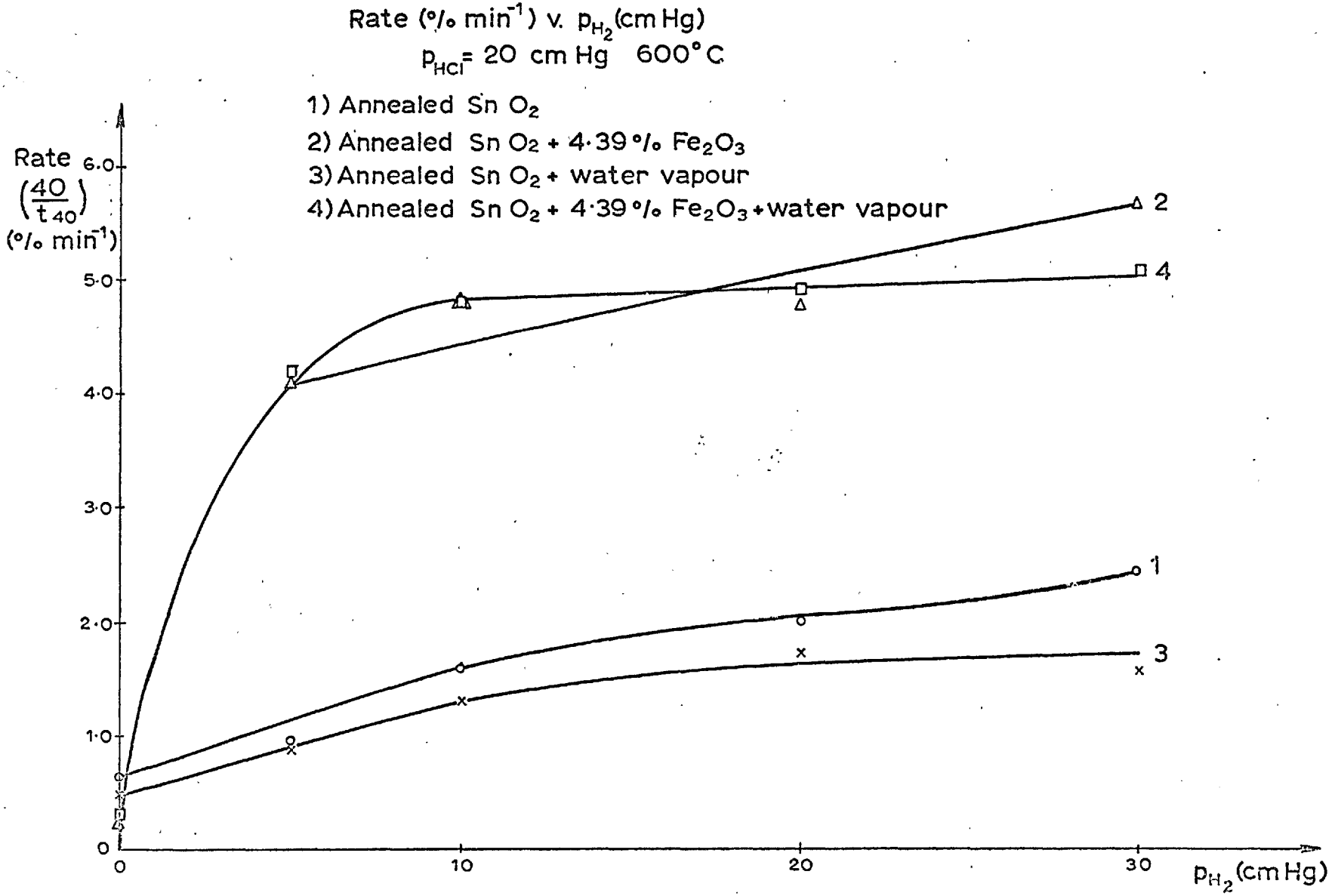

Fig. 15 Effect of varying p_{H_2} and adding water vapour. Annealed crystals ± Fe_2O_3. 600°C.

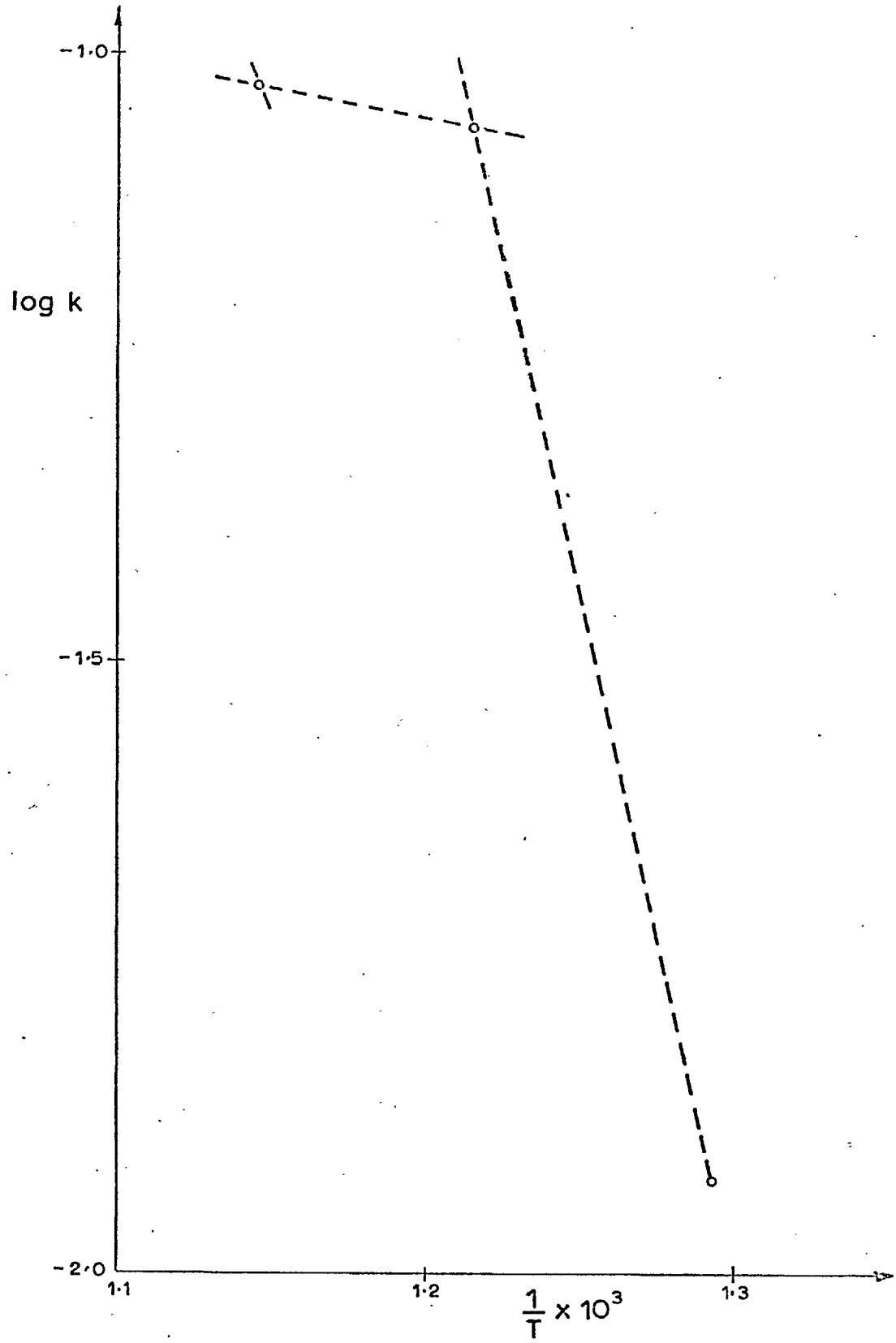

Fig.16 Activation energy of reaction of annealed crystals + H_2/HCl.

4.2.3.3. Effect of Fe_2O_3 on annealed crystals.

Annealed crystals mixed with 4.39% Fe_2O_3 were reacted in H_2/HCl at 500°, 550 and 600°C. All the rate curves obtained were sigmoidal and the variation of the rate of reaction is shown in Figures 13, 14 and 15 (curves 2). The catalytic effect of Fe_2O_3 appears to increase with temperature and there is a finite rate of reaction at 600°C in the absence of hydrogen, where, presumably, $SnCl_4$ is produced. As with the non-annealed crystals, this reaction in inhibited by the Fe_2O_3. Also curves 3 and 4 of Figure 15 show the slight decrease in rate in the presence of approximately 2 mm Hg of water vapour (one of the products of reaction) with and without the addition of Fe_2O_3.

A sequence of experiments similar to those described in section 4.2.2.3. to determine whether the Fe_2O_3 was consistently active throughout the chlorination of a crystal, was carried out using a mixture of annealed crystals and Fe_2O_3. The mixture was reacted to completion in HCl only, volatilising Fe_2O_3 as $FeCl_3$. Hydrogen was admitted at this point and the mixture reacted to approximately 10% where a sigmoid curve was obtained. The apparatus was evacuated at the reaction temperature and HCl readmitted. The mixture reacted to 11% in 60 min. The results are shown in Figure 17.

The sigmoid rate curve suggests that some of the Fe_2O_3 had gone into solution in the crystal surface and was catalytically active. Neither the residual Fe_2O_3 nor the original

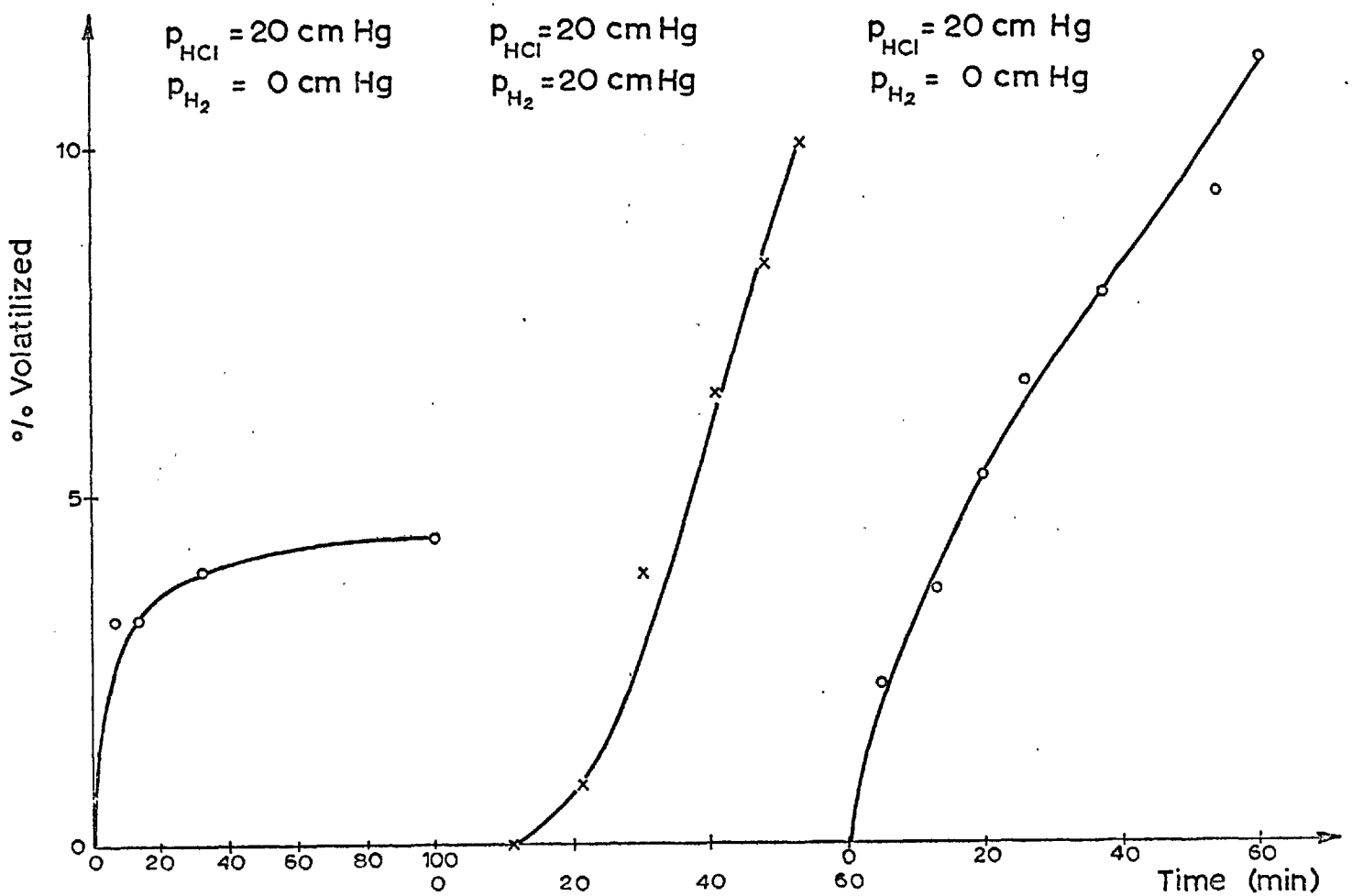

Fig. 17 Effect of Fe_2O_3 on reaction of annealed SnO_2 in successive mixtures of HCl and H_2/HCl. 500°C.

annealing inhibited the HCl only reaction, immediately after reaction in H_2/HCl.

4.2.3.4. Effect of varying the percentage of Fe_2O_3.

Experiments were performed on annealed crystals at 550°C in which both the proportion of Fe_2O_3 and the hydrogen pressure were varied. The results given in Figure 18 show that increasing the proportion of Fe_2O_3 causes increased catalysis. In order to determine whether catalysis required only a very small amount of Fe_2O_3 which is not used up or alternatively is regenerated, an attempt was made to uniformly distribute a trace of Fe_2O_3 over the surface of the SnO_2 crystals and to react the mixture thus obtained. To approximately 0.1g SnO_2 crystals was added 1 ml of $Fe(NO_3)_3$ solution containing the equivalent of 0.05g Fe_2O_3. This was evaporated to dryness and heated to 550°C to decompose the nitrate; in reaction with H_2/HCl there was no sign that the 0.05% Fe_2O_3 had any catalytic effect (see Appendix p145 for detailed results).

4.2.3.5. Reaction with SnO_2 and physically separate Fe_2O_3.

It was considered possible that the mechanism of catalysis involved some gaseous intermediate e.g. $FeCl_3$; physical separation of the two solid phases, while reducing the catalytic effect to some extent, should still render the latter discernible if a gaseous compound is involved.

Accordingly, experiments were performed with the Fe_2O_3

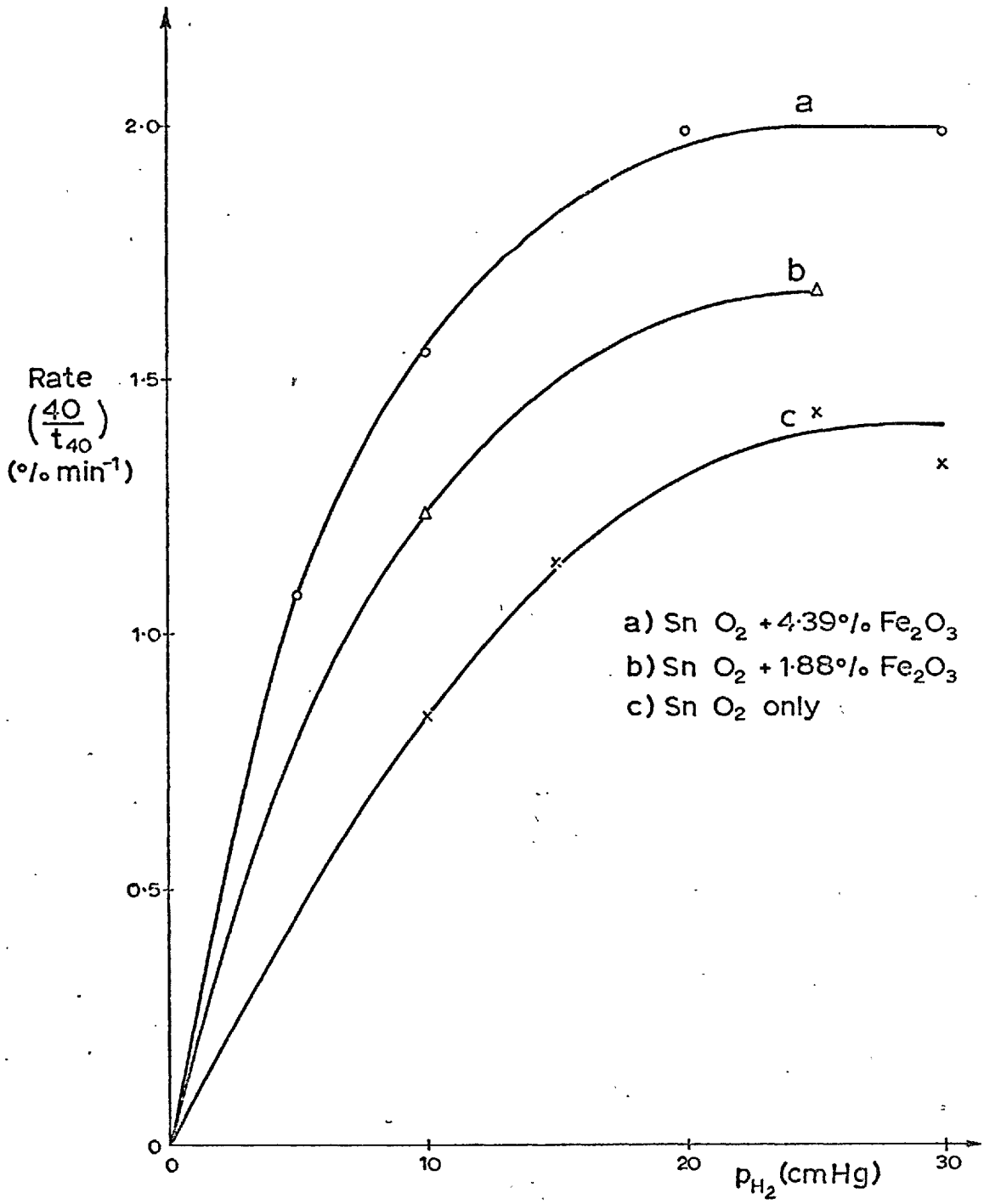

Fig. 18 Effect of variation in amount of Fe_2O_3. 550°C.

out of contact with the SnO_2 in the sample holder described in Figure 3, section 3.1.1. These gave reaction rates comparable to those for SnO_2 only and examination of the residue showed that the ferric oxide had been converted to ferrous chloride (Appendix p147).

As any gaseous compound had good opportunity of contact with the SnO_2 substrate and as no catalytic effect was observed, it may be concluded that the mechanism of catalysis does not involve a gaseous intermediate with an appreciable lifetime.

4.2.3.6. Effect of Fe_2O_3 on reduction of SnO_2 by H_2.

It has been suggested in preceding sections that the rate-controlling step in the reaction of SnO_2 in H_2/HCl is one of reduction by H_2. Thus any mechanism of catalysis must either increase the rate of this reduction or alternatively provide a completely new route for reaction. Iron metal produced by hydrogen reduction of its oxides is widely used as a heterogeneous catalyst in reduction reactions by H_2;[44] this is due to the ability of the metal, so produced, to chemisorb H_2, simultaneously activating it by dissociation. It was thus considered pertinent to determine whether the presence of Fe_2O_3, as intimately mixed as possible, would appreciably catalyse the reduction of solid SnO_2.

Accordingly, experiments were performed in which annealed crystals, with and without 4.39% Fe_2O_3, were reacted in H_2 at 550°C. The SnO_2 crystals alone did not react at a measurable rate at this temperature (less than 1% in 7ks) but

the presence of Fe_2O_3 caused approximately 22 and 17% reduction to tin in 9.6 ks in 25 and 10 cm Hg of H_2 respectively. Clearly Fe_2O_3 causes marked catalysis of the reduction of SnO_2 to Sn.

The rate curve, 3, given in Figure 19, shows certain discontinuities but as the experiment was not repeated, it is not possible to state that these discontinuities represent a real effect. However, it is possible, though unlikely, that these may be explained by the film of liquid tin produced denying access to the SnO_2 substrate by the H_2 until the film agglomerates or by lack of sensitivity of the suspension system. Reaction of Fe_2O_3 alone in H_2 at 550°C has shown that it is completely converted into iron metal.

4.2.3.7. Effect of other metal oxides on the reaction of annealed crystals in H_2/HCl.

As the presence of Fe_2O_3 catalysed the reduction of SnO_2 by H_2, it was thought that the catalysis observed in the reaction of SnO_2 in H_2/HCl was similarly produced. In this case a small quantity of iron metal would be required to account for the rectilinear portions observed in the catalysed reaction rate curves; eventually this iron would be converted to ferrous chloride by reaction with HCl. Owing to the difficulty of detecting in situ what need only be a small amount of elemental iron, it was decided to test the above hypothesis by analogy. A number of SnO_2/metal oxide mixtures were prepared as described in section 3.4.1.; these metal oxide additives were selected on the basis of whether they could be reduced to metal, under the

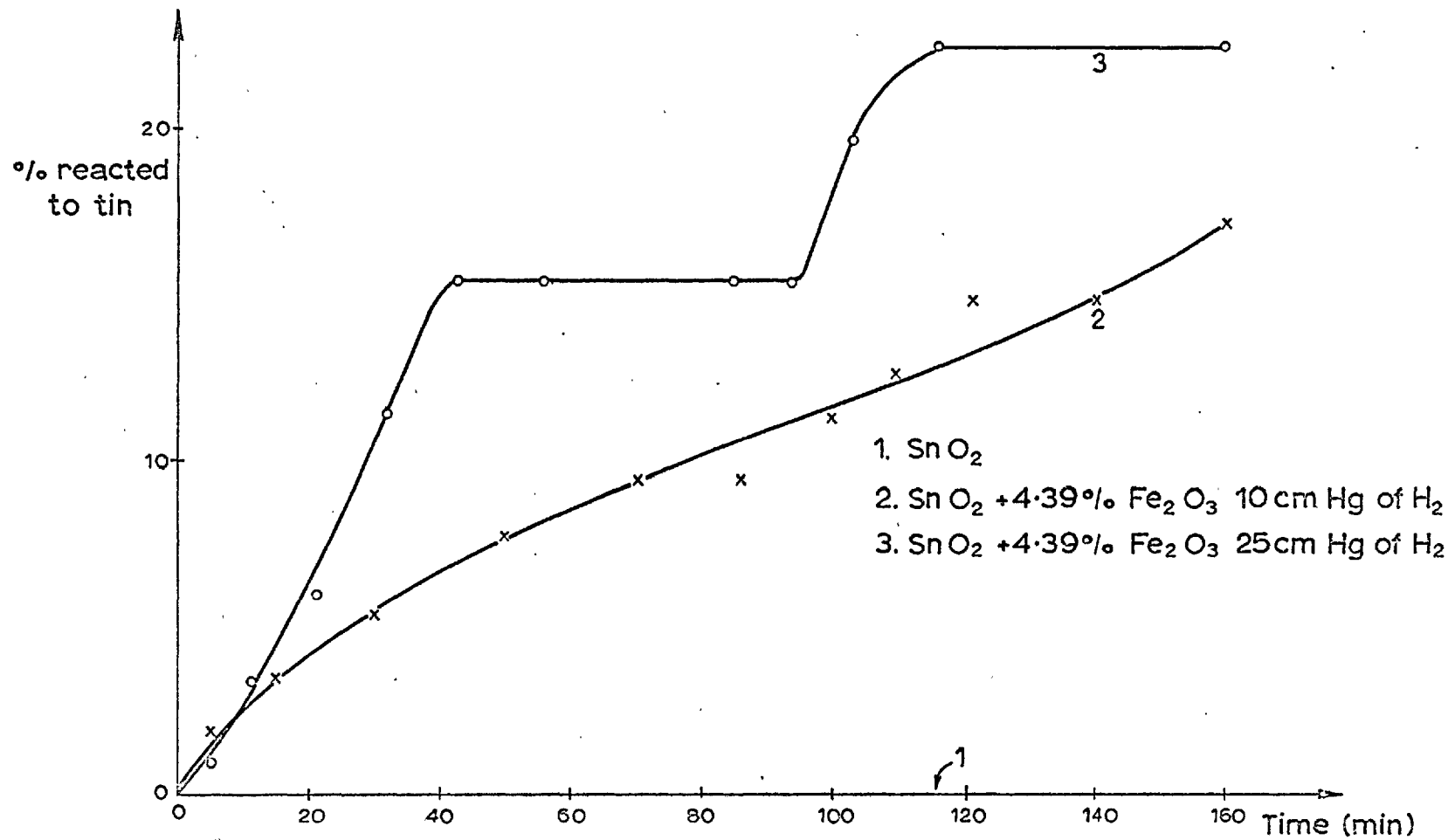

Fig. 19 Effect of Fe_2O_3 on reduction of $Sn\ O_2$ by H_2 at 550°C.

prevalent reaction conditions, no matter how transient the metallic species, and whether the latter were capable or not of chemisorbing H_2.

The mixtures of annealed SnO_2 crystals and 4.74% metal oxides were reacted at 550°C in P_{HCl} = 20 cm Hg and P_{H_2} = 10, 25 cm Hg. The additives used were: NiO, Co_3O_4, Pt, MoO_3, V_2O_5, TiO_2, CuO, PbO, Ag_2O, Ta_2O_5, Nb_2O_5 and WO_3. These additives were also reacted alone at 550°C in $P_{HCl} = P_{H_2}$ = 20 cm Hg (Appendix p159) and they remained effectively constant in mass.

The addition of NiO, Co_3O_4, Pt, MoO_3, V_2O_5 and TiO_2 resulted in sigmoidal rate curves and marked catalysis; the mixtures containing CuO, PbO, Ag_2O and Ta_2O_5 reacted at rates comparable to that for SnO_2 only. WO_3 caused some initial retardation of reaction but thereafter reacted as SnO_2 whilst the mixture with Nb_2O_5 exhibited an induction period of approximately 2.4ks in P_{H_2} = 25 cm Hg and did not react (in 6.6ks) in P_{H_2} = 10 cm Hg (Appendix 152). The rate curves for SnO_2 only, SnO_2 -Pt and SnO_2 -Nb_2O_5 are shown in Figure 20.

For catalysis to involve the chemisorption of H_2 it is usually necessary for the oxide to be reduced to metal. This is possible for NiO, Co_3O_4, MoO_3, CuO, PbO and Ag_2O and marginally for WO_3; Pt is already present in metallic form. V_2O_5, TiO_2, Ta_2O_5 and Nb_2O_5 cannot be reduced to metal. The complete results are presented in Table 2.

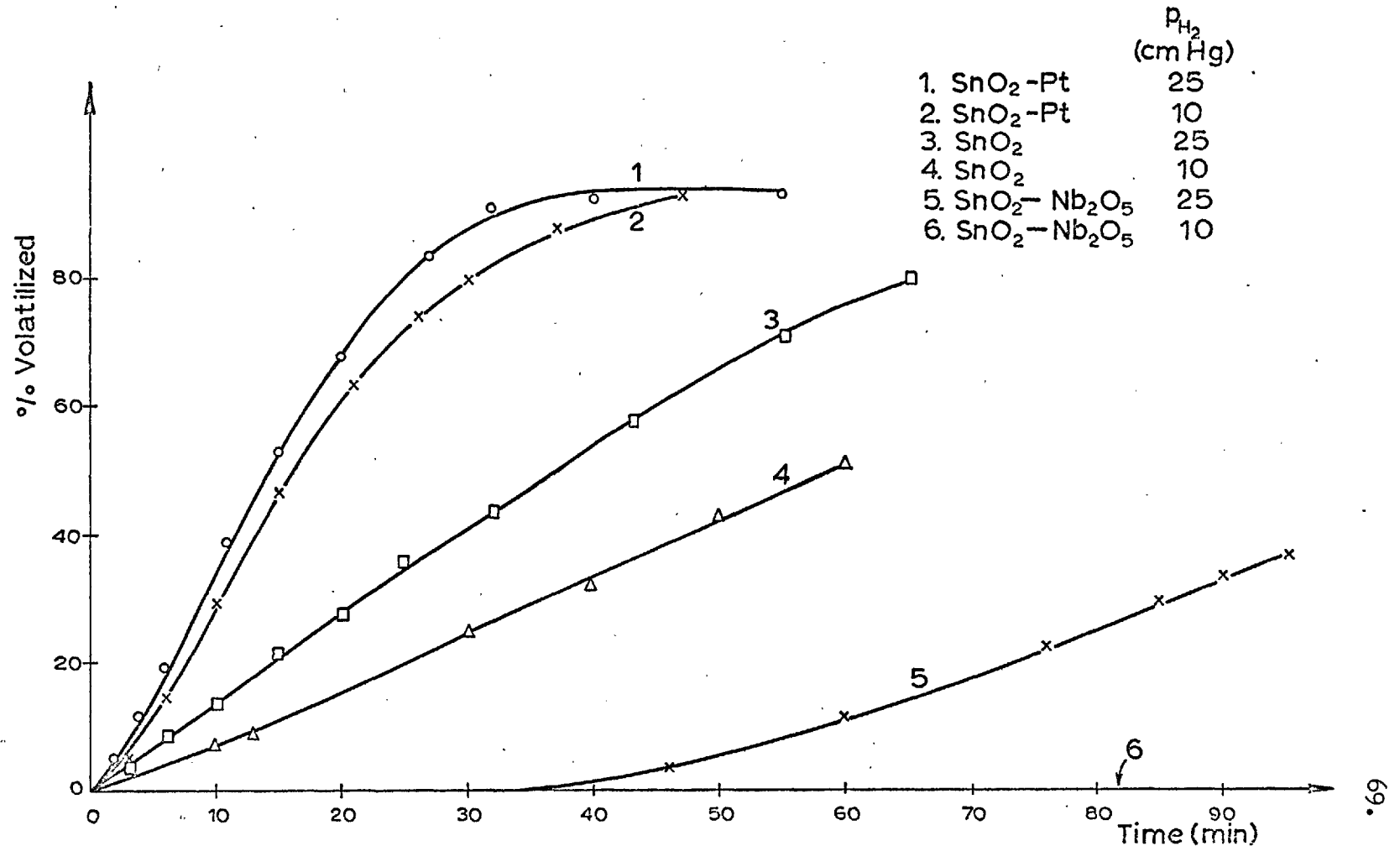

Fig. 20 Effect of Pt, Nb_2O_5 on the H_2/HCl reaction at 550°C.

Table 2. Effects of synthetic additives on the reaction of SnO_2 in H_2/HCl.

Additive	Std. free energy of reduction to metal by H_2. at 550°C kcal/mole H_2	Dissociative chemisorption of H_2 by metal [45]	Shape of reaction curves	Rate of reaction (% sec^{-1})	
				P_{H_2}=10 cm Hg	P_{H_2}=25 cm Hg
SnO_2	+ 2.1	NO	Normal	1.4×10^{-2}	2.4×10^{-2}
Fe_2O_3	+ 0.3	YES	Sigmoid	2.6×10^{-2}	
NiO	- 8.6	YES	Sigmoid	4.4×10^{-2}	6.7×10^{-2}
Co_3O_4	-14.8	YES	Sigmoid	1.9×10^{-2}	6.7×10^{-2}
MoO_3	- 4.2	YES	Slightly sigmoid	2.3×10^{-2}	3.9×10^{-2}
Cu_2O	-21.6	NO	Normal	1.3×10^{-2}	
Ag_2O	-42.7	NO	Normal		1.7×10^{-2}
PbO	- 9.7	NO	Normal	1.3×10^{-2}	
WO_3	+ 1.8	YES	Sigmoid	1.6×10^{-2}	2.2×10^{-2}
V_2O_5	+ 9.9	YES	Sigmoid	2.8×10^{-2}	5.1×10^{-2}
TiO_2	+46.9	YES	Sigmoid	2.8×10^{-2}	4.9×10^{-2}
Ta_2O_5	+32.4	YES	Normal		1.6×10^{-2}
Nb_2O_5	+25.8	YES	Induction period	Approx. 0	1.3×10^{-2}
Pt	-	YES	Sigmoid	5.8×10^{-2}	6.7×10^{-2}

Of the oxides which can be reduced to metal, only those which can chemisorb H_2 catalyse the reaction. V_2O_5 can only be reduced as far as VO; this lower oxide resembles a metal by virtue of its high density of point defects and could thus

chemisorb H_2 into lattice vacancies[46]. TiO_2, on the other hand, cannot be reduced by H_2 at 550°C, though the lower oxides are similar to VO in their non-stoichiometry.[47] Clearly the action of TiO_2, Nb_2O_5 and WO_3 must be explained by reference to other factors.

4.2.4. Electron spin resonance of SnO_2 and reacted SnO_2/Fe_2O_3 mixtures.

If the production of iron metal is postulated as an intermediate step in the catalytic mechanism, then the process may occur either inside or outside the SnO_2 crystal matrix. It has been shown in section 4.1. that catalysis by iron compounds within a particular grain of cassiterite occurs only within strictly defined regions i.e. the catalytic intermediate is not very mobile. It is thus more probable that catalysis takes place by a process within the SnO_2 lattice. If this is so, then differences in the state of the residual iron present in the SnO_2 crystals, at various stages in their reaction treatment, should be detected by e.s.r. methods.

Accordingly, four specimens were prepared for e.s.r. analysis which was performed by Dr. T.I. Barry of the National Physical Laboratory. These were:

1) Annealed crystals which were supposedly iron-doped (these had reacted at rates as for SnO_2 only. cf. section 3.3.4.).
2) Annealed crystals +4.39% Fe_2O_3, heated to and kept at 550°C for 3.6ks.

3) Annealed crystals +4.39% Fe_2O_3, reacted in H_2/HCl at 550°C.

4) Annealed SnO_2 +4.39% Fe_2O_3, reacted in H_2 at 550°C.

In all cases the excess iron oxide was removed in aqueous concentrated HCl.

The following interpretation was made by Dr. Barry of the spectra shown in Figures 21-23. An explanatory diagram is given in Figure 24. The spectra from specimens 1-3 were rather complex while specimen 4 could not be tuned in the e.s.r. cavity, probably because of the presence of a ferromagnetic phase.

Specimens 1 and 2 were basically the same; each contained Fe^{3+} as individual ions in at least four sites and in addition a broad resonance arising from magnetically coupled groups of paramagnetic ions which were probably Fe^{2+} or Fe^{3+}.

The four types of spectra from individual Fe^{3+} ions are characterised by the ratio of the strength of the orthorhombic crystal field to the axial crystal field. This ratio is denoted $E' = E/D$. The intensities of the four types are different in the two specimens and, in Table 3 values are given for E', for the intensity ratio I_1/I_2, and for the fields of the various transitions expressed as fractions of the applied magnetic field, Ho (= 3308 gauss). X,Y and Z are the crystal axes.

Fig. 21 E.S.R. spectrum $Sn O_2$ (1).
Total attenuation = 33 db = factor of 45.

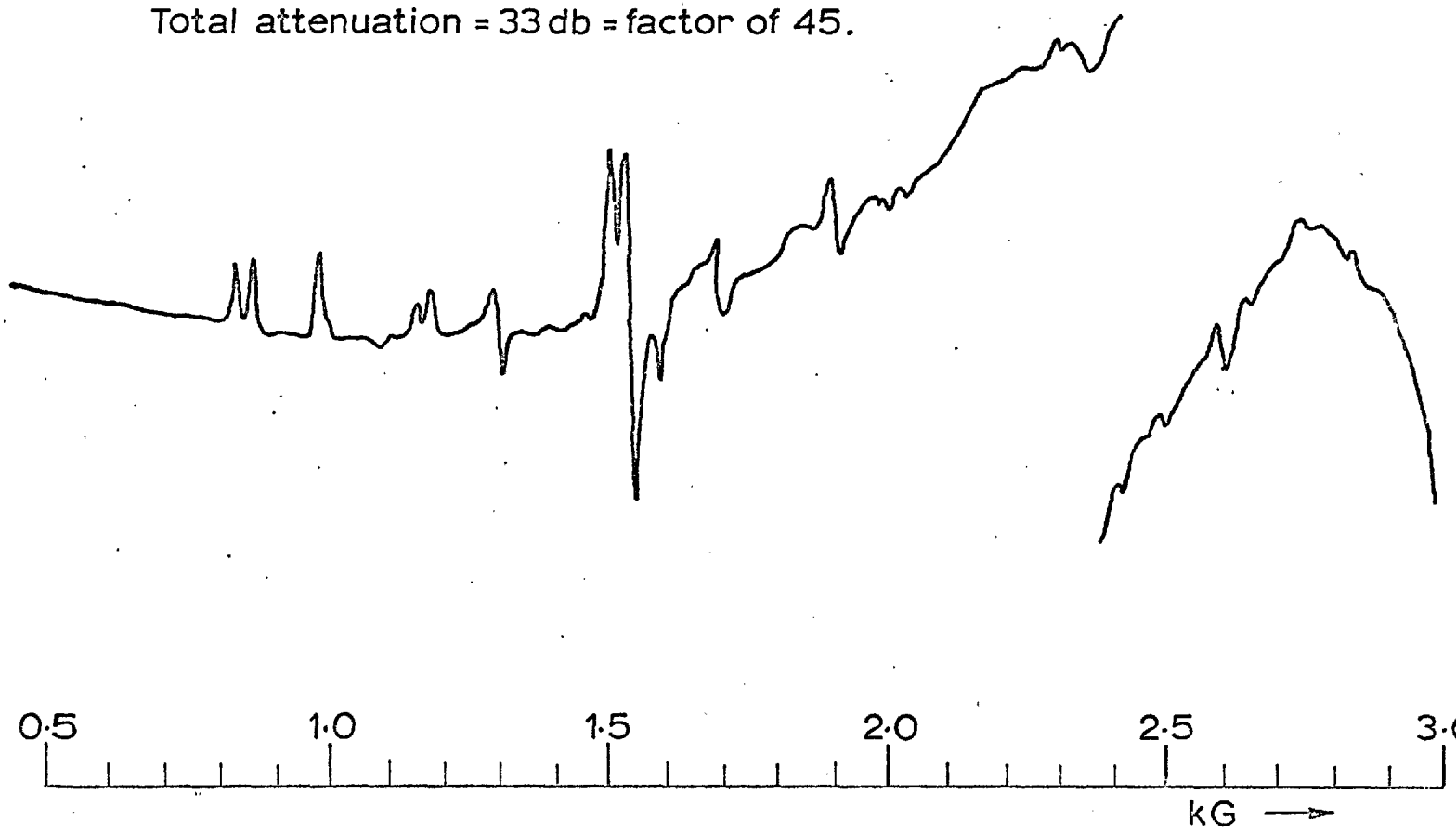

Fig. 22 E.S.R. spectrum $Sn O_2$ (2).
Total attenuation = 33db = factor of 45.

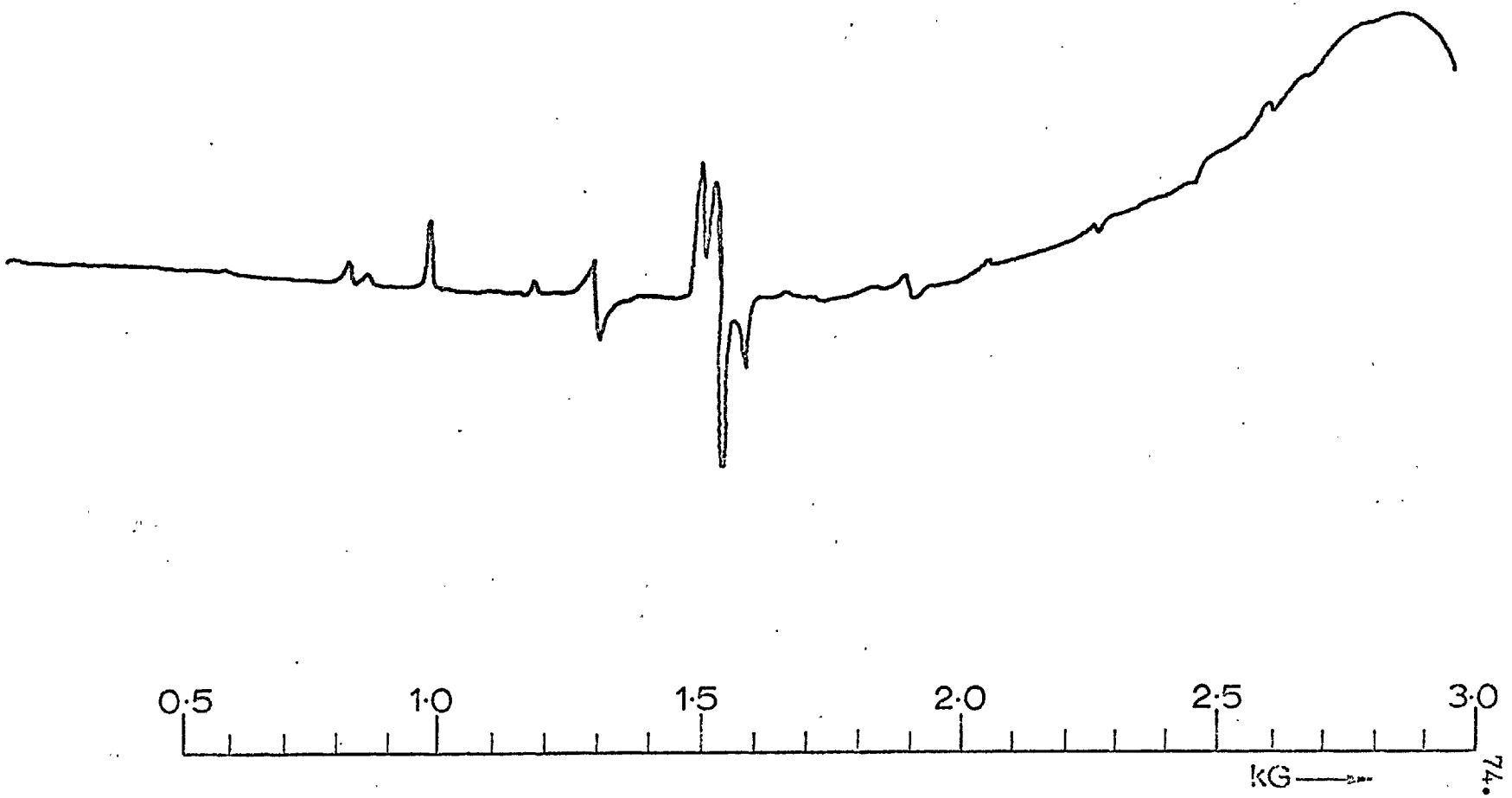

Fig. 23 E.S.R. spectrum $Sn O_2$ (3).
Total attenuation 33 db.

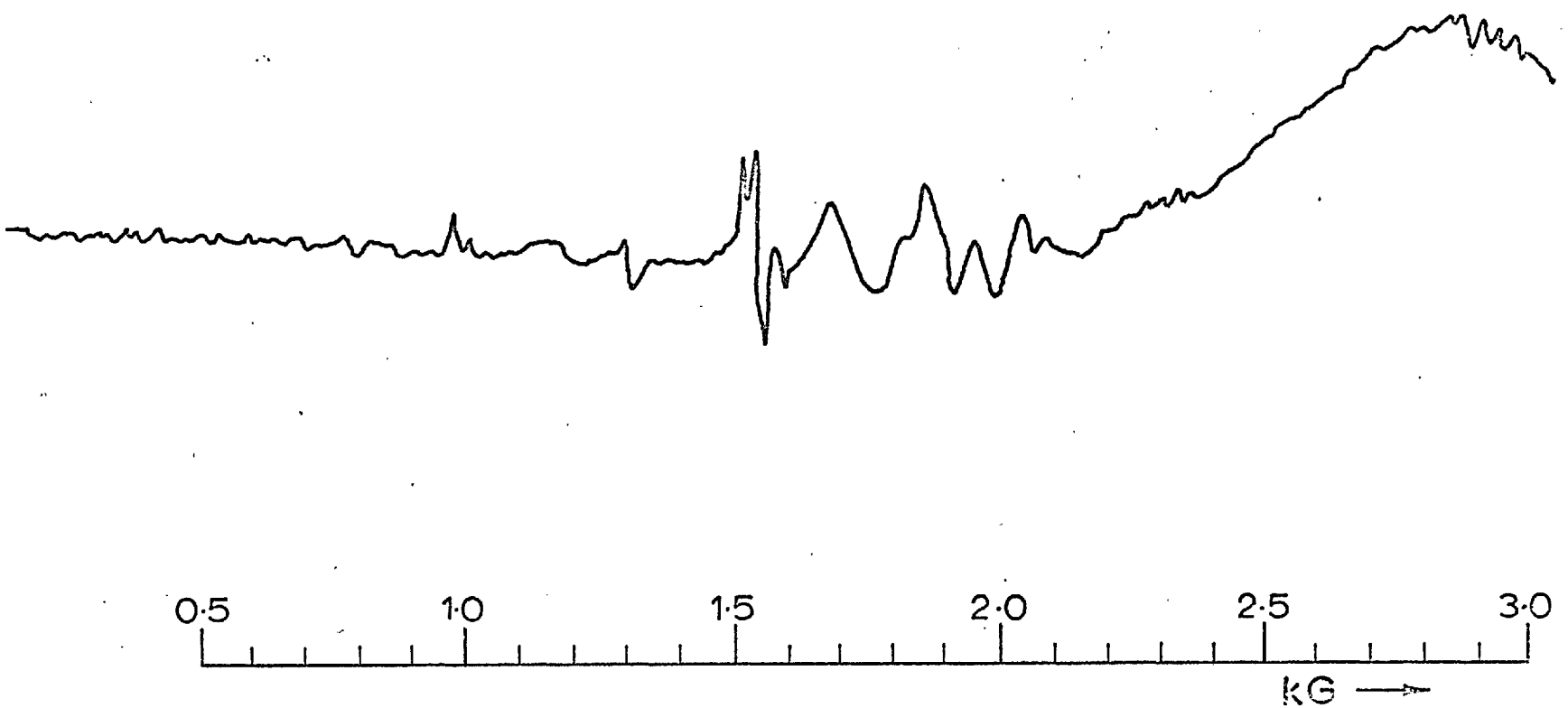

Fig. 24 E.S.R. spectra. Explanatory diagram.

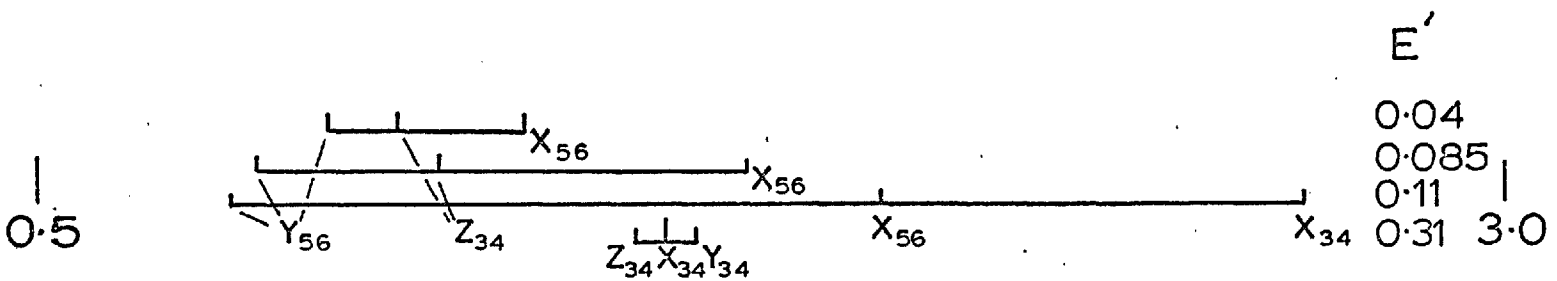

Table 3. E.S.R. transitions of specimens 1 and 2

E'	0.04	0.085	0.11	0.31
I_1/I_2	1	7	3	1*
Y_{5-6}	0.293	0.256	0.247	
Z_{3-4}	0.336	0.348	0.356	0.456
X_{5-6}	0.393	0.519	0.579	
X_{3-4}			0.795	0.467
Y_{3-4}				0.482

* Dr. Barry states that at 77°K the centres with E' = 0.31 saturate easily and that this distinguishes them from centres with E' = 0.04 which have a similar value for I_1/I_2.

The centre with E' = 0.11 has a spectrum closely similar to that of Fe^{3+} in rutile, so that this centre is probably substitutional as in rutile.[48]

Specimen 3 has the same spectrum as 2 but with additional complex features. Amongst others there are broad peaks at 1170, 1710 and 1880 gauss and two groups of five narrowly spaced peaks centred at about 2300 and 2900 gauss. These additional features complicate the spectrum and it is not amenable to interpretation. One considered possibility, which unfortunately does not fit the data, is that the HCl treatment may have produced Fe^{3+} centres compensated by Cl^- in anion sites. However, the major Cl^- isotope has a nuclear

spin of 3/2 which would give rise to a four line hyperfine splitting, not a five line splitting as was observed.

The Fe^{3+} content is less than 100 p.p.m. and specimens 1-3 do not differ by orders of magnitude in this respect.

Even though the interpretation of these data remains vague, the possible presence of elemental iron in specimen 4 and the fact that the other three specimens differ in both the amount and state of their iron content, lends support to the hypothesis that the mechanism of catalysis involves some change in the iron species present within the SnO_2 crystal.

4.2.5. Effect of iron-bearing minerals on the reaction of annealed crystals.

Iron occurs in various compounds with which cassiterite is commonly associated; it was decided to simulate naturally occurring cassiterite by investigating the effect of the presence of a wide variety of iron-bearing minerals on the reaction of annealed crystals.

Samples of SnO_2 mixed with 10% of various iron minerals were reacted at 550°C in P_{HCl} = 20 cm Hg and P_{H_2} = 10,25 cm Hg. The minerals used were: hematite, magnetite, pyrite, columbite, biotite and ilmenite. They were in the size-range 75-150 μm (see section 3.4.2.).

Hematite, magnetite, ilmenite and pyrite catalysed the reaction giving sigmoidal rate curves, although the degree of catalysis was much less than observed when using synthetic

Fe_2O_3. Columbite and biotite retarded the reaction though not as much as when synthetic Nb_2O_5 was present. Microscopic examination of the residues showed that the hematite, magnetite, ilmenite and pyrite had reacted but there was no clear evidence that the columbite and biotite had changed (cf. Appendix p174).

The occurrence of catalysis is coincident with the capacities of the minerals concerned to be reduced to metal under the prevalent reaction conditions.

4.2.6. Odegi cassiterite - effect of Fe_2O_3.

The annealed crystals used reacted at a faster rate than that obtained with natural cassiterite (see section 4.2.1.) i.e. there was a greater incidence of crystal imperfections in the synthetic material. As the catalytic process might proceed via some modification to these imperfections by the iron compounds it was decided to investigate the degree of catalysis by Fe_2O_3 when using crystals relatively free of imperfections i.e. natural cassiterite.

A primary cassiterite from Odegi in Nigeria in the size-range 75-105 μm was reacted in H_2/HCl at 600°C both with and without 4.39% Fe_2O_3. From the results shown in Figures 25 and 26, it will be seen that Fe_2O_3 produces sigmoidal rate curves and catalyses the reaction, the rate being taken from the slopes after the accelerating period as with synthetic SnO_2. The increase in rate is of the order of 100% compared with approximately 150% when synthetic crystals were used.

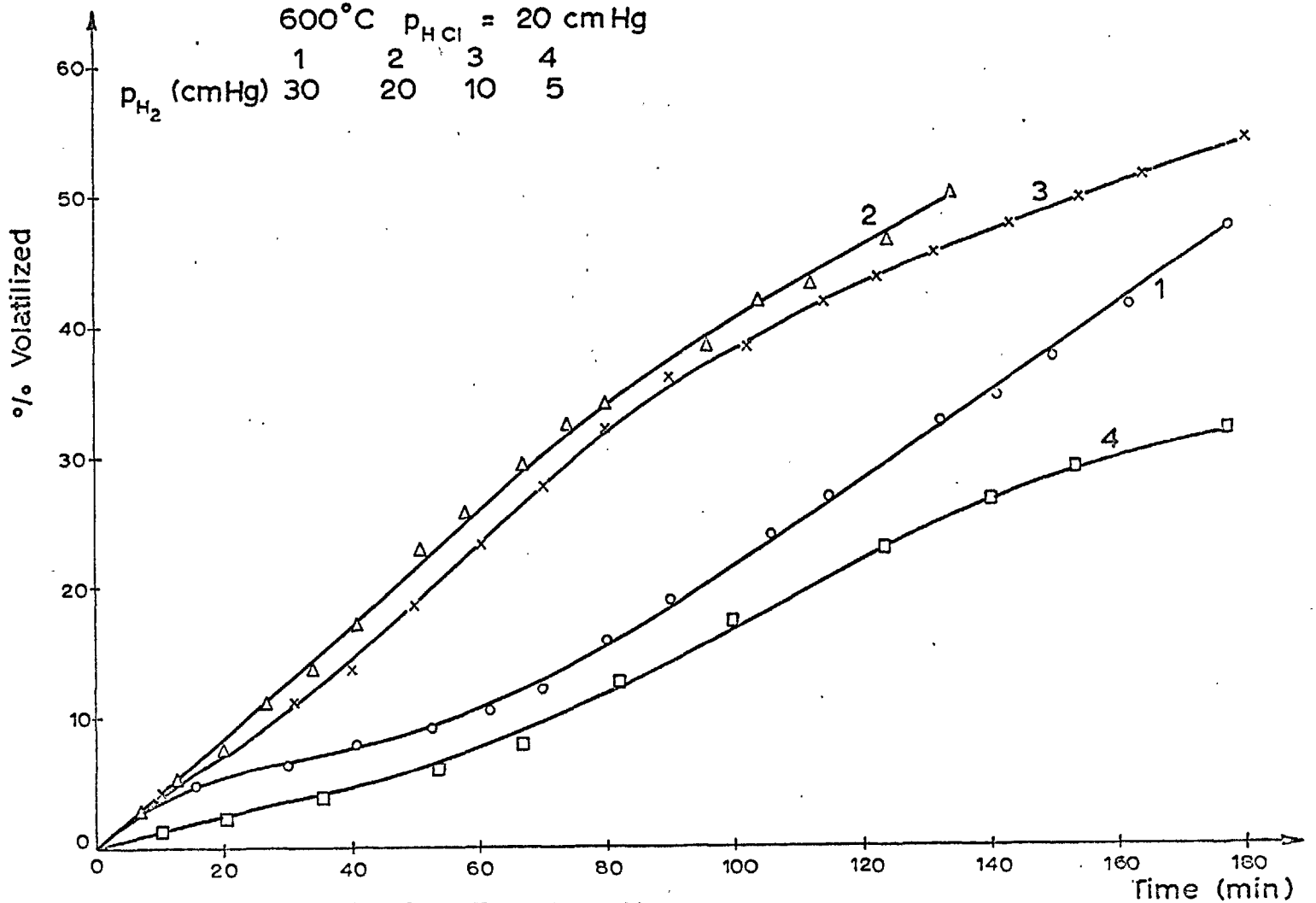

Fig. 25 Odegi Cassiterite. Effect of H_2 pressure.

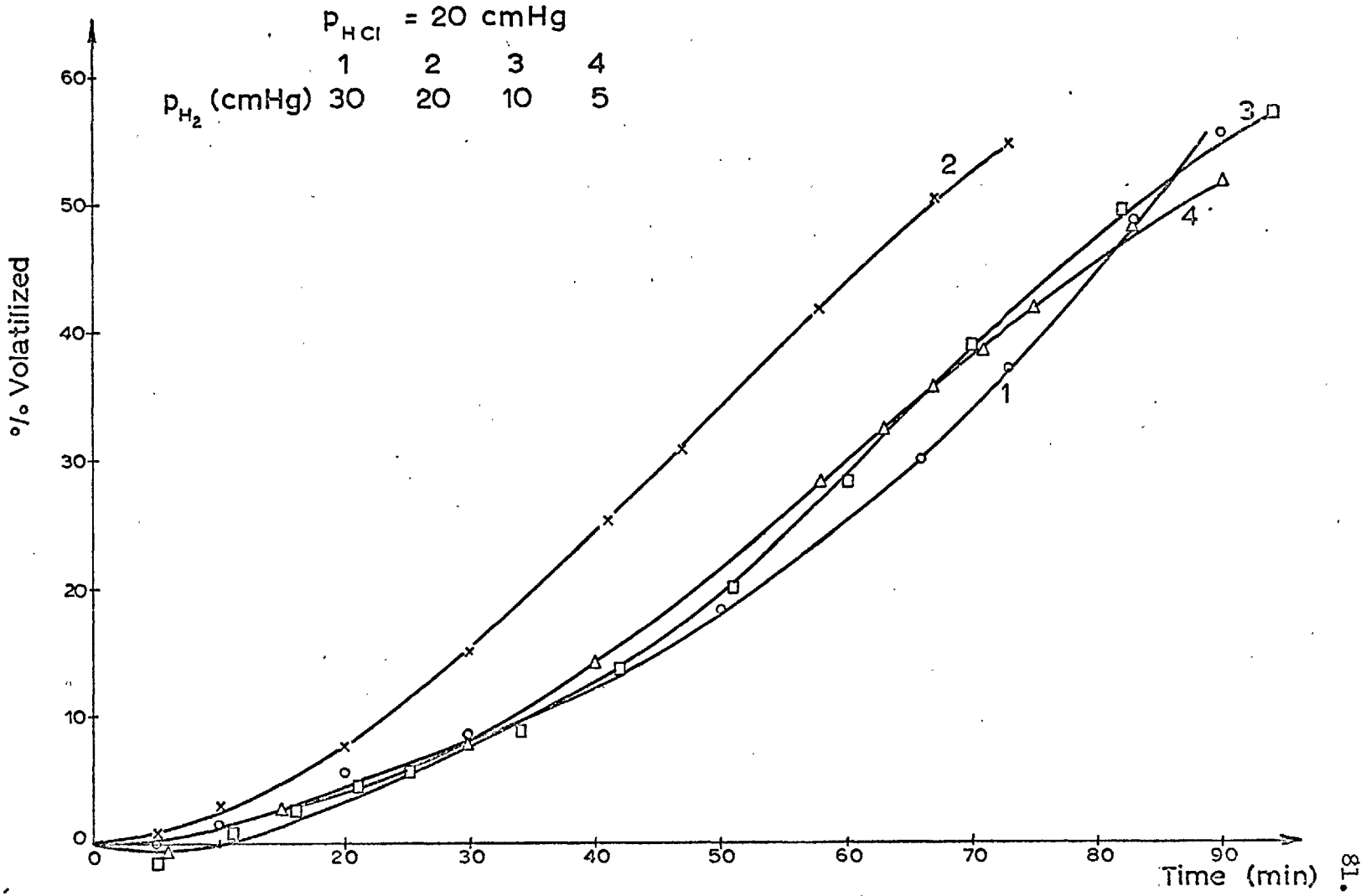

Fig. 26 Odegi Cassiterite. Effect of Fe_2O_3 at 600°C.

4.2.7. The reaction of annealed SnO_2 in CO/HCl.

Another possible method of effecting volatilisation of $SnCl_2$ from SnO_2 is to use CO as the reductant instead of H_2, again using HCl as the chlorinating agent. This reaction has been investigated by Nieuwenhuis[31] using a low-grade tin concentrate containing approximately 5% Sn, 1.25% Fe and 68% SiO_2; a summary of his results has been given in section 2.5. As stated in that section, he found that the rate of volatilisation of $SnCl_2$ was proportional to the HCl concentration and independent of the CO pressure. Conducting the reaction between 700 and 800°C, he also found that the rate increased with decreasing $CO:CO_2$ ratio (above the value 0.061). As this dependence on HCl pressure and not on reductant pressure seemed to be at variance with the results described here, it was decided to investigate this reaction in a similar manner to the H_2/HCl reaction using synthetic SnO_2 and various additives.

4.2.7.1. Kinetics of reaction of SnO_2 alone.

Annealed SnO_2 crystals were reacted at 700°C in various CO/HCl mixtures; all the rate curves were sigmoidal and some are shown in Figure 27; the incipient induction period indicates the build-up of some reaction intermediate. It may be seen from the results shown in Figure 28 (1, 2) that the reaction is first order with respect to HCl and is not a function of P_{CO}; this corroborates the findings of Nieuwenhuis(31).

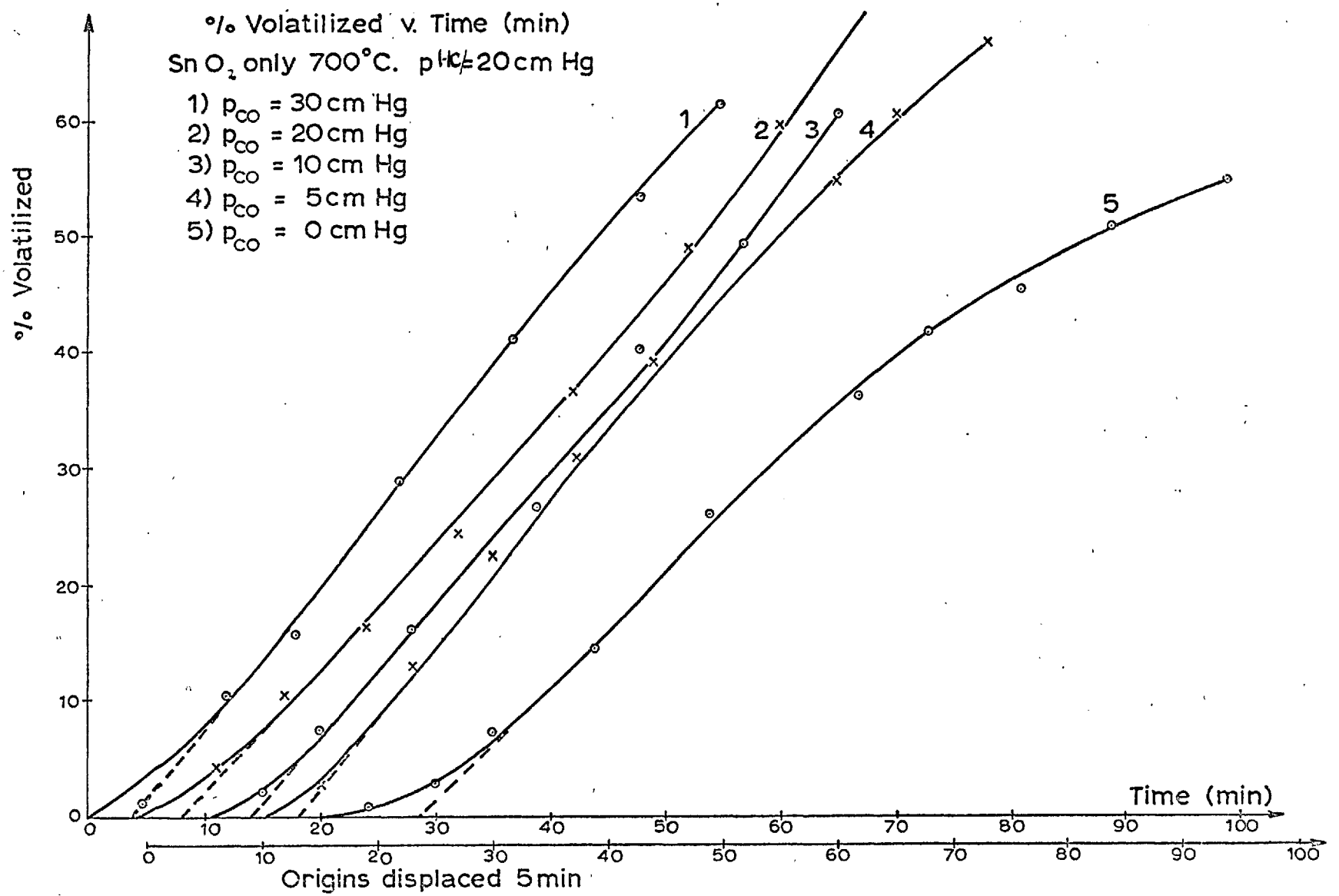

Fig. 27 Effect of p_{CO}. 700°C. Annealed crystals and CO/H Cl.

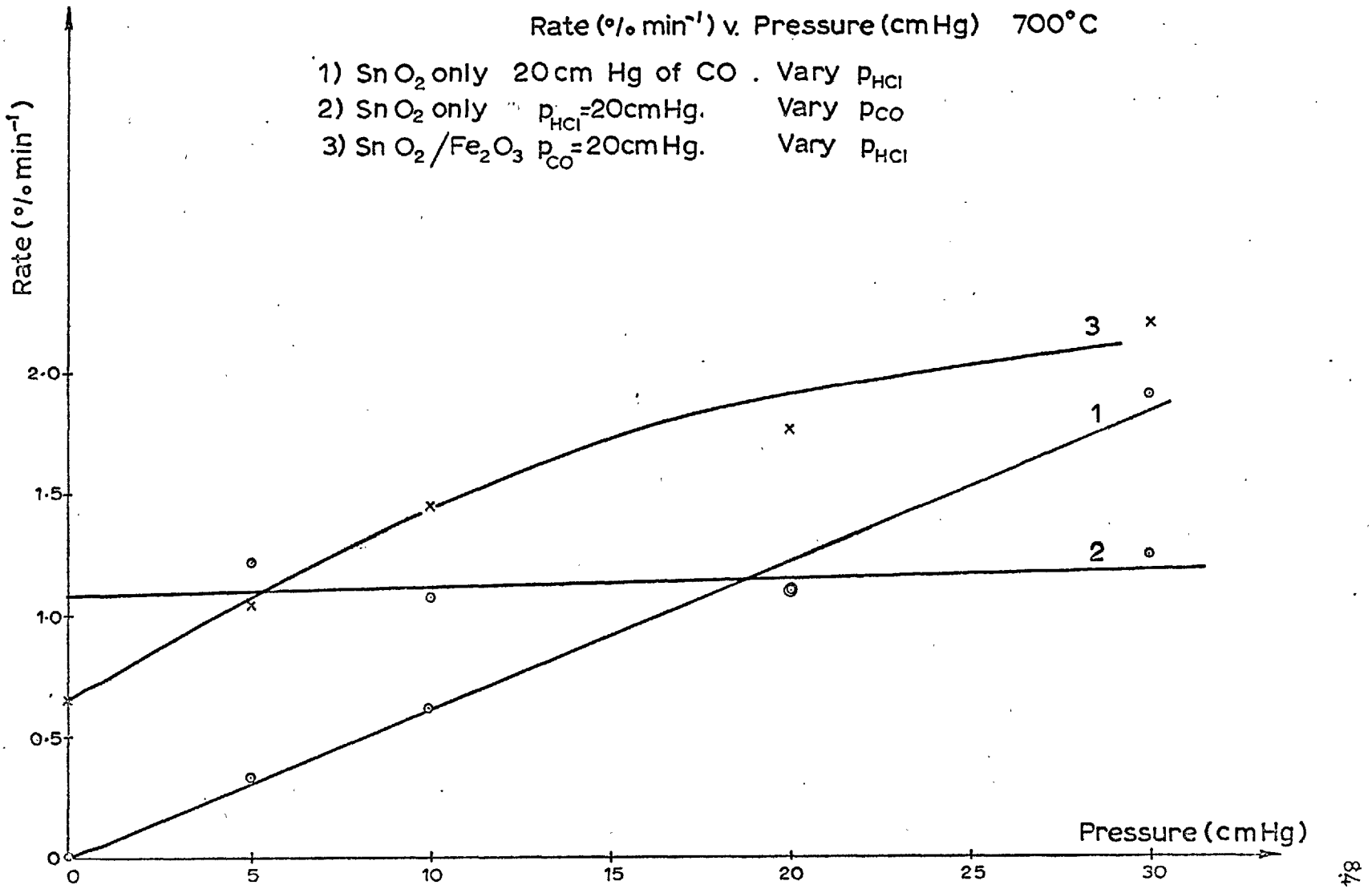

Fig. 28 Effect of p_{CO} and p_{HCl}. Annealed crystals. 700°C.

4.2.7.2. Effect of Fe_2O_3 on the CO/HCl reaction.

SnO_2/Fe_2O_3 mixtures were reacted in CO/HCl at 700°C and various P_{HCl}. The rate curves were markedly less sigmoidal than those obtained in the absence of Fe_2O_3 and are shown in Figure 29. Inspection of the results given in Figure 28, (1, 3) shows that the presence of Fe_2O_3 causes marked catalysis. These results indicate that Fe_2O_3 accelerates the production of the reaction intermediate which gave rise to the sigmoidal rate curves obtained in section 4.2.7.1.

As curve 2 in Figure 28 has a finite value of rate at $P_{CO} = 0$ there must be a reaction with HCl only (this was also observed at 600°C with the H_2/HCl reaction). Similarly curve 3, but not curve 1, has a finite value of rate at $P_{HCl} = 0$, i.e. the reduction of SnO_2 is catalysed by Fe_2O_3 at 700°C. The reaction of reduced SnO_2 with HCl is expected to produce $SnCl_2$, but the reaction with HCl alone would produce $SnCl_4$. The addition of Fe_2O_3 is, therefore, expected to cause a change in the $SnCl_2$:$SnCl_4$ ratio in the products.

The effect of varying the CO pressure, in the presence of Fe_2O_3, was not investigated as the reduction step was not rate-controlling.

These results differ from those obtained when dealing with reaction in H_2/HCl as Fe_2O_3 now appears to catalyse a chlorinating step. Another difference is also found in that the presence of 4.74% Nb_2O_5 causes catalysis in CO/HCl (see Figure

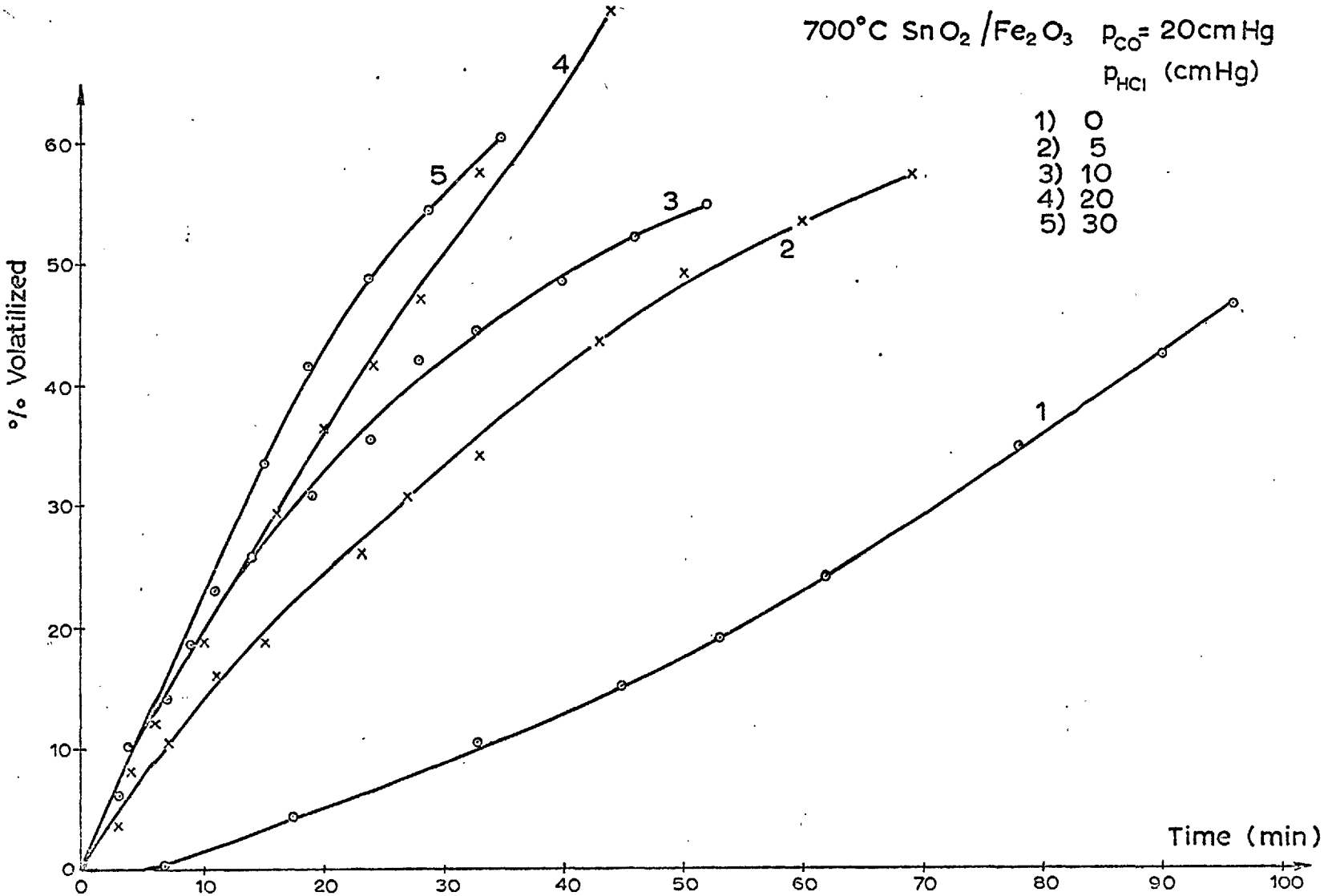

Fig. 29 Effect of Fe_2O_3 and p_{CO}. Annealed crystals. 700°C.

30) whereas it retarded reaction in H_2/HCl.

4.2.7.3. Effect of other metal oxides on reduction by CO.

As has been seen in section 4.2.7.2., Fe_2O_3 catalyses the reduction of SnO_2 in CO; this may have occurred via chemisorption of CO on reduced iron metal. It was decided to check by analogy whether the catalytic process was one of chemisorption. SnO_2 crystals admixed with 4.74% Pt, Nb_2O_5 or Bi_2O_3 were reacted in P_{CO} = 20 cm Hg at 700°C. Pt will chemisorb CO, Bi_2O_3 can be reduced to metal under the above reaction conditions but Bi will not chemisorb CO[45] and Nb_2O_5 cannot be reduced to metal at this temperature.

Inspection of the results shown in Figure 31 indicates that Fe_2O_3, Pt and Bi_2O_3 catalyse the reduction whereas Nb_2O_5 does not. The behaviour of Fe_2O_3, Pt and Nb_2O_5 in this reduction is similar to their effects on the reaction of SnO_2 in H_2/HCl. The hypothesis of chemisorption of CO as one step in the catalytic mechanism of the reduction of SnO_2 has not been conclusively demonstrated owing to the anomalous behaviour of Bi_2O_3.

4.2.7.4. Effect of CO_2 on reaction in CO/HCl.

Carbon dioxide as the oxidation product of CO might be expected to retard the rate of reaction of SnO_2 in CO/HCl if it is sufficiently near the temperature at which $\Delta G^o_T = 0$.

SnO_2 crystals were reacted at 700°C in $P_{CO} = P_{HCl}$ = 10 cm Hg, while varying the P_{CO_2}:P_{CO} ratio. The results,

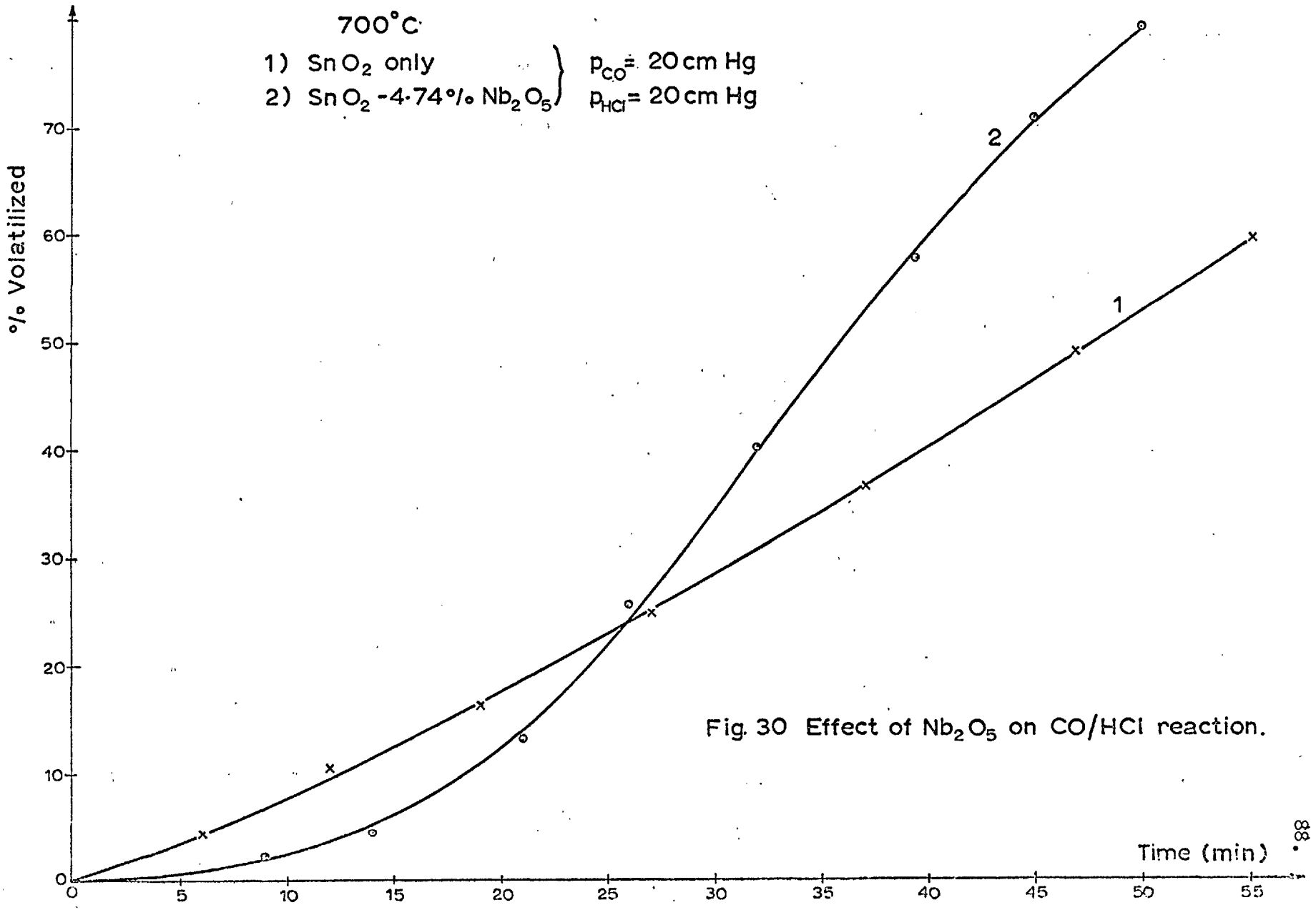

Fig. 30 Effect of Nb_2O_5 on CO/HCl reaction.

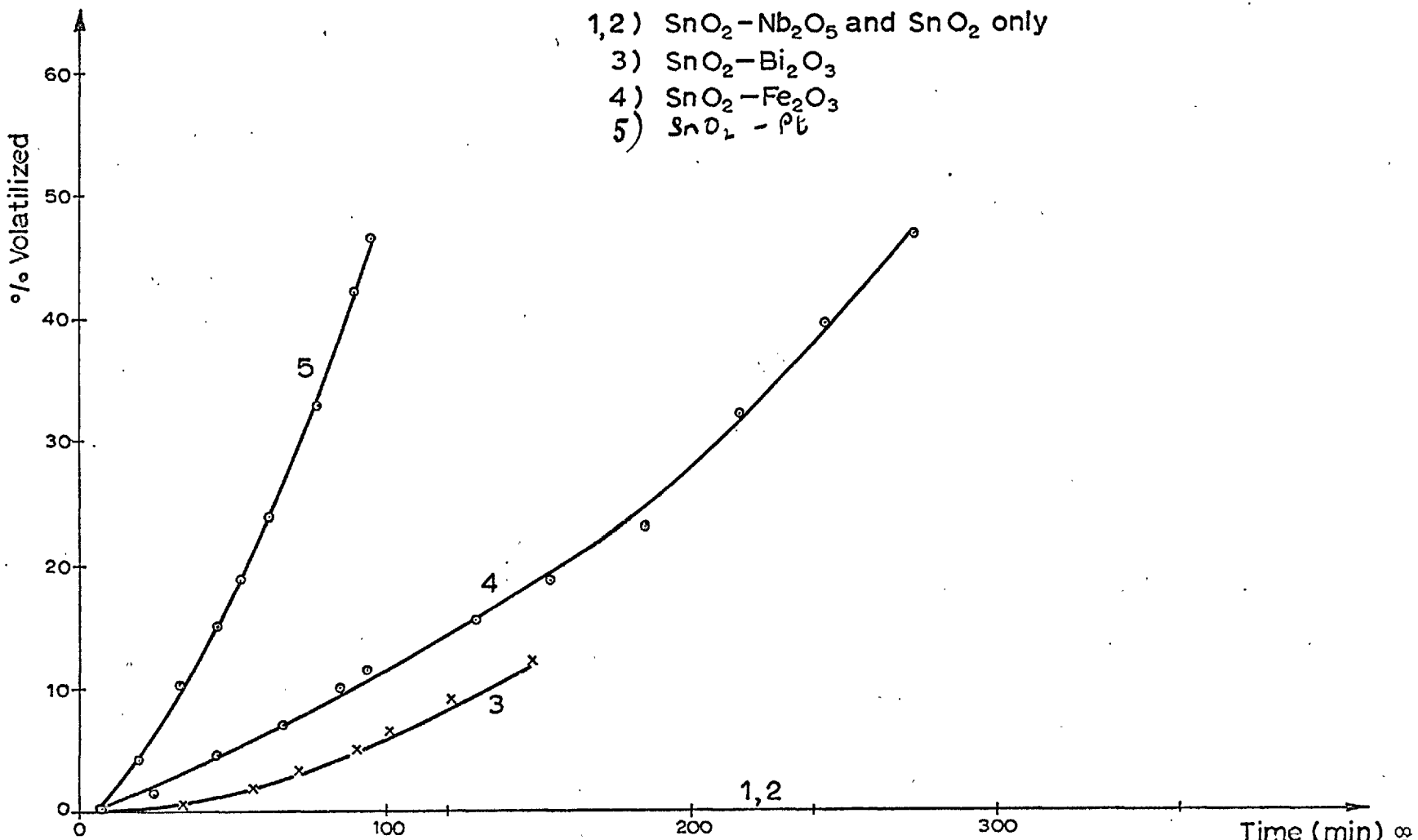

Fig. 31 Effect of additives on reduction of SnO_2 by CO at 700° C.

given in Figure 32, show that increasing the $P_{CO_2}:P_{CO}$ ratio retards the reaction. This result is at variance with that of Nieuwenhuis[31], who found that the reverse was the case above $P_{CO}:P_{CO_2} = 0.061$. This point is discussed further in sections 5.2. and 5.3.3.

4.3. Analysis of products.

A study has been made of the products of reaction of SnO_2 crystals in the following atmospheres: H_2/HCl; HCl; CO/HCl. As discussed in section 4.2.7.2. the results in Figure 28 suggest that the products of reaction in CO/HCl may change by addition of Fe_2O_3. Accordingly, analyses were made of the products of the following reactions at 700°C:

1) SnO_2 in H_2/HCl
2) SnO_2 in HCl
3) SnO_2 in CO/HCl
4) SnO_2/Fe_2O_3 in CO/HCl.

The reaction products were removed from where they had condensed in the cooler parts of the apparatus by dissolution in 50 ml A.R. concentrated HCl. The solution was made up to 250 ml with distilled water in a volumetric flask. 25 ml aliquots of the solution were added to 25 ml lots of acidified standard potassium dichromate solution; the residual dichromate was titrated against standard ferrous ammonium sulphate solution using diphenylamine as indicator. The pertinent equations are as follows:

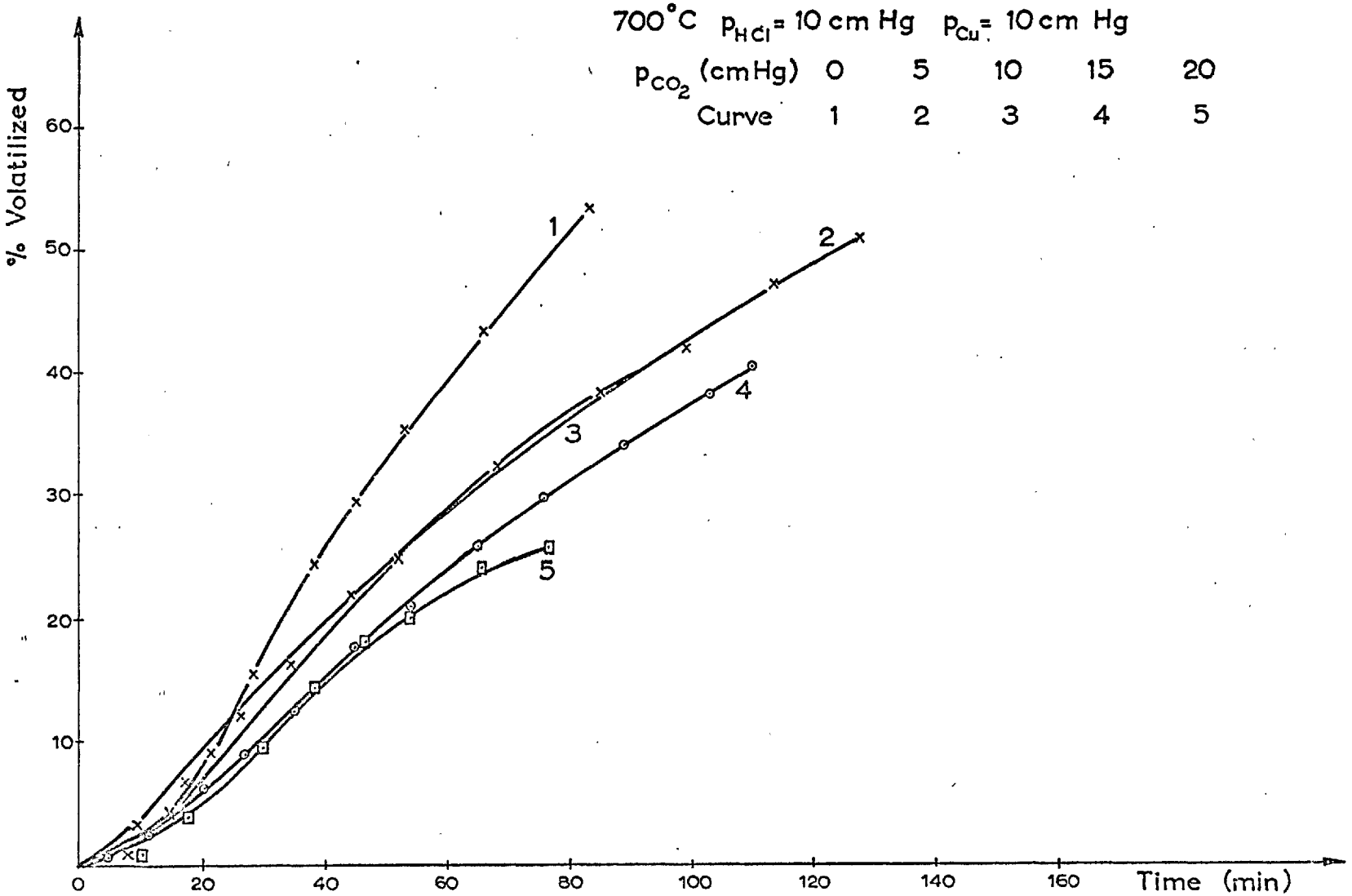

Fig. 32 Effect of CO_2 pressure on CO reduction of $Sn O_2$ at 700°C.

$3\ Sn^{2+} + Cr_2O_7^{2-} + 14H^+ = 3\ Sn^{4+} + 2Cr^{3+} + 7H_2O$

$6\ Fe^{2+} + Cr_2O_7^{2-} + 14H^+ = 6\ Fe^{3+} + 2Cr^{3+} + 7H_2O.$

Sn^{2+} was determined by the above method while the total tin content of the solution was analysed using atomic absorption spectrophotometry; a calibration curve had been drawn up using solutions of known amounts of A.R. tin in 2N.HCl. The results are shown in Table 4.

Table 4. Analysis of products.

Reaction	Sample wt. loss. mass	%	Sn(II) in condensate (% of original sample)	Total Sn in condensate (% of original sample)	Sn(II):Sn(IV)
SnO_2 in H_2/HCl	0.5568g	57.3	56.6	57.0	140
SnO_2 in HCl	0.1758g	23.5	<1.3	17.4	<0.08
SnO_2 in CO/HCl	0.1727g	20.8	3.6	13.7	0.36
SnO_2/Fe_2O_3 in CO/HCl	0.1100g	41.2	17.6	28.7	1.59

Within the limits of analysis, Table 4 shows that reaction with H_2/HCl yields only Sn(II) and with HCl alone yields only Sn(IV). The actual products are presumably $SnCl_2$ and $SnCl_4$. The product from reaction of SnO_2 with CO/HCl is mainly Sn(IV) but also a significant quantity of an Sn(II) compound was produced. This implies that the CO is taking little part in the reaction, acting only as an inert diluent. The presence of Fe_2O_3 in the CO/HCl reaction causes a great increase in the Sn(II):Sn(IV) ratio. This suggests that two reactions occur in this case: one producing $SnCl_4$ and the

other catalysed by Fe_2O_3, producing $SnCl_2$. This point is further discussed in section 5.2 . The loss of Sn in the last three analyses is probably due to the partial incondensibility of $SnCl_4$ (s.v.p. of $SnCl_4$ = 32.6 mm at 20°C), which if it had been recovered, would have decreased the $SnCl_2$: $SnCl_4$ ratio in the products from those reactions.

5. Discussion of results.

5.1. Rate-controlling process.

Several possibilities arise as to the nature of the rate-controlling step in heterogeneous reaction of the type studied here; they may be broadly divided into two sections, viz. control by mass-transport processes such as the rate of evaporation of products or by a particular chemical step in the reaction mechanism. It is contended that the latter is the case and the following sections are adduced in evidence. They deal largely with reaction in H_2/HCl but, by extension of the argument, the same conclusions were found to apply with equal validity to the reaction of SnO_2 in CO/HCl mixtures.

5.1.1. Control by evaporation of products.

Stannous chloride is the least volatile of the products of reaction and control by evaporation implies that the gas phase is in equilibrium with $SnCl_2$ liquid on the particles. Stannous chloride in the gas phase is, therefore, at the saturation vapour pressure at the reaction temperature. The rate of mass change is approximately determined by the rate of volatilisation of $SnCl_2$, which is proportional to the rate of flow of the gas phase. The vapour pressure of $SnCl_2$ has been expressed as a function of temperature, viz.

$\log p(\text{mm Hg}) = -4480/T + 7.73$ [49]

At 500 and 600°C, the ends of the temperature range in which the reaction was performed, the values of p are 1.14×10^{-1}

and 5.23×10^{-1} atmospheres respectively. Assuming a flow-rate of 17 $cm^3 sec^{-1}$, saturated with $SnCl_2$, the maximum rates of volatilisation of stannous chloride are 0.06 and 0.26g sec^{-1} at 500 and 600°C respectively. As the rates of reaction found at these temperatures are equivalent to approximately 10^{-5}g sec^{-1}, the reaction is clearly not controlled by the rate of flow of the gas phase saturated with $SnCl_2$. Also, varying the gas circulation rate would be expected to change the rate of reaction if the above process was rate-controlling; however, this was not so (see section 4.2.2.1.).

5.1.2. Control by diffusion of products and reactants.

If the rate-controlling step in the reaction is diffusion of products away from the solid surface, through a boundary layer of gas, then the concentration at the crystal surface would be equal to the saturated vapour pressu and in the main bulk would be virtually zero. As the particle size was approximately 100 μm, the distance from the crystal surface at which P_{SnCl_2} was zero was taken as 10 μm; larger distances would not apply owing to the presence of adjacent crystals. As the distance from the reaction interface, where $P_{SnCl_2} = 0$, is one order of magnitude less than the particle diameter, a linear-diffusion model was employed in the following calculation, with the concentration gradient everywhere constant. The number of molecules crossing unit area in unit time under unit negative concentration gradient is the coefficient of diffusion, D, given in the following equation:

$$D = \frac{3}{8\sigma^2 n} \left(\frac{3kT}{8m}\right)^{\frac{1}{2}} \quad [50]$$

σ = molecular diameter (cm)

n = number of molecules per unit volume (cm^{-3})

m = mass of one molecule (g)

k = Boltzmann Constant (erg/molecule-degree)

T = absolute temperature. (^{o}K)

Taking the $SnCl_2$ molecular diameter to be 50 nm and the surface area of the SnO_2 sample to be 8.7 cm^2, this would give rise to rates of diffusion of $SnCl_2$ of approximately 3g sec^{-1} at the temperatures used in the experiments. These rates are five orders of magnitude greater than those observed viz. 10^{-5}g sec^{-1}, and, thus, the reaction is not controlled by this stage.

Another possibility to be considered is rate-control by diffusion of the H_2 and HCl to the crystal surface when th react immediately. Taking their bulk pressures to be 20 cm Hg and their corresponding molecular diameters to be 27.8 and 18.1 nm[51] and using the above equation, rates of 0.23 and 0.13g sec^{-1} at 500^{o}C are obtained. Comparison of these with observed rates, shows that this type of diffusion is not rate-controlling.

If the reaction were diffusion-controlled then the most likely possibility is that the slowest step would be the diffusion of $SnCl_2$ away from the surface of the bed of crystals i.e. the rate would be independent of bed-depth.

Taking the boundary layer to be 1mm thick and the surface area to be that of the sample holder then the above equation gives 0.03g sec^{-1} as the rate obtained at 500 - 600°C. This is still three orders of magnitude larger than the experimentally determined rates of reaction.

5.1.3. Heterogeneity of reaction of particles.

Differences in the extent of reaction over the surfaces of single crystals have been observed with both synthetic and natural cassiterite. In section 4.1., the influence of small iron-bearing inclusions, in a non-uniform distribution, on the rate of reaction of the adjacent SnO_2 was described. Although heterogeneity of reaction is possible in a diffusion-controlled process e.g. crystal growth or evaporation, owing to the higher partial pressure existing over high energy sites, it is difficult to envisage any mechanism whereby the incidence of imperfections in the surface of the SnO_2 lattice could influence the rate of diffusion of $SnCl_2$. Thus non-uniform reaction provides further evidence for chemical control rather than mass-transfer control.

5.1.4. Sensitivity of rate to temperature and to small quantities of additives.

It has been shown that the activation energy of the H_2/HCl reaction is 52Kcal in the range 500 - 550°C and that this decreases as the temperature rises to 600°C (cf. section 4.2.3.2.). Gas-diffusion-controlled processes have low

activation energies, usually less than 10Kcal, so that this is another indication that the reaction is chemically controlled.

From consideration of the results described in section 4.2. and especially 4.2.3, it may be seen that the rate of reaction of synthetic SnO_2 crystals is susceptible to the presence of less than 5% of metal or metal oxide additives. In particular, the presence of 4.74% Pt caused an increase in rate at 550°C of almost 250%. It is improbable that this effect can be attributed to some modification of a diffusion step. Indeed, as the particle size of these additives was of the order of 1 μm, their presence would have been expected to impede any gaseous diffusion process. Thus the catalysis caused by these additions must arise either from some modification of the crystal matrix i.e. by promotion of crystal imperfections or by the formation in situ of some reactive intermediate which increases the rate of a chemically controlled step in the reaction mechanism.

5.2. Products of reaction in the absence of additives.

Inspection of the results obtained in section 4.3. shows that in general at least two overall reactions are taking place: one of them occurs in HCl only and the other involves both HCl and the reductant. The reaction in HCl only results in the production of a Sn(IV) species, presumably $SnCl_4$, and this is reasonable as no reductant is present. The reactions of SnO_2 in H_2/HCl and CO/HCl differ

in that the former produces mostly $SnCl_2$ whilst the product from the latter reaction is predominantly a Sn(IV) species.

The appearance of Sn(IV) as the major product from reaction in CO/HCl is at variance with the results found by Nieuwenhuis[31], whose work has been described in section 2.5. Using a low-grade tin concentrate containing 5% Sn and 1.25% Fe, he found that $SnCl_2$ was formed as 99.9% of the product providing the $pCO:pCO_2$ ratio was greater than 6.1×10^{-2} at 1000°K to prevent conversion according to the following equation:

$$2\ SnCl_2(g) + 2\ CO_2(g) \rightleftharpoons SnCl_4(g) + SnO_2(c) + 2\ CO(g)$$

for which $\Delta G^o_T = -18{,}370 - 3.46\ T \log T - 3.26 \times 10^{-3} T^2 + 62.45T$.

The standard free energy change at 1000°K is 26.2 kcal but the reaction becomes more favourable as the temperature is lowered and if both the stannous and stannic chlorides remain in the gas phase ($\Delta G_{300^oK} = -3.6$ kcal). If the materials are present in their standard states at 300°K then $\Delta G^o_{300^oK} = 30$ kcal. The above reconversion may be split up as follows:

$$2SnCl_2(g) + O_2(g) \rightleftharpoons SnCl_4(g) + SnO_2(c) \quad \ldots\ (1)$$

$\Delta G^o_T = -153{,}370 - 3.46\ T \log T - 3.26 \times 10^{-3} T^2 + 99.95T$

and the reduction equilibrium of CO_2

$$2\ CO_2 \rightleftharpoons 2\ CO + O_2 \quad \ldots\ (2)$$

$\Delta G^o_T = -135{,}000 - 37.5\ T$

If the minimum $pCO:pCO_2$ ratio is 400 (based on 0.1g SnO_2 having reacted), then $pO_2 = 0.5 \times 10^{-95}$ as $Kp_{(2)} = 7.9 \times 10^{-91}$ at

$300^{o}K$. $K_{p(1)} = 4.0 \times 10^{92}$ at $300^{o}K$ so that $p^{2}_{SnCl_2} \simeq 500$. Less than 5% of the $SnCl_2$ would be reconverted by this process. Also, in the experiments in which the $pCO:pCO_2$ ratio was varied (section 4.2.6.4.) within the range $0.5-\infty$, no obvious change in products was found. The presence of iron in Nieuwenhuis's experiments[31] may account for the predominance of $SnCl_2$; this point is discussed further in section 5.4.3.

It is possible to account for the production of $SnCl_2$ and $SnCl_4$ in a number of ways dependent on the oxidation-reduction equilibria of the tin chlorides in the gas mixtures used in the temperature range 0 - $700^{o}C$; sequences of reaction are outlined as follows:

a) 1) $SnO_2 + H_2 = SnO + H_2O$

$SnO + 2HCl = SnCl_2 + H_2O$

2) $SnO_2 + 2H_2 = Sn + 2H_2O$

$Sn + 2HCl = SnCl_2 + H_2$

3) $SnO_2 + CO = SnO + CO_2$

$SnO + 2HCl = SnCl_2 + H_2O$

4) $SnO_2 + 2CO = Sn + 2CO_2$

$Sn + 2HCl = SnCl_2 + H_2$

b) $SnO_2 + 4HCl = SnCl_4 + 2H_2O$

c) 1) $2\ SnCl_2 + 2H_2O = SnCl_4 + SnO_2 + 2H_2$

2) $2\ SnCl_2 + 2CO_2 = SnCl_4 + SnO_2 + 2CO$

d) 1) $SnCl_4 + H_2 = SnCl_2 + 2HCl$

2) $SnCl_4 + CO = SnCl_2 + COCl_2$

The thermodynamic feasibility of these reaction schemes is discussed below; for convenience, 1000°K is taken as the temperature of the sample.

a) Liquid tin is the only stable tin species in the Sn-O-H and Sn-O-CO systems at 1000°K; the standard free energies of reduction of SnO_2 to Sn by H_2 and CO are -2.4 and -4.1 Kcal respectively. Tin will react with HCl at this temperature to produce $SnCl_2$ ($\Delta G^0 = -10$ kcal).

b) SnO_2 will react with HCl to produce $SnCl_4$ providing the latter is removed from the reaction site; the standard free energy change of reaction at 1000°K is 7.7 kcal.

c) The reaction of $SnCl_2$ with CO_2 has been treated above and it has been shown that less than 5% of the $SnCl_2$ would react at 300°K. For the overall reaction:

$$2\ SnCl_2(g) + 2H_2O(g) = SnCl_4(g) + SnO_2(c) + 2H_2(g)$$

$$\Delta G^0_T = -35{,}570 - 3.46\ T \log T - 3.26 \times 10^{-3} T^2 + 73.75\ T$$

which may be simplified into:

$$2\ SnCl_2 + O_2 \rightleftharpoons SnCl_4 + SnO_2 \qquad \ldots\ (\alpha)$$

$$\Delta G^0_T = -153{,}370 - 3.46\ T \log T - 3.26 \times 10^{-3} T^2 + 99.95T$$

and

$$2H_2O \rightleftharpoons 2H_2 + O_2 \qquad \ldots\ (\beta)$$

$$\Delta G^0_T = 117{,}800 - 26.2T.$$

The free energy change for the overall reaction is 24.5 kcal at 1000°K but -16.0 kcal at 300°K, so that the reaction becomes more favourable as the temperature is lowered. If the minimum $pH_2:pH_2O$ ratio is 70 (based on 0.55g SnO_2 reacted),

then $pO_2 = 1.8 \times 10^{-85}$ as $Kp_{(\beta)} = 9.1 \times 10^{-82}$ at 300°K.

$Kp_{(\alpha)} = 4.0 \times 10^{92}$ so that $p^2SnCl_2/pSnCl_4 = 1.4 \times 10^{-8}$.

Thus almost all the $SnCl_2$ would be reconverted by this process; however, this is not observed, the gases issuing from the hot zone are cooled sufficiently rapidly to freeze in the high temperature equilibrium.

d) Hydrogen will reduce $SnCl_4$ to $SnCl_2$ at 1000°K ($\Delta G^o = -16.7$ kcal) but the reaction becomes less favourable at lower temperatures ($\Delta G^o_{300°K} = 12$ kcal). CO, on the other hand, will not reduce $SnCl_4$ in this temperature range ($\Delta G_{1000°K} = 35.7$ kcal, $\Delta G^o_{300°K} = 40$ kcal).

The production of $SnCl_2$ is thus thermodynamically feasible in either H_2/HCl or CO/HCl, as is also the formation of $SnCl_4$ by reaction of SnO_2 with HCl alone. As hydrogen reduction of $SnCl_4$ becomes progressively more difficult as the temperature is lowered, the production of $SnCl_2$ via the intermediate formation of $SnCl_4$ would only occur at high temperatures. The intermediate formation of $SnCl_4$, by reaction of SnO_2 in CO/HCl to produce $SnCl_2$, probably does not occur as CO will not reduce $SnCl_4$ in the temperature range 0 - 700°C.

5.3. <u>Kinetics and mechanisms of reaction in the absence of additives.</u>

The rate-dependency of the reaction of SnO_2 with the three gas mixtures used is discussed under separate headings.

5.3.1. Kinetics and mechanism of reaction in HCl only.

As analysis of the product of reaction in HCl only has shown that it consists in the majority of Sn(IV) (cf. section 4.3.), the most probable reaction is that previously quoted, viz.

$$SnO_2(c) + 4HCl(g) \longrightarrow SnCl_4(g) + 2H_2O(g)$$

for which $\Delta G^{o}_{500^{o}C} = 5.2$ kcal. Inspection of the results obtained from those experiments where non-annealed crystals were reacted in HCl only at 500°C, shows that the reaction is first order with respect to HCl.

At 500°C in p_{HCl} = 20 cm Hg, a maximum rate of reaction may be found from the partial pressure of $SnCl_4$ in equilibrium with SnO_2. Under these conditions, $p_{SnCl_4} = 5.46 \times 10^{-2}$ atmos. ; assuming a gas flow-rate of 17cm^3 sec^{-1} saturated with $SnCl_4$ at this pressure, the rate of volatilisation of $SnCl_4$ is 3.7×10^{-3}g sec^{-1}. This corresponds to a rate of reaction of SnO_2 of approximately 2.1% sec^{-1} and is two orders of magnitude larger than the rate actually found in PHCl = 20 cm Hg viz. 3.5×10^{-3}% sec^{-1} (cf. section 4.2.2.2.). and thus is not rate-controlling. Control by diffusion of $SnCl_4$ through a boundary layer of 1 mm. would give rise to rates which are more than three orders of magnitude too large (cf. section 5.1.2.). Therefore, the reaction is controlled by the rate of a chlorinating step.

The rate dependence upon p_{HCl} indicates that the reaction occurs in stages, probably involving the stepwise

chemisorption of HCl molecules at surface active sites. This hypothesis is corroborated by the fact that annealing the crystals inhibits the reaction in HCl only (cf. section 4.2.3.1.). No quantitative data on the dislocation density in cassiterite crystals has been obtained but Hirthe and Brittain[52] have shown that by maintaining rutile crystals, which have the same tetragonal structure as cassiterite, at 1375°C for 2.7 ks, they were able to reduce the dislocation density four-fold. It would thus appear that the rate of formation of $SnCl_4$ is a function of the number of crystal imperfections i.e. high energy sites, present in the crystal surface. This point is further attested by the preferential reaction occurring at edges and corners where non-annealed crystals have been reacted in HCl only (cf. section 4.2.2.4.).

5.3.2. Kinetics and mechanism of the reaction of SnO_2 in H_2/HCl.

The reaction of annealed crystals in H_2/HCl mixtures is first order with respect to H_2 at 500°C (cf. section 4.2.3.1.), but at higher temperatures and high p_{H_2}, the order decreases. As the reaction is not diffusion controlled, within the temperature-pressure zone where the rate is a function of p_{H_2} and independent of p_{HCl}, the rate-controlling step is probably one of reduction. Also, the rate of reduction of non-annealed crystals in H_2 only is comparable to the rate of their overall chlorination (cf. Figure 8, section

4.2.2.2.). The hydrogen and hydrogen chloride were always in considerable excess compared with the SnO_2 (> x 75); also, the products, $SnCl_2$ and H_2O, were condensed in the cooler parts of the apparatus. Thus the conditions remained thermodynamically favourable for the reaction to proceed until all the SnO_2 was exhausted, a fact confirmed by the results. It has also been shown in section 5.2. that any reactions in the gas phase within the low temperature regions are sufficiently slow to be discounted and thus it is assumed that the overall reaction takes place at the temperature of the sample.

The following three mechanisms, involving some well-established compounds as intermediate products, are thermodynamically feasible under the conditions used in these studies. The free energies of reaction are given at 500°C:

1a. $SnO_2(c) + H_2(g) \longrightarrow SnO(c) + H_2O(g)$, ΔG^0 = 1 kcal

1b. $SnO(c) + 2HCl(g) \longrightarrow SnCl_2(l) + H_2O(g)$, ΔG^0 = -12 kcal

2a. $SnO_2(c) + 2H_2(g) \longrightarrow Sn(l) + 2H_2O(g)$, ΔG^0 = 3 kcal

2b. $Sn(l) + 2HCl(g) \longrightarrow SnCl_2(l) + H_2(g)$, ΔG^0 = -14 kcal

3a. $SnO_2(c) + 4HCl(g) \longrightarrow SnCl_4(g) + 2H_2O(g)$, ΔG^0 = 3.5 kcal

3b. $SnCl_4(g) + H_2(g) \longrightarrow SnCl_2(l) + 2HCl(g)$, ΔG^0 = -14.5 kcal

As reaction 3a has been shown to occur at a negligible rate when annealed crystals are used (cf. section 4.2.3.1.) it is possible to discard the third mechanism as playing only a minor role in the overall reaction. Mechanism 2, as set out, may also be discarded as it would give rise to a rate

dependence on $p^2_{H_2}$ and the reaction has been observed to be first order with respect to H_2; however, reaction 2a could occur in two or more steps involving chemisorbed hydrogen, etc. and, therefore, give rise to an apparent first order reaction. Also, if the formation of liquid tin is a stepwise process involving the intermediate formation of SnO, then it is not possible to distinguish between mechanisms 1 and 2 by the experiments performed. Neither of these mechanisms is limited by the rate of removal of $SnCl_2$ (cf. section 5.1.).

5.3.3. Kinetics and mechanism of reaction in CO/HCl.

The reaction of SnO_2 in CO/HCl at 700°C results in a mixture of products, viz. $SnCl_4$ and $SnCl_2$, in which the higher chloride predominates. The reaction is first order with respect to HCl and is independent of P_{CO}. It has been shown in section 5.2. that low temperature oxidation of $SnCl_2$ or reduction of $SnCl_4$ does not occur to a sufficient extent to account for the proportions present in the product. Therefore, the reactions to produce the two chlorides probably take place at the sample temperature.

As $SnCl_2$ is the minor product, the rate dependence of the reaction to produce this chloride cannot be deduced from the results of the experiments performed. However, a number of mechanistic schemes may be put forward to account for the presence of $SnCl_2$ at 700°C:

1a. $SnO_2(c) + CO(g) \longrightarrow SnO(c) + CO_2(g)$, $\Delta G^o = -4$ Kcal.

1b. $SnO(c) + 2HCl(g) \longrightarrow SnCl_2(g) + H_2O(g)$, $\Delta G^o = -10$ Kcal

2a. $SnO_2(c) + 2\,CO(g) \longrightarrow Sn(l) + 2CO_2(g)$, $\Delta G^o = -6$ Kcal

2b. $Sn(l) + 2HCl(g) \longrightarrow SnCl_2(g) + H_2(g)$, $\Delta G^o = -8$ Kcal

3a. $SnO_2(c) + 4HCl(g) \longrightarrow SnCl_4(g) + 2H_2O(g)$, $\Delta G^o = -1$ Kcal

3b. $SnCl_4(g) + CO(g) \longrightarrow SnCl_2(g) + COCl_2(g)$, $\Delta G^o = 36$ kcal.

Reaction 3b. would probably not occur owing to its unfavourable free energy change and it is not possible to decide conclusively between the first two mechanisms proposed.

The production of $SnCl_4$ probably takes place according to reaction 3a (see curve 2, Figure 28 at $P_{CO} = 0$). As stated in section 5.2., the rate-dependence on P_{HCl} indicates that the reaction probably occurs according to a complex mechanism involving chemisorbed intermediates which have not been characterised.

5.4. Influence of Fe_2O_3 and other additives.

The effect of Fe_2O_3 on the reaction of SnO_2 varies with the chlorinating system used; these effects are discussed in separate sections, each dealing with reaction occurring in a particular gaseous mixture.

5.4.1. Effect of Fe_2O_3 on the reaction of SnO_2 crystals with HCl.

It has been argued in section 5.2. that the reaction of SnO_2 crystals with HCl takes place predominantly at high energy sites in the crystal lattice and that this reaction is

inhibited by annealing the crystals at 1265°C. Mixing and heating non-annealed crystals with Fe_2O_3 to 500°C causes an almost identical effect to that of annealing in that the reaction of SnO_2 crystals with HCl only is repressed (cf. section 4.2.2.3.). It is suggested that Fe_2O_3 inhibits this reaction either by dissolution in the surface or body of the crystal, relieving crystal imperfections in the process or by adsorption at a surface active site thus denying it for reaction. Experiments have been described in section 4.2.2.3. (Figures 11 and 12) in which a mixture composed of non-annealed SnO_2 and Fe_2O_3 was reacted to completion in HCl; the residual SnO_2 was partly reacted in H_2/HCl and the residue from this second part of the experiment subsequently reacted in HCl only. It is thus apparent that the effect of the residual Fe_2O_3 did not extend throughout the crystal. A mixture of Fe_2O_3 and annealed crystals was subjected to the same sequence of experiments and similar behaviour was observed (cf. section 4.2.3.3.); neither the residual Fe_2O_3 nor the annealing repressed the reaction in HCl only, immediately after reaction in H_2/HCl.

5.4.2. Influence of Fe_2O_3 on the reaction of SnO_2 with H_2/HCl.

Inspection of the results described in sections 4.2.3.3.-6. shows that Fe_2O_3 catalyses the reaction of SnO_2 in H_2/HCl; the catalytic effect is an increasing function of temperature and amount of Fe_2O_3. This catalysis may occur

according to one or a combination of four different mechanisms; these are:

1) by a cyclic reaction involving $FeCl_3$

2) by Vol'kenshtein's Effect

3) by nucleation of reaction using metal particles

4) by chemisorption and activation of H_2 on metal particles.

Descriptions of these possible processes and the evidence for and against them are given in the following sections.

5.4.2.1. Catalysis by $FeCl_3$

If $FeCl_3$ is the reagent responsible for catalysis the mechanism would involve the cyclic consumption and regeneration of $FeCl_3$ according to a reaction scheme of which the following is an example:

$$Fe_2O_3(c) + 6HCl(g) \longrightarrow 2FeCl_3(g) + 3H_2O(g)$$

$$2FeCl_3(g) + Sn(l) \longrightarrow 2FeCl_2(c) + SnCl_2(l)$$

$$2FeCl_2(c) + 2HCl(g) \longrightarrow 2FeCl_3(g) + H_2(g)$$

Several types of catalysis involving this chlorination-exchange mechanism with $FeCl_3$ have been studied but they occur largely in molten systems.[53]

It has been shown in section 4.2.3.5. that it is unlikely that a gaseous intermediate is involved and this is further confirmed by the strictly defined areas over which catalysis occurred in grains of natural cassiterite. Also, such a process as the one described above would increase the rate of a chlorination step but the reaction has been found to

be reduction-controlled (cf. section 5.3.2.); it is thus possible to discard this mechanistic scheme.

5.4.2.2. Catalysis by promotion of active sites in the SnO_2 crystal surface.

One method by which catalysis may occur is by the propagation of crystal lattice disturbances due to the presence of impurities; this is known as Vol'kenshtein's Effect.[54] According to this process, which may catalyse either a chlorination or reduction step, ions which are too large to be absorbed substitutionally are sorbed in surface layers as interstitials causing lattice disturbances over a distance of 10.A.U. or more i.e. they promote high energy sites. This catalytic effect is directly related to the ionic volume and electronic charge of the additives. Typical of this mode of catalysis is the increased reduction of FeO by CO in the presence of small amounts (less than 1 atomic percent) of the large alkali and alkaline earth metal ions.[55]

This type of catalysis probably does not play a large part in the catalytic mechanism as Sn^{4+} and Fe^{3+} have similar ionic radii (6.5 and 6.7nm respectively[51]) and homogeneous solid solutions are known[42]. Also, it has been shown in section 5.4.1. that mixing and heating of SnO_2 with Fe_2O_3 tends to anneal the crystal surface i.e. to reduce the number of lattice imperfections.

5.4.2.3. Nucleation of reduction by metal particles.

One way to catalyse the reduction of a metallic oxide in H_2 is to nucleate the reaction with particles of the metal concerned.[56-60] Delmon[57,59] et al have found that it is possible to increase the rate of H_2 reduction of NiO and CuO by the addition of one of a number of finely divided metals i.e. by artificially germinating the reaction. In this case the degree of catalysis would be an increasing function of the tendency of the reduced metal to form an alloy with the metal additive and this is confirmed by the catalytic effect of Cu on the reduction of NiO.

This type of catalysis is unlikely to prevail in the reaction under discussion for a number of reasons. It has been found that the H_2 reduction of SnO does not show this phenomenon[58] and as the reduction of SnO_2 to Sn must proceed stepwise (as the reaction is first order with respect to H_2), this process must catalyse the reduction of SnO_2 to SnO, when the possibility of metallic nucleation is lost. Also, it has been found that the presence of copper oxide does not catalyse the overall reaction at 550°C even though metallic copper is stable in HCl at this temperature.

5.4.2.4. Catalysis by chemisorption and activation of H_2

As the rate-controlling process is one of reduction and as this would involve the breaking of an H-H bond, it would be reasonable to suppose that any mechanism which

facilitated the fracture of this bond would also accelerate the reduction process. Hydrogen molecules will not normally dissociate neither will hydrogen atoms recombine in the gas phase at an appreciable rate as the energy requirements are too great. However, in the presence of some other body which will stabilise the transition state and provide an energy sink, both of these processes may be facilitated. It is apparent that such a chemisorptive process is operative to some extent in the overall reaction in the absence of additives as the maximum activation energy is 52 kcal while the dissociation energy of H_2 is 104 kcal. Chief among the substances which provide the necessary substrate are certain transition metals, of which iron is one, which will dissociatively chemisorb hydrogen, i.e. the dissociation takes place with a decreased activation-energy on the surface of these metals. It is contended that the enhancement of the rate of reaction of SnO_2 in H_2/HCl owing to the presence of Fe_2O_3 is due to the dissociative chemisorption of hydrogen on iron metal.

Attempts have been made, and the results are given in section 4.2.3.7., to prove this hypothesis by analogy i.e. by adding other metal oxides the behaviour of which is predictable if such a mechanism operates. It has been shown that the incidence of catalysis is consistent with the reduction of the oxide additives to metal and the ability of the latter to chemisorb H_2. Only two exceptions were found viz. V_2O_5 and

TiO_2; as explained in section 4.2.3.7., the non-stoichiometric VO is the stable oxide in H_2 at the temperature used (550°C) and this may catalyse the reaction by absorption of H_2 by a vacancy mechanism. TiO_2, however, cannot be reduced by H_2 at this temperature so perhaps it increases the rate of reaction by some such process as the following:

$TiO_2(c) + 4HCl(g) \longrightarrow TiCl_4(g) + 2H_2O(g)$, $\Delta G^o = 30$ Kcal

$TiO_2(g) + SnO_2(c) + 2H_2(g) \longrightarrow SnCl_2(l) + 2H_2O(g) + TiO_2(c)$,

$\Delta G^o = -41$ kcal.

The first stage is, however, thermodynamically unfavourable.

SnO_2 may be reduced to Sn but the latter will not chemisorb H_2[45] so that the reaction is not autocatalytic.

Of those oxides which can be reduced to metals and will chemisorb H_2, some of the latter will also be converted to non-volatile chlorides in the course of the reaction. The standard free energy changes when these metals react with HCl at 550°C to form chlorides are given as follows:

$Fe(c) + 2\,HCl(g) \longrightarrow FeCl_2(c) + H_2(g)$, $\Delta G^o = -9.8$ Kcal

$Co(c) + 2\,HCl(g) \longrightarrow CoCl_2(c) + H_2(g)$, $\Delta G^o = -2.3$ kcal

$Ni(c) + 2\,HCl(g) \longrightarrow NiCl_2(c) + H_2(g)$, $\Delta G^o = 4.4$ kcal

$Mo(c) + 2\,HCl(g) \longrightarrow MoCl_2(c) + H_2(g)$, $\Delta G^o = 25.6$ kcal

$Pt(c) + 2\,HCl(g) \longrightarrow PtCl_2(c) + H_2(g)$, $\Delta G^o = 46$ kcal.

Where applicable, the free energies of reaction to higher chlorides are more unfavourable.

The retarding action of Nb_2O_5 and WO_3 may perhaps be explained by the fact that the stable oxides of Nb and W under the conditions used are NbO_2 and WO_2; both of these oxides have the same crystal structure as cassiterite and both Nb^{4+} and W^{4+} have similar ionic radii to that of Sn^{4+}. It is possible that epitactic growth of these oxides has taken place on the surface of the SnO_2 thus denying the latter to reaction.

Further evidence that the catalysis by Fe_2O_3 is by a process of chemisorption may be attested in that Fe_2O_3 also catalyses the reduction of SnO_2 by H_2 (cf. section 4.2.3.6). This could not occur by any of the other mechanisms described for the same reasons given earlier in sections 5.4.2.1. - 3.

If catalysis occurs by this type of process then it requires the viable existence of elemental iron throughout the period of reaction represented by the rectilinear sections of the rate curves shown in Figure 10. This may come about by reduction of Fe_2O_3 to Fe by H_2 followed by chlorination to ferrous chloride, the process occurring throughout the time taken for reaction of SnO_2. It is possible that iron metal may also be produced according to the following equation:
$Sn(l) + FeCl_2(c) = SnCl_2(l) + Fe(c)$, $\Delta G^{o}_{550^{o}K} = -2.3$ kcal.
It is, however, improbable as Prosser and Romero[35] have shown that tin reacts with HCl almost instantaneously at this temperature.

Another objection to this process is that the size of the iron particles may be extremely small and that the surface

characteristics of particles consisting of only a few atoms may differ considerably from those in the massive phase. However, Bond has shown that particles of 150 nm diameter consisting of arrays of only two hundred atoms still retain their catalytic effectiveness[61].

Assuming the existence of particles of iron, it is suggested that the following scheme of catalysis applies:

$H_2 \rightleftharpoons 2H^{\bullet}$ on the surface of iron metal

$SnO_2 + 2H^{\bullet} \longrightarrow SnO + H_2O$

followed by

$SnO + 2HCl \longrightarrow SnCl_2 + H_2O$

or

$SnO + 2H^{\bullet} \longrightarrow Sn + H_2O$

$Sn + 2HCl \longrightarrow SnCl_2 + H_2$

with the first step rate-controlling and proportional to P_{H_2}, as found experimentally (cf. Figures 3-5).

As hydrogen atoms are very reactive one would expect that their subsequent adsorption and reaction would take place at a site not too far removed from their point of origin i.e. that a catalytic intermediate of this type would have limited mobility. Thus, further evidence for this mechanism is found in the fact that only rigidly defined areas of natural cassiterite containing iron-bearing inclusions showed preferential reaction (cf. section 4.1.1.).

It has been suggested by Grubb et al[40,42] that the

colour-zoning of cassiterite is due to different valency states of iron, the darker the colour, the higher the Fe^{2+}/Fe^{3+} ratio and it has not been found possible to correlate differences in the rate of reaction with colour-zoning. It has been postulated that pyrophorism (and thus catalytic activity) of iron particles is a function of the original oxide from which they were produced[62]. Thus the catalytic activity of the iron particles should vary with the atomic packing density of the original oxide; iron produced from magnetite is denser and much less active as a catalyst than that produced from hematite. Therefore, it might be expected to find preferential reaction in those regions of high Fe^{3+}/Fe^{2+} ratio as compared with areas of low $Fe^{3+}:Fe^{2+}$ for constant iron content; as stated above, this has not been observed. This may be explained by the fact that the iron in particles which exhibited colour-zoning was present in solid solution and thus was not in its own oxide lattice. Also, below 570°C the reduction of Fe_2O_3 takes place stepwise via magnetite.[63]

Catalysis of the reaction of SnO_2 crystals by such a process of chemisorption may take place in one of two ways dependent upon the solubility of Fe_2O_3 in SnO_2 under the prevalent reaction conditions.

If Fe_2O_3 has dissolved homogeneously throughout the crystal matrix then as the reaction interface advances fresh iron atoms are produced i.e. the mechanism does not require

the cyclic regeneration of metallic iron, given above. In this case it would be required that H_2 diffuse into the crystal lattice faster than HCl and that the state of the iron content, in the surface layers at least, would be changed. It has been shown in section 3.3.4. that it has not been possible to dissolve more than 100 p.p.m. of iron in the SnO_2 matrix and that such crystals reacted at the same rate as pure SnO_2 crystals. Also, inspection of the results obtained in sections 4.2.2.3. and 4.2.3.3., after undissolved Fe_2O_3 and the surface layers of the crystals had been removed, shows that the residue reacted in HCl only i.e. Fe_2O_3 was not active over all the crystal surface. On the other hand, e.s.r. analysis of crystals which had been previously mixed, heated and reacted with Fe_2O_3 showed some difference in the state of the iron content, though interpretation of the results is difficult (cf. section 4.2.3.). In particular, the presence of a ferromagnetic phase within the crystals reduced with hydrogen, lends support to the hypothesis that H_2 diffuses into the lattice and reduces the dissolved Fe_2O_3.

The other alternative is that reaction occurs entirely on the crystal surface at those points where iron atoms are produced by reduction of the adjacent Fe_2O_3. Evidence for this is provided by the fact that the degree of catalysis is an increasing function of the amount of Fe_2O_3 present even though the concentration of dissolved Fe_2O_3 does not change

(cf. section 4.2.3.4.).

It is thus probable that catalysis by chemisorption of H_2 takes place by a combination of the above two processes.

5.4.3. Effect of Fe_2O_3 on the reaction of SnO_2 in CO/HCl.

It has been suggested in section 5.3.3. that SnO_2 crystals undergo two reactions in CO/HCl mixtures; one of these reactions produces the major product $SnCl_4$ while the other produces $SnCl_2$. The presence of Fe_2O_3 in the reaction causes an increase in the proportion of the reduced Sn(II) species in the products (cf. section 4.3.), i.e. Fe_2O_3 catalyses a reaction involving both CO and HCl in competition to the reaction occurring in HCl only. As CO played very little part in the reaction in the absence of Fe_2O_3 i.e. reduction was difficult, it is probable that the rate- controlling step in the catalysed reaction is one of reduction by CO. No experiments were performed to test this directly but evidence is provided by curves 1 and 3 of Figure 28, which are almost parallel at low P_{HCl}; this implies that Fe_2O_3 catalyses some reaction other than that occurring in HCl only and no reaction took place at $P_{HCl} = 0$ in the absence of Fe_2O_3. This type of process would explain the results of Nieuwenhuis[31] in that the presence of Fe_2O_3 in the concentrate used would catalyse the production of $SnCl_2$ and thus account for its predominance in the reaction product. The first order rate-dependence upon P_{HCl} found by Nieuwenhuis[31] in his

experiments at high P_{CO} does not preclude the existence of reduction control at low pressures of CO.

Both Fe_2O_3 and SnO_2 may be reduced to metals by CO at 700°C; iron will chemisorb CO whereas tin will not do so. It is thus possible that catalysis of the reaction of SnO_2 in CO/HCl occurs by chemisorption of CO on iron metal in a similar manner to that described when H_2 is used as the reducing agent. The iron, once again, is subsequently converted to ferrous chloride. However, the presence of Nb_2O_5 also catalysed the reaction of SnO_2 in CO/HCl and as Nb_2O_5 is stable in CO/HCl at 700°C it is difficult to envisage any process by which this occurs (cf. section 4.2.6.2.).

Attempts to show that catalysis of the reduction of SnO_2 by CO was consistent with a chemisorption mechanism also gave inconclusive results (cf. section 4.2.7.3.). Both Fe_2O_3 and Pt catalysed the reduction while the absence of catalysis by Nb_2O_5 was also predictable; however, the catalytic behaviour of Bi_2O_3 is anomalous as Bi will not chemisorb CO[45].

6. Conclusions.

The results of the investigation into the role of iron-bearing impurities in the chlorination of cassiterite using H_2/HCl and CO/HCl mixtures are summarised as follows:

a) cassiterite undergoes two reactions in H_2/HCl mixtures; the major reaction, which produces $SnCl_2$, is controlled by the rate of reduction of SnO_2 and is first order with respect to H_2; the reaction rate is independent of the pressure of HCl. The second reaction produces $SnCl_4$ and is first order with respect to HCl; it occurs predominantly at high energy sites.

b) Fe_2O_3 catalyses the reaction to produce $SnCl_2$ by a process involving the chemisorption of hydrogen on iron metal produced by reduction of the iron oxide. It also inhibits the reaction which forms $SnCl_4$ by relieving crystal imperfections.

c) The presence of Nb_2O_5 and WO_3, the oxides of two elements which are commonly associated with cassiterite, retard the reaction of SnO_2 with H_2/HCl. It is probable that NbO_2 and WO_2, which have the same structure as cassiterite and which are stable under the reaction conditions, form an epitactic layer on the surface of the cassiterite, the phase change being nucleated by the latter.

d) cassiterite also undergoes two reactions in CO/HCl; the major reaction in this system produces $SnCl_4$ and is the same reaction occurring with HCl only described in a). The second reaction produces $SnCl_2$ and the rate is probably some function

of the pressure of CO.

e) Fe_2O_3 catalyses the production of $SnCl_2$ by reaction of SnO_2 in CO/HCl; the catalytic process is probably one of chemisorption of CO on elemental iron.

f) Nb_2O_5 catalyses the overall reaction occurring in CO/HCl but the mechanism of catalysis is not clear.

It is concluded that iron-bearing impurities catalyse the production of $SnCl_2$ by reaction of cassiterite in the above system; thus the presence of these impurities lower the temperature required for reaction at a given rate.

References.

1) Berman, H., Frondel, C. and Palache, C. 'Dana's System of Mineralogy'. p576(John Wiley and Sons Inc. 1944).

2) Report of U.S. Bur. Mines. No. 5095 (1954).

3) Bulletin of U.S. Bur. Mines. No. 585 (1960).

4) Report of U.S. Bur. Mines. No. 5161 (1955).

5) Carlsson, F. and Trostler, F. U.S. Patent 2,219,411 (1940).

6) Tainton, U.C. U.S. Patent 2,238,194 (1941).

7) Large, A. 'Advances in Extractive Metallurgy', p206, Symposium of the Institution of Mining and Metallurgy, London (1967).

8) Decroly, C. and Ghodsi, M. Mém. Scient. Revue Métall., 63, (1966), 109-25.

9) Decroly, C., Ghodsi, M. and Winand, R. Trans. Instn Min. Metall. (Sect. C: Mineral Process. Extr. Metall.) 76, (1967) C259.

10) Report of U.S. Bur. Mines No. 5501 (1959).

11) Roy, M.R.W. Trans. Instn Min. Metall. (Sect. C: Mineral Process. Extr. Metall.) 76, (1967) C101.

12) Report of U.S. Bur. Mines. No. 2247 (1921).

13) Report of U.S. Bur. Mines. No. 5281 (1956).

14) Report of U.S. Bur. Mines. No. 5349 (1957).

15) Report of U.S. Bur. Mines. No. 6612 (1965).

16) Report of U.S. Bur. Mines. No. 6635 (1965).

17) Report of U.S. Bur. Mines. No. 6649 (1965).

18) Gibson, A.R. and Buddery J.H. 'Extractive metallurgy of some of the less common metals'. p49. Symposium of Institution of Mining and Metallurgy. London (1956).

19) Henderson, A.W., May S.L. and Higbie, K.B. Ind. and Eng. Chem. 50, (1959), 611.

20) Henderson, A.W. J. Metal. 16, (1964), 155.

21) Fridman and Bogoraz. J. Appl. Chem. (U.S.S.R.) (1946), 833.

22) Richards, A. Netherlands Patent 2,062 (1919).

23) Wood, L.A. and Sulman, H.L. U.S. Patent 1,931,944 (1934).

24) Fletcher, A.W., Jackson, D.V. and Valentine. Trans. Instn Min. Metall. (Sect. C: Mineral Process. Extr. Metall.) 76, (1967), C145.

25) Frents, G.S. Tsvetnye Metally, 4, (1937), 25.

26) Ashcroft, E.A. Brit. patent 302,851 (1928).

27) Ashcroft, E.A. U.S. Patent 1,843,060 (1932).

28) Malan, H.L. Min. Mag. 81, 1949(Sept.), 137.

29) Chizikov, D.M., Frents, G.S. and Tratsevnitskaya, B.Ya, 'Chloride Metallurgy of Tin', (Russian). Akad. Nauk S.S.S.R., (1963).

30) Chizikov, D.M. and Balikhina, G.S., Tsvetnye Metally, 8, (1937), 68.

31) Nieuwenhuis, J.A.M. 'Advances in Extractive Metallurgy', p455. Symposium of the Institution of Mining and Metallurgy, London, (1967).

32) Report of U.S. Bur. Mines. No.5298 (1957).

33) Report of U.S. Bur. Mines. No. 5459 (1959).

34) Report of U.S. Bur. Mines No. 5811 (1961).

35) Prosser, A.P. and Romero, R. to be published.

36) Prosser, A.P. Chem. and Ind. (1966), 1545.

37) Prosser, A.P. and Lythe, R.G. 'Advances in Extractive Metallurgy'. Contribution to discussion. p521, Symposium of the Institution of Mining and Metallurgy, London (1967)

38) Wright, P.A. 'Extractive Metallurgy of Tin', p205, (Elsevier, 1966).

39) Fischer, W. and Gewehr, R. Z. anorg. Chem. 209, (1932),22.

40) Grubb, P.L.C. and Hannaford, P. Nature, 5024, (1966), 677.

41) Kohnke, H.F. and Kunkle, E.E. J. Appl. Phys., 36, (1965), 1489.

42) Grubb, P.L.C. and Hannaford, P. Mineralium Deposita, 2, (1966), 148.

43) Noack, J. Z. physik. Chem. 219, (1962), 417.

44) Bond, G.C. 'Catalysis by Metals'. p372. (Academic Press. New York,1962).

45) Bond, G.C. 'Catalysis by Metals'. p66 (Academic Press. New York, 1962).

46) Cotton, F.A. and Wilkinson, G. 'Advanced Inorganic Chemistry' p680, (1st edn. Interscience, (1962)).

47) Cotton, F.A. and Wilkinson, G. op cit. p672.

48) Barry, T.I. 'Method of Application of Electron Spin Resonance of Ions with S = $^{5}/_{2}$ (Fe^{3+}) for Polycrystalline Materials and Glasses'. p7. National Physical Laboratory, 1967.

49) Wright, P.A. op cit. p9.

50) Chapman, S. Proc. Roy. Soc. A93, (1917), 1.

51) Moelwyn-Hughes, E.A. 'Physical Chemistry', p24, (2nd edn. Pergamon, 1961).

52) Hirthe, W.M. and Brittain, J.O. J. Am. Ceram. Soc., 45, (1962), 546.

53) Bezukladnikov, A.B. and Vil'nyanski Ya. E. Zh. Prik. Khim. 34 (1), (1961), 49.

54) Vol'kenshtein, F.F. Zh. Fiz. Khim., 22, (1948), 311.

55) Khalafalla, S.E. and Weston, P.L. Trans. A.I.M.E. Met. Soc. (1967), 1494.

56) Lambiev, D., Boyadzhiev, A., Kuncheva, K. C.R. Acad. Bulg. Sci. 19 (11), (1966), 1031.

57) Pouchot, M.-T., Verhoeven, W. and Delmon, B. Bull. Soc. Chim. France., 3, (1966), 911.

58) Delmon, B. and Verhoeven, W. Bull. Soc. Chim. France., 10, (1966), 3065.

59) Delmon, B. and Verhoeven, W. C.R. Acad. Sci. Paris. Ser. C., 262, (1966), 33.

60) Delmon, B. and Verhoeven, W. Bull. Soc. Chim. France, 10, (1966), 3073.

61) Bond, G.C. Trans. Faraday Soc. 52, (1956), 1235.

62) Crowley, H.L. U.S. Patent 2,716,603 (1955).

63) Lu, W-K. and Bitsianes, G. Can. Met. Quart., 7 (1), (1968), 3.

APPENDIX

Alluvial Nigerian cassiterite - reaction in H_2/HCl at 610°C

P_{H_2} = 35.7 cm Hg P_{HCl} = 2.6 cm Hg		P_{H_2} = 19.3 cm Hg P_{HCl} = 9.6 cm Hg		P_{H_2} = 19.3 cm Hg P_{HCl} = 16.3 cm Hg	
Time (min)	% volatilised	Time (min)	% volatilised	Time (min)	% volatilised
0	0.0	0	0.0	0	0.0
5	0.3	5	0.9	3	0.6
8	0.6	10	1.5	6	1.2
10	0.6	15	2.1	10	0.9
13	0.9	20	2.4	15	1.0
15	0.9	25	2.4	19	1.0
18	1.5	35	3.7	25	1.0
20	1.2	40	5.2	30	1.0
25	1.5	45	7.0	35	1.0
30	1.5	50	7.9	40	1.9
35	1.5	65	11.3	45	2.8
40	1.5	71	13.1	50	4.0
45	1.5	80	16.5	55	5.9
50	2.2	85	18.0	60	7.8
55	2.5				
60	3.1				
67	3.7				
75	4.6				
85	6.2				
95	7.7				
100	8.9				
105	9.9				

Reagent grade SnO_2 powder - effect of bed-depth on reaction in H_2/HCl.

P_{H_2} = 20.5 cm Hg P_{HCl} = 20.5 cm Hg 320°C.

Average bed depth	0.1 cm		0.8 cm	
	Time (min)	% volatilised	Time (min)	% volatilised
	0	0.0	00	0
	5	14.1	05	2.3
	10	29.8	10	5.8
	15	44.2	15	9.2
	20	59.8	20	13.6
	27	79.1	30	22.6
	30	87.7	42	31.9
	37	97.5	55	41.0
			70	49.8
			85	58.1
			100	64.9

Non-annealed SnO_2 crystals (75-105 μm) - effect of bed-depth on reaction in H_2/HCl.

P_{H_2} = 20.5 cm Hg P_{HCl} = 20.5 cm Hg 500°C

Average bed-depth	< 0.1 cm		0.5 cm	
Time (min)	% volatilised		Time (min)	% volatilised
0	0.0		0	0.0
7	6.4		5	2.3
15	13.8		10	5.5
25	19.0		20	11.1
30	23.3		25	14.1
40	27.3		35	16.6
50	31.9		40	22.4
60	38.3		50	30.7
75	43.2		60	32.5
97	46.3		80	42.6
118	51.5		110	55.5

Non-annealed SnO_2 crystals - effect of gas circulation rate in H_2/HCl.

P_{H_2} = 15 cm Hg. P_{HCl} = 15 cm Hg. 550°C

Fast circulation		Slow circulation	
Time (min)	% volatilised	Time (min)	% volatilised
0	0.0	0	0.0
5	4.7	5	4.8
10	8.3	10	8.0
15	12.7	15	10.8
20	16.9	20	14.0
25	20.7	25	19.6
30	24.6	30	22.2
41	31.9	35	27.2
46	35.8	40	32.2
60	45.2	50	41.2
75	56.8	60	46.0
90	66.5	75	57.0
105	74.9	90	68.4
125	83.9	100	75.8
		110	80.8
		120	85.4

Non-annealed crystals - effect of varying P_{H_2} at 500°C

P_{HCl} = 20 cm Hg

P_{H_2} = 0 cm Hg		P_{H_2} = 2.5 cm Hg		P_{H_2} = 5 cm Hg.	
Time (min)	% volatilised	Time (min)	% volatilised	Time (min)	% volatilised
0	0.0	0	0.0	0	0.0
5	1.8	10	6.3	5	2.8
13	3.6	20	11.8	10	5.1
21	5.8	30	16.1	15	7.6
30	8.1	40	19.5	20	9.9
41	11.2	55	24.7	25	11.6
50	13.8	72	29.0	35	15.6
60	17.4	85	33.0	46	19.6
71	20.7	96	36.0	55	22.0
81	22.8	111	42.9	66	25.2
90	25.2	133	47.1	75	27.9
100	25.9	146	50.5	86	31.0
111	26.9			91	32.1
				100	34.8
				110	37.7
				120	39.8

P_{H_2} = 10 cm Hg		P_{H_2} = 13 cm Hg		P_{H_2} = 15 cm Hg.	
Time (min)	% volatilised	Time (min)	% volatilised	Time (min)	% volatilised
0	0.0	0	0.0	0	0.0
5	3.1	5	2.4	12	10.3
10	5.8	10	5.9	21	17.5
16	9.3	15	9.3	30	23.3
20	11.2	20	12.5	40	30.1
30	16.7	30	17.8	54	39.1
42	22.1	40	23.1	60	41.7
51	25.6	50	27.5	70	48.6
60	29.6	60	32.0	80	54.5
65	31.7	72	39.7	90	59.3
88	40.4	80	43.6	100	64.8
95	42.5	90	48.0	110	70.4
100	45.0	100	52.5	120	75.2
111	48.8	110	57.1	130	80.5
		120	61.2		

P_{H_2} = 20 cm Hg		P_{H_2} = 25 cm Hg		P_{H_2} = 30 cm Hg	
Time (min)	% volatilised	Time (min)	% volatilised	Time (min)	% volatilised
0	0	0	0	0	0
5	3.6	5	5.7	10	11.6
15	10.3	10	9.9	15	16.2
25	15.7	20	17.1	20	20.6
37	21.4	30	24.0	25	25.1
46	25.6	42	31.0	30	29.5
62	32.0	54	37.2	40	38.4
72	35.8	63	42.5	50	47.6
87	42.4	70	47.4	61	57.1
96	46.1	80	53.6	70	64.3
108	52.8	90	60.0	80	71.4
120	56.6	100	65.0	91	78.8
		110	71.4	100	83.9
		122	79.3	110	88.7
				120	91.2

Non-annealed crystals - effect of varying P_{HCl} at 500°C

P_{H_2} = 0 cm Hg

P_{HCl} = 10 cm Hg		P_{HCl} = 20 cm Hg		P_{HCl} = 30 cm Hg	
Time (min)	% volatilised	Time (min)	% volatilised	Time (min)	% volatilised
0	0	0	0	0	0.0
10	1.5	10	4.4	10	3.8
20	3.0	20	7.4	20	6.9
34	4.3	30	9.9	30	10.2
45	5.1	40	12.6	40	15.5
60	7.0	50	13.7	50	20.5
76	8.1	60	16.9	60	26.9
90	9.6	70	19.2	70	32.4
105	11.0	80	21.6	80	38.2
135	13.1	90	23.6	90	43.4
		104	27.0	100	47.1
		110	28.9		
		120	31.6		
		130	35.3		
		140	38.0		
		150	40.9		

Non-annealed crystals - effect of varying P_{HCl} at 500°C. P_{H_2} = 20 cm Hg.

P_{HCl} = 0		P_{HCl} = 5cm Hg		P_{HCl} = 10cm Hg		P_{HCl} = 15cm Hg		P_{HCl} = 25cm Hg		P_{HCl} = 30cm Hg	
Time (min)	% volatilised	Time (min)	% volatilised	Time (min)	% volatilised	Time (min)	% volatilised	Time (min)	% volatilised	Time (min)	% volatilised
0	0.0	0	0.0	0	0.0	0	0.0	0	0.0	0	0.0
30	0.0	10	4.6	10	8.9	10	7.5	10	8.8	10	13.3
45	0.0	20	10.8	18	16.5	20	13.5	20	16.4	20	20.0
60	1.5	30	16.7	30	26.2	32	20.0	30	24.7	30	29.4
75	3.2	40	21.5	46	35.8	40	24.3	40	32.9	37	34.3
90	5.3	50	26.2	61	44.6	50	29.2	50	40.2	50	42.9
107	7.4	60	31.9	70	51.8	60	34.4	62	49.1	61	47.9
120	8.8	70	36.3	80	56.6	70	40.6	70	55.9	71	54.1
137	10.1	80	40.3	91	61.7	80	47.6	82	65.6	80	58.5
151	11.4	91	45.9	100	65.2	90	53.1	92	73.1	90	63.7
		101	50.0	110	69.3	100	61.0	99	77.3	101	68.2
		112	53.4	120	73.1	113	70.0	110	83.5	110	72.9
		120	56.2					120	88.3	119	77.1

Non-annealed SnO_2 + 4.39% Fe_2O_3 - effect of varying P_{HCl} = 20 cm Hg. 500°C.

P_{H_2} = 0cm Hg		P_{H_2} = 2.5cm Hg		P_{H_2} = 5cm Hg		P_{H_2} = 10cm Hg	
Time (min)	% vol-atilised	Time (min)	% vol-atilised	Time (min)	% vol-atilised	Time (min)	% vol-atilised
0	0.0	0	0.0	0	0.0	0	0.0
10	2.3	10	1.9	10	2.4	11	6.1
20	3.2	20	7.6	20	9.4	20	14.1
30	4.2	30	14.8	30	16.2	30	24.3
40	4.2	40	22.9	40	23.7	35	28.6
56	4.2	51	31.7	50	30.7	48	40.3
66	4.2	60	38.0	60	37.4	60	48.5
120	4.2	70	44.7	72	45.6	70	55.0
		80	51.1	80	51.3	81	61.8
		91	58.3	91	58.3	90	66.9
		100	63.6	100	65.1	100	72.4
		110	69.5	111	69.4	113	78.5
		120	75.2	122	76.9	120	80.9
		135	82.1			130	85.3

Repeat of P_{H_2} = 0cm Hg.

Time(min)	0	[illegible]	10	15	20	30	40	50	60	100	120
% volatilised	0.0	0.9	3.3	3.9	3.9	4.2	5.4	5.4	5.4	5.4	5.4

P_{H_2}=15 cm Hg		P_{H_2}=20 cm Hg		P_{H_2}=30 cm Hg	
Time (min)	% vol-atilised	Time (min)	% vol-atilised	Time (min)	% vol-atilised
0	0.0	0	0.0	0	0.0
5	1.5	5	2.1	5	4.8
10	5.7	10	9.5	10	10.5
15	10.2	17	16.9	15	15.9
20	14.2	25	22.3	20	20.7
30	22.8	30	27.4	30	31.1
40	30.8	40	33.5	40	43.1
50	38.7	51	41.1	50	56.4
60	46.8	60	47.5	60	66.4
71	55.2	70	53.8	70	75.8
80	62.3	82	59.2	80	83.8
90	70.0	95	71.0	90	88.2
100	77.7	100	74.2	100	91.8
120	89.2	110	77.4	110	93.2
130	91.5	120	80.7	120	93.7

Non-annealed crystals + 4.39% Fe_2O_3 - effect of varying P_{HCl}.

P_{H_2} = 20 cm Hg. 500°C

P_{HCl} = 0 cm Hg		P_{HCl} = 5 cm Hg		P_{HCl} = 10cm Hg		P_{HCl} = 30 cm Hg	
Time (min)	% volatilised	Time (min)	% volatilised	Time (min)	% volatilised	Time (min)	% volatilised
0	0.0	0	0.0	0	0.0	0	0.0
15	0.0	10	3.7	10	6.3	10	7.2
30	0.0	20	9.9	20	14.5	20	15.0
45	0.6	30	15.4	30	24.3	30	23.1
60	2.6	40	23.2	40	32.6	40	28.4
75	3.0	50	28.9	50	41.1	50	33.0
90	3.2	60	35.9	61	48.9	60	42.7
115	3.6	70	41.5	70	55.7	65	43.4
135	5.5	81	46.9	80	62.6	70	47.8
150	5.5	90	51.6	90	69.4	80	53.1
165	5.8	100	56.4	100	75.3	91	58.6
180	6.2	110	61.4	110	81.5	100	63.9
195	6.2	120	65.6	120	86.3	110	67.7
210	6.7					120	72.8

Annealed SnO_2 - variation with P_{H_2}. P_{HCl} = 20 cm Hg 500°C.

P_{H_2} = 0cm Hg		P_{H_2} = 10cm Hg		P_{H_2} = 20cm Hg		P_{H_2} = 30cm Hg	
Time (min)	% vol-atilised	Time (min)	% vol-atilised	Time (min)	% vol-atilised	Time (min)	% vol-atilised
0	0.0	0	0.0	0	0.0	0	0.0
10	1.7	10	1.3	10	2.2	10	5.5
20	2.7	20	3.0	20	5.9	20	10.5
30	3.0	30	5.1	30	9.1	30	15.9
40	3.0	40	6.9	40	13.3	41	20.6
50	3.0	50	9.1	50	16.5	50	25.0
60	3.0	60	11.2	63	22.0	61	30.9
70	2.7	70	13.3	70	23.6	72	36.4
110	2.3	80	15.5	85	28.9	80	39.6
		108	19.5	100	33.4	90	44.9
		135	26.1	120	39.3	100	49.5
		172	31.1	125	41.2		
		200	34.1				
		220	36.9				
		250	41.1				

Annealed SnO_2 + 4.39% Fe_2O_3 - effect of varying P_{H_2}.

P_{HCl} = 20 cm Hg. 500°C.

P_{H_2}=0 cm Hg		P_{H_2}=10 cm Hg		P_{H_2}=20 cm Hg		P_{H_2}=30 cm Hg	
Time (min)	% vol-atilised	Time (min)	% vol-atilised	Time (min)	% vol-atilised	Time (min)	% vol-atilised
0	0.0	0	0.0	0	0.0	0	0.0
7	3.3	10	0.0	10	0.0	10	0.0
14	3.3	17	0.0	20	0.6	20	4.4
33	4.0	29	0.2	30	2.3	30	10.8
100	4.4	40	4.3	40	4.8	42	16.2
130	4.5	50	8.9	50	8.4	50	20.7
		61	13.5	60	12.1	60	25.1
		70	17.9	70	15.3	70	29.5
		76	20.7	80	18.6	80	35.7
		90	27.2	90	23.1	90	40.1
		100	31.5	110	31.1	100	45.4
		110	34.7	130	39.1	119	53.7
		120	38.9	135	40.2		
		130	43.0				

Annealed SnO_2-effect of varying P_{H_2}. P_{HCl} = 20 cm Hg. 550°C.

P_{H_2} = 0 cm Hg		P_{H_2} = 10 cm Hg		P_{H_2} = 15 cm Hg	
Time (min)	% vol-atilised	Time (min)	% vol-atilised	Time (min)	% vol-atilised
0	0.0	0	0.0	0	0.0
10	0.4	10	7.2	5	4.8
20	0.4	13	8.9	10	9.7
30	0.4	30	24.7	15	16.8
40	0.4	40	31.9	20	21.9
50	0.6	50	42.9	31	34.4
65	0.6	60	51.3	35	40.1
100	0.6			45	53.6

P_{H_2} = 20 cm Hg		P_{H_2} = 25 cm Hg		P_{H_2} = 30 cm Hg	
Time (min)	% vol-atilised	Time (min)	% vol-atilised	Time (min)	% vol-atilised
0	0.0	0	0.0	0	0.0
10	16.7	5	5.5	10	9.5
15	26.2	10	13.0	20	25.5
20	35.8	16	22.4	30	39.2
25	45.6	21	30.0	40	54.1
30	54.8	25	36.1		
		30	42.2		
		36	51.7		
		40	56.5		

Repetition of P_{H_2} = 25 cm Hg.

Time(min)	0	3	6	10	15	20	25	32	43	55	65	75	94	106
% vol-atilised	0.0	3.7	8.3	13.9	21.0	27.8	34.5	43.7	57.5	70.7	79.9	87.3	96.7	99.8

Repetition of P_{H_2} = 10 cm Hg.

Time (min)	0	5	10	18	30	42	50	60
% vol-atilised	0.0	5.8	10.5	16.7	25.5	34.9	41.4	46.4

Annealed crystals + 4.39% Fe_2O_3 - effect of varying P_{H_2}.

P_{HCl} = 20 cm Hg. 550°C.

P_{H_2} = 0 cm Hg		P_{H_2} = 5 cm Hg		P_{H_2} = 10 cm Hg	
Time (min)	% vol-atilised	Time (min)	% vol-atilised	Time (min)	% vol-atilised
0	0.0	0	0.0	0	0.0
5	4.1	5	-1.3	5	0.0
10	4.2	10	2.9	10	0.0
20	4.3	15	8.4	15	10.1
35	4.4	20	15.0	20	22.7
71	4.4	25	22.7	25	35.5
101	4.4	33	37.4	30	48.1
120	4.4	40	50.1	36	61.6
		45	58.7	41	72.2

P_{H_2} = 20 cm Hg		P_{H_2} = 25 cm Hg		P_{H_2} = 30 cm Hg	
Time (min)	% vol-atilised	Time (min)	% vol-atilised	Time (min)	% vol-atilised
0	0.0	0	0.0	0	0.0
6	4.6	3	-2.0	5	0.6
12	20.2	5	1.2	10	15.1
16	29.6	8	6.4	15	27.6
19	35.9	11	12.9	20	37.9
23	43.3	16	23.3	23	43.6
27	49.7	20	31.6	35	66.9
32	58.0	23	38.0	41	77.3
39	68.6	27	46.2		
		30	52.2		
		35	63.1		
		40	74.1		
		45	83.9		
		50	91.0		
		55	95.0		
		63	97.0		
		71	97.7		
		81	97.8		

Annealed crystals + 1.88% Fe_2O_3 - effect of varying P_{H_2}.

P_{HCl} = 20 cm Hg. 550°C

P_{H_2} = 10 cm Hg		P_{H_2} = 25 cm Hg	
Time (min)	% vol-atilised	Time (min)	% vol-atilised
0	0.0	0	0.0
3	-0.7	2	-0.8
5	1.1	5	2.2
11	8.1	8	6.8
15	15.1	10	10.4
18	20.0	14	18.5
22	26.8	17	25.1
26	32.7	21	34.2
32	47.5	24	40.1
35	51.6	28	49.1
38	55.2	36	64.6
43	59.7		

Annealed crystals + $Fe(NO_3)_3$ solution. P_{H_2} = 15 cm Hg.

P_{HCl} = 20 cm Hg. 550°C.

Time(min)	% volatilised	Time (min)	% volatilised
0	0.0	36	36.2
3	2.8	41	40.2
5	4.8	48	47.2
8	8.1	56	54.1
12	12.5	67	63.5
16	16.6	78	71.8
19	19.6	98	83.8
22	22.7	118	93.0
26	26.6	140	97.5
31	31.4	170	99.6

Fe-doped crystals. P_{H_2} = 0 cm Hg. P_{HCl} = 20 cm Hg. 500°C.

Time (min)	% volatilised
0	0.0
5	0.0
11	2.7
17	4.6
21	5.5
30	8.1
40	12.5
53	17.0
60	20.3
69	23.6
91	31.7
101	34.6
123	42.8
140	49.0

Annealed crystals out of contact with 4.39% Fe_2O_3. 550°C.

P_{HCl} = 20 cm Hg.

P_{H_2} = 15 cm Hg		P_{H_2} = 25 cm Hg	
Time (min)	% volatilised	Time(min)	% volatilised
0	0.0	0	0.0
4	0.5	3	-1.5
8	3.1	5	1.9
12	7.1	7	3.1
15	11.2	10	9.3
21	18.8	13	13.3
26	24.5	20	28.3
31	30.3	29	39.8
37	37.8	33	45.1
42	43.9		
47	49.2		

Annealed crystals + 4.74 NiO. P_{HCl} = 20 cm Hg. 550°C.

P_{H_2} = 10 cm Hg		P_{H_2} = 25 cm Hg	
Time (min)	% volatilised	Time (min)	% volatilised
0	0.0	0	0.0
3	2.6	3	5.7
8	15.9	6	15.2
10	21.4	10	29.8
13	29.5	16	51.6
16	37.2	22	68.9
20	46.5	30	83.5
25	58.1	38	91.1
31	70.3	52	94.4
42	85.6		
50	91.1		
62	93.9		

Annealed crystals + 4.74% CuO.
550°C. P_{H_2} = 10cm Hg.
P_{HCl} = 20 cm Hg.

Time (min)	% volatilised
0	0.0
3	3.3
6	5.4
11	9.3
26	21.2
37	29.3
46	35.9
54	41.7
68	49.6
87	54.4

Annealed crystals + 4.74% PbO
550°C P_{H_2} = 10cm Hg.
P_{HCl} = 20 cm Hg.

Time (min)	% volatilised
0	0.0
3	1.8
5	3.3
10	7.5
16	12.2
24	18.9
30	24.1
36	28.8
45	36.5
55	44.8
66	53.0
85	65.2
97	70.3
134	87.8

Annealed crystals + 4.74% Co_3O_4. P_{HCl} = 20 cm Hg. 550°C.

P_{H_2} = 10 cm Hg		P_{H_2} = 25 cm Hg	
Time (min)	% volatilised	Time(min)	% volatilised
0	0.0	0	0.0
3	-1.4	3	5.3
6	-1.3	6	13.7
10	0.0	10	28.5
15	2.9	13	39.9
20	7.9	16	50.4
25	13.3	20	63.7
30	19.3	25	77.0
37	27.7	31	88.6
41	32.5	36	94.8
48	39.4	42	96.9
55	48.0	60	98.3
61	54.8		
70	62.8		
91	79.3		
124	90.2		
153	92.5		

Annealed crystals + 4.74% Ag_2O

550°C. P_{H_2} = 25 cm Hg.

P_{HCl} = 20 cm Hg.

Time (min)	% volatilised
0	0.0
3	3.5
6	8.2
11	15.2
15	20.6
20	24.9
25	29.7
30	54.3
35	38.1
38	40.8
48	48.3
61	57.5
75	61.3
120	85.3

Annealed crystals +4.74% Ta_2O_5

P_{H_2} = 25 cm Hg. P_{HCl} = 20 cm Hg

550°C

Time (min)	% volatilised
0	0.0
3	3.1
6	6.7
10	11.3
15	17.2
20	22.2
25	26.5
35	33.9
52	45.8
67	55.7
86	70.2
128	90.8
154	94.0

Annealed crystals + 4.74% Nb_2O_5. 550°C P_{HCl} = 20 cm Hg.

P_{H_2} = 10 cm Hg		P_{H_2} = 25 cm Hg	
Time(min)	% volatilised	Time(min)	% volatilised
0	0.0	0	0.0
4	0.0	3	0.0
10	0.0	6	0.0
15	0.0	10	0.0
27	0.0	15	0.0
40	0.0	30	0.0
52	0.0	46	3.0
60	0.0	60	11.1
75	0.0	76	22.4
82	0.0	85	29.3
98	0.0	90	33.4
110	0.0	95	36.8
130	0.0	101	40.9
150	0.0		
180	0.0		

Annealed crystals + 4.74% Pt. 550°C. P_{HCl} = 20 cm Hg.

P_{H_2} = 10 cm Hg		P_{H_2} = 25 cm Hg	
Time (min)	% volatilised	Time (min)	% volatilised
0	0.0	0	0.0
3	4.4	2	4.5
6	14.4	4	11.8
10	29.3	6	19.4
15	46.6	11	39.1
21	63.1	15	53.0
26	73.8	20	68.1
30	79.4	27	83.4
37	87.5	33	90.5
47	92.4	40	92.2
58	93.9	55	93.1

Annealed crystals + 4.74% TiO_2. 550°C. P_{HCl} = 20 cm Hg.

P_{H_2} = 10 cm Hg.		P_{H_2} = 25 cm Hg.	
Time (min)	% volatilised	Time(min)	% volatilised
0	0.0	0	0.0
3	2.0	3	4.6
7	7.5	6	10.8
10	12.1	11	22.0
15	20.5	15	31.2
20	29.2	19	40.2
25	37.6	23	48.6
30	46.3	27	57.4
35	54.3	31	65.9
42	65.6		

Repetition of P_{H_2} = 25 cm Hg.

Time(min)	0	3	5	11	18	21	25	30
% volatilised	0.0	5.6	10.5	21.8	35.0	40.1	48.6	58.9

Annealed crystals + 4.74% MoO_3. 550°C. P_{HCl} = 20 cm Hg.

P_{H_2} = 10 cm Hg.		P_{H_2} = 25 cm Hg.	
Time (min)	% volatilised	Time (min)	% volatilised
0	0.0	0	0.0
4	7.8	3	6.0
8	12.4	7	14.5
12	17.9	11	23.1
17	23.8	16	35.4
22	30.0	20	44.1
33	45.2	25	54.4
39	52.8	30	64.4
46	64.3	36	74.4
55	77.5		

Annealed crystals +4.74% V_2O_5. 550°C. P_{HCl} = 20 cm Hg.

P_{H_2} = 10 cm Hg		P_{H_2} = 25 cm Hg.	
Time (min)	% volitilised	Time (min)	% volatilised
0	0.0	0	0.0
3	3.7	3	6.6
6	8.7	7	17.9
10	15.6	11	30.6
14	22.6	16	45.8
20	32.0	24	66.7
25	40.9		
33	53.3		
43	68.1		

Annealed crystals +4.74% WO_3. 550°C. P_{HCl} = 20 cm Hg.

P_{H_2} = 10 cm Hg		P_{H_2} = 25 cm Hg	
Time (min)	% volatilised	Time(min)	% volatilised
0	0.0	0	0.0
3	1.5	3	1.2
7	3.1	6	2.3
11	4.1	11	4.2
15	5.9	15	6.5
21	8.9	22	11.8
30	15.1	28	17.4
36	19.7	33	23.2
47	28.0	41	32.9
56	35.0	47	41.1
73	49.5	54	51.1
86	59.2	60	59.7
		66	69.0

Fe_2O_3. P_{H_2} = 20 cm Hg = P_{HCl}.

500°C		550°C		600°C	
Time(min)	% wt. increase	Time(min)	% wt. increase	Time(min)	% wt. increase
0	0.0	0	0.0	0	0.0
3	17.4	3	19.2	3	7.8
7	30.2	6	30.0	5	16.6
11	41.9	11	43.0	8	26.4
15	45.2	14	45.0	10	33.6
20	46.6	22	47.2	15	45.9
25	47.2	29	47.2	21	45.3
30	47.7	38	46.6	27	44.3
38	47.7	49	46.6	33	42.2
54	47.7	58	45.6	39	41.6
75	47.7	68	45.6	50	38.8
94	47.7	79	45.0	66	34.8
145	47.7	90	43.9	82	31.2
		120	43.0	96	27.8
				114	24.1
				145	18.3
				190	10.0

Reaction of metal oxide additives alone at 550°C.

$P_{H_2} = P_{HCl} = 20$ cm Hg.

Nb_2O_5

Time (min)	% volatilised
0	0.0
5	0.5
11	0.5
16	0.6
20	0.7
25	0.9
30	1.3
35	1.3
40	1.7
45	2.7
51	3.6
56	3.9
65	3.9
78	6.0
91	6.5
109	7.9
120	8.8
137	9.4
150	10.5
165	11.5

Co_3O_4

Time (min)	% volatilised
0	0.0
2	-21.3
7	0.4
10	22.7
12	25.8
15	27.2
20	27.9
34	27.9
50	27.9
217	27.9

Ag_2O

Time (min)	% volatilised
0	0.0
3	2.6
7	4.8
13	6.1
20	6.1
33	6.1
54	6.2
64	6.2
79	6.6
98	7.2
120	7.7

CuO

Time (min)	% volatilised
0	0.0
2	16.6
6	27.3
11	29.0
16	29.0
26	30.2
48	31.3
64	31.3
180	33.4

Ta_2O_5

Time (min)	% volatilised
0	0.0
5	1.0
11	1.3
20	1.4
30	1.4
42	1.4
77	1.4
93	1.4

V_2O_5

Time (min)	% volatilised
0	0.0
3	15.4
7	18.0
12	20.4
19	22.7
26	24.2
33	26.2
40	27.8
47	28.2

WO_3

Time (min)	% volatilised
0	0.0
4	0.3
10	4.5
15	7.3
20	10.0
27	13.7
35	17.8
45	23.5
56	29.1
70	36.7
91	48.0

TiO_2

Time (min)	% volatilised
0	0.0
5	0.0
11	0.0
24	0.0
45	0.0
62	0.0
94	0.0

MoO_3

Time (min)	% volatilised
0	0.0
2	50.6
6	62.6
11	63.0
17	63.0
40	63.0
59	63.0

PbO

Time (min)	% volatilised
0	0.0
2	-11.5
8	-6.3
15	1.8
26	13.3
38	22.9
48	28.9
58	34.3
71	39.8
90	47.3
158	71.4
180	77.1

Odegi cassiterite - effect of varying P_{H_2}. P_{HCl} = 20 cm Hg.

600°C.

P_{H_2} = 5 cm Hg		P_{H_2} = 10cm Hg		P_{H_2} = 20cm Hg		P_{H_2}=30 cm Hg.	
Time (min)	% vol-atilised	Time (min)	% vol-atilised	Time (min)	% vol-atilised	Time (min)	% vol-atilised
0	0.0	0	0.0	0	0.0	0	0.0
10	1.2	10	4.1	7	2.9	16	4.9
20	2.2	20	7.6	13	5.4	30	6.4
35	3.9	31	11.0	20	7.8	41	7.9
53	6.0	40	13.6	27	11.0	53	9.2
66	8.0	50	18.6	34	13.6	62	10.5
82	12.5	60	23.2	41	17.1	70	12.1
100	17.2	70	27.2	51	22.8	80	15.9
123	22.9	80	32.1	58	25.6	90	18.9
140	26.5	90	35.9	67	29.3	106	23.7
153	29.0	102	38.2	74	32.4	115	26.5
177	31.7	114	41.7	80	33.9	132	32.4
197	34.5	122	43.5	96	38.4	141	34.5
220	38.1	131	45.2	104	41.7	150	37.4
240	40.6	143	47.6	112	43.1	162	41.4
277	45.0	154	49.7	124	46.7	177	47.4
297	45.9	164	51.3	134	50.0	191	52.4
		180	54.3			210	59.1

Odegi cassiterite +4.39% Fe_2O_3 - effect of varying P_{H_2}.

P_{HCl} = 20 cm Hg. 600°C.

P_{H_2} = 5cm Hg		P_{H_2} 10cm Hg		P_{H_2} = 20cm Hg		P_{H_2} = 30cm Hg	
Time (min)	% vol-atilised	Time (min)	% vol-atilised	Time (min)	% vol-atilised	Time (min)	% vol-atilised
0	0.0	0	0.0	0	0.0	0	0.0
5	-1.3	6	-0.8	5	0.5	5	0.0
11	0.9	10	-0.8	10	3.0	10	1.4
16	2.7	15	2.7	20	7.9	21	5.3
21	4.5	30	7.7	30	14.9	30	8.7
25	5.8	40	14.1	41	25.1	42	13.7
34	9.0	58	28.1	47	30.6	50	18.3
42	13.4	63	32.2	58	41.9	66	29.9
51	21.1	67	35.7	67	50.2	73	37.0
60	28.2	71	38.6	73	54.6	83	48.6
70	38.6	75	41.9			90	55.5
82	49.1	83	47.9				
94	56.7	90	51.8				
103	61.1						

Annealed crystals - effect of varying P_{H_2}.

P_{HCl} = 20 cm Hg. 600°C.

P_{H_2} = 0 cm Hg		P_{H_2} = 5 cm Hg		P_{H_2} = 10 cm Hg	
Time (min)	% vol-atilation	Time (min)	% vol-atilation	Time (min)	% vol-atilation
0	0.0	0	0.0	0	0.0
11	8.4	3	3.3	2	2.6
20	14.6	8	9.5	5	7.5
30	20.6	11	12.8	10	15.7
40	27.3	15	16.8	13	20.5
50	33.5	21	22.5	16	25.2
60	38.9	26	27.0	20	31.4
71	43.4	34	34.1	25	38.9
78	46.1	39	38.0	30	46.6
90	50.2	44	42.4	35	53.9
		50	46.2	45	69.1
		61	53.6	60	89.4
		74	61.2		
		95	73.6		

P_{H_2} = 20 cm Hg		P_{H_2} = 30 cm Hg	
Time (min)	% volatilised	Time (min)	% volatilised
0	0.0	0	0.0
2	3.1	3	4.9
4	7.1	6	17.7
7	13.0	9	23.8
10	19.5	12	30.7
14	28.3	15	37.2
18	37.8	18	43.9
22	46.9	25	59.3
26	55.4	30	69.9
30	64.3	38	86.2
35	74.0	47	98.9
46	91.2		
59	99.2		

Annealed crystals +4.39% Fe_2O_3 - effect of varying P_{H_2}.

P_{HCl} = 20 cm Hg. 600°C

P_{H_2} = 0 cm Hg		P_{H_2} = 5 cm Hg		P_{H_2} = 10 cm Hg	
Time (min)	% vol-atilised	Time (min)	% vol-atilised	Time (min)	% vol-atilised
0	0.0	0	0.0	0	0.0
10	8.1	3	-0.9	2	0.0
20	13.4	5	6.2	4	9.4
30	18.2	7	14.1	6	19.2
40	22.4	10	26.2	8	28.3
50	26.9	13	38.1	10	37.2
60	29.8	16	48.6	12	45.7
71	32.4	19	58.6	15	58.6
80	35.2	27	80.8	21	77.9
92	34.0			25	86.9
103	34.7				
126	36.1				
140	37.3				
159	39.3				
170	42.2				
177	43.6				

P_{H_2} = 20 cm Hg		P_{H_2} = 30 cm Hg	
Time (min)	% volatilised	Time (min)	% volatilised
0	0.0	0	0.0
2	3.3	2	3.7
4	12.9	4	13.8
6	21.6	6	25.2
8	30.5	9	42.0
10	40.2	12	58.3
13	53.4	14	67.9
17	68.7	18	84.5
21	81.3	22	94.2
25	90.1	26	98.7
30	95.3		

Annealed crystals - effect of varying P_{H_2}. $P_{H_2O} \simeq 2mm$.

P_{HCl} = 20 cm Hg. 600°C.

P_{H_2} = 0 cm Hg		P_{H_2} = 5 cm Hg		P_{H_2} = 10 cm Hg	
Time (min)	% vol-atilised	Time (min)	% vol-atilised	Time (min)	% vol-atilised
0	0.0	0	0.0	0	0.0
5	6.3	2	1.5	2	3.0
10	10.7	5	5.9	6	9.2
16	13.1	10	11.3	10	14.4
21	15.8	15	16.1	15	21.4
27	19.0	20	20.6	20	24.5
34	22.9	25	25.4	25	32.6
44	26.9	30	29.3	30	39.1
52	30.9	37	34.9	35	44.0
57	32.8	42	38.1	41	51.9
64	36.1	49	42.6	45	57.4
74	38.2	59	49.1	51	64.2
82	40.8	69	54.2	60	74.3
94	43.9	86	62.0		
106	46.0				

P_{H_2} = 20 cm Hg		P_{H_2} = 30 cm Hg	
Time (min)	% volatilised	Time (min)	% volatilised
0	0.0	0	0.0
2	3.2	2	2.3
4	6.6	4	5.0
7	11.8	6	7.8
10	16.5	10	14.5
14	24.4	14	22.2
19	33.7	19	29.8
23	40.9	25	38.6
17	47.4	30	46.4
33	57.8	35	55.9
38	65.3	40	65.8
		45	73.3

Annealed crystals +4.39% Fe_2O_3. - effect of varying P_{H_2}. 600°C

P_{H_2O} = 2 mm. P_{HCl} = 20 cm Hg.

P_{H_2} = 0 cm Hg		P_{H_2} = 5 cm Hg		P_{H_2} = 10 cm Hg	
Time (min)	% vol-atilised	Time (min)	% vol-atilised	Time (min)	% vol-atilised
0	0.0	0	0.0	0	0.0
5	5.1	2	-1.1	2	-2.3
12	6.8	4	5.4	4	5.9
18	8.3	6	14.0	6	15.8
26	11.1	8	22.3	8	24.4
33	14.0	10	30.3	10	34.3
41	17.2	13	41.6	12	42.4
50	20.6	17	55.8	14	49.3
57	23.6	19	60.1	16	52.4
65	25.7	23	72.1	19	65.4
72	27.9	30	87.7	23	76.5
82	30.8			28	84.8
90	33.5			32	92.8
100	35.1				
107	35.7				
120	38.0				
129	39.1				
139	41.5				
154	41.9				
163	42.8				

P_{H_2} = 20 cm Hg		P_{H_2} = 30 cm Hg	
Time (min)	% volatilised	Time (min)	% volatilised
0	0.0	0	0.0
2	1.8	2	2.0
4	10.7	4	11.7
6	19.9	6	20.9
8	29.2	8	30.5
10	38.5	10	40.7
12	46.5	12	49.6
15	58.3	15	61.2
18	69.0	18	70.3
21	78.2	24	87.9
		38	96.9

Annealed crystals + 10% iron mineral additives. 550°C.

P_{HCl} = 20 cm Hg. Hematite.

P_{H_2} = 10 cm Hg		P_{H_2} = 25 cm Hg	
Time (min)	% volatilised	Time (min)	% volatilised
0	0.0	0	0.0
4	-0.9	2	0.0
7	-1.3	6	-1.7
10	-1.4	11	-2.7
15	-0.2	16	-3.2
20	4.5	22	-0.5
27	14.0	27	3.9
33	24.0	32	10.4
38	32.3	36	15.5
43	40.7	41	21.7
48	48.2	47	30.0
53	54.3	52	36.3
60	62.8	57	42.5
67	71.5	64	51.5
73	77.2	69	57.6
81	83.4	76	65.8
91	9[illegible].6	84	72.1
		90	75.4

Pyrite.

P_{H_2} = 10 cm Hg		P_{H_2} = 25 cm Hg	
Time (min)	% volatilised	Time (min)	% volatilised
0	0.0	0	0.0
2	0.7	3	8.0
5	5.4	6	15.4
8	9.6	9	21.1
12	16.3	13	27.6
17	24.1	16	32.1
21	30.6	20	37.9
26	37.6	26	45.9
30	42.8	30	50.6
36	50.5	35	56.9
40	55.9	40	63.3
45	63.0	46	70.0
50	70.4	51	75.1
58	76.2	64	85.1
65	81.9		

Magnetite

P_{H_2} = 10 cm Hg		P_{H_2} = 25 cm Hg	
Time (min)	% volatilised	Time (min)	% volatilised
0	0.0	0	0.0
2	0.3	2	0.0
5	2.2	5	2.9
10	6.9	10	9.8
15	12.5	15	16.7
20	17.4	20	22.3
25	22.3	26	29.4
30	27.3	31	35.7
35	32.4	35	40.0
40	37.8	42	47.9
45	42.2	52	56.0
50	47.4	69	78.0
55	51.4	75	84.5
60	55.6		
66	59.5		
70	62.6		
78	68.4		
95	78.0		

Columbite.

P_{H_2} = 10 cm Hg		P_{H_2} = 25 cm Hg	
Time (min)	% volatilised	Time (min)	% volatilised
0	0.0	0	0.0
3	0.5	2	1.0
8	2.8	6	3.7
14	5.5	10	7.3
19	8.0	15	11.2
25	11.1	21	16.0
31	14.1	26	20.2
38	17.9	30	22.6
44	20.1	35	26.0
49	22.5	40	30.2
54	24.9	51	38.5
60	27.4	56	41.6
70	31.4	61	44.4
86	38.1	67	48.0
100	42.0	72	50.9
112	46.3	81	55.0
124	49.8	90	58.4
145	55.7	100	61.9
155	58.6	111	64.4

Biotite.

P_{H_2} = 10 cm Hg		P_{H_2} = 25 cm Hg	
Time (min)	% volatilised	Time (min)	% volatilised
0	0.0	0	0.0
5	1.6	5	3.2
11	4.4	14	10.2
17	8.3	20	13.8
21	10.4	25	17.0
30	15.3	30	20.4
36	18.3	37	24.9
42	20.8	44	29.2
48	23.5	50	52.6
55	26.1	60	40.0
70	32.9	70	45.7
77	35.8	82	52.0
86	39.8	90	55.2
93	42.6	100	58.6
103	45.4		
114	49.0		
126	52.2		
137	55.7		

Ilmenite.

P_{H_2} = 10 cm Hg		P_{H_2} = 25 cm Hg	
Time (min)	% volatilised	Time (min)	% volatilised
0	0.0	0	0.0
7	6.1	5	3.2
12	12.2	11	9.5
20	21.4	17	15.9
27	29.2	21	19.9
35	37.6	26	26.5
42	43.3	31	32.2
47	48.5	38	41.0
53	53.0	46	51.6
63	60.2	52	60.5

Annealed crystals. - effect of varying P_{CO}. P_{HCl} = 20 cm Hg. 700°C.

P_{CO} = 0 cm Hg		P_{CO} = 5 cm Hg		P_{CO} = 10 cm Hg	
Time (min)	% vol-atilised	Time (min)	% vol-atilised	Time (min)	% vol-atilised
0	0.0	0	0.0	0	0.0
4	0.9	5	2.7	5	2.1
10	2.8	13	13.0	10	7.5
15	7.3	20	22.5	18	16.1
24	15.6	27	30.8	29	26.7
34	26.2	34	39.0	38	40.2
47	36.1	40	44.3	47	49.1
53	41.7	50	54.7	55	60.4
61	45.3	55	60.0		
69	50.7	63	66.4		
79	54.8				

P_{CO} = 20 cm Hg		P_{CO} = 30 cm Hg	
Time (min)	% volatilised	Time (min)	% volatilised
0	0.0	0	0.0
6	4.3	5	1.2
12	10.6	12	10.4
19	16.4	18	15.7
27	24.9	27	29.8
37	37.1	37	41.0
47	49.0	48	53.5
55	59.6	55	61.3
67	74.8		
74	81.8		
81	88.5		
90	94.7		

Annealed crystals - effect of varying P_{HCl}. $P_{CO=20cm\ Hg}$. 700°C.

P_{HCl} = 0 cm Hg		P_{HCl} = 5 cm Hg	
Time (min)	% volatilised	Time (min)	% volatilised
0	0.0	0	0.0
8	0.0	6	-1.4
23	0.0	13	0.0
37	0.0	24	1.8
53	0.0	36	4.1
85	0.0	47	7.3
106	0.0	65	12.6
140	0.0	82	18.7
173	0.0	93	23.1
		117	31.0
		127	34.1
		141	38.5
		152	43.2
		192	54.6

P_{CO} = 10 cm Hg		P_{CO} = 30 cm Hg	
Time (min)	% volatilised	Time (min)	% volatilised
0	0.0	0	0.0
4	0.4	6	5.4
8	3.4	12	16.8
13	7.3	18	28.2
18	10.3	25	42.0
26	15.6	30	51.0
32	19.0	35	60.6
43	26.3	38	65.6
52	31.1		
61	35.6		
68	39.9		
75	43.8		
83	48.0		
94	52.6		
106	58.1		

Annealed crystals +4.39% Fe_2O_3 - effect of varying P_{HCl}.

P_{CO} = 20 cm Hg. 700°C.

P_{HCl} = 0 cm Hg		P_{HCl} = 5 cm Hg		P_{HCl} = 10 cm Hg	
Time (min)	% vol-atilised	Time (min)	% vol-atilised	Time (min)	% vol-atilised
0	0.0	0	0.0	0	0.0
7	0.3	3	3.7	4	10.1
20	4.4	7	10.6	9	18.7
33	10.4	11	16.0	14	26.0
45	15.0	15	18.9	19	30.9
53	19.1	23	26.2	24	35.6
62	24.1	27	30.7	28	42.1
78	34.9	33	34.1	33	44.5
90	42.4	43	43.6	40	48.5
96	46.5	50	49.0	46	52.2
		60	53.4	52	54.7
		69	57.0		

P_{HCl} = 20 cm Hg		P_{HCl} = 30 cm Hg	
Time (min)	% volatilised	Time (min)	% volatilised
0	0.0	0	0.0
4	8.0	3	6.1
6	12.4	7	14.3
10	18.8	11	23.3
16	29.5	15	33.3
20	36.1	19	41.2
24	41.6	24	48.9
28	47.2	29	54.5
33	57.6	35	60.7
44	70.9		

Annealed crystals + 4.74% additives. P_{CO} = 20 cm Hg.

P_{HCl} = 0 cm Hg 700°C

Pt		Nb_2O_5		Bi_2O_3	
Time (min)	% vol-atilised	Time (min)	% vol-atilised	Time (min)	% vol-atilised
0	0.0	0	0.0	0	0.0
3	0.5	11	0.0	14	0.0
9	0.5	24	0.0	26	0.0
16	0.7	33	0.0	34	0.5
24	1.5	46	0.0	42	0.5
34	2.7	60	0.0	56	1.9
45	4.6	95	0.0	71	3.3
58	5.9	114	0.0	90	4.9
66	7.1	130	0.0	101	6.6
75	8.3			121	9.1
85	10.0			148	12.1
94	11.5				
130	15.6				
154	19.0				
174	23.2				
216	32.3				
244	39.6				
273	46.8				

Annealed crystals +4.74% Nb_2O_5. $P_{CO} = P_{HCl} = 20$ cm Hg. 700°C.

Time (min)	% volatilised
0	0.0
4	-0.8
9	2.4
14	3.5
21	13.3
26	25.8
32	40.4
39	57.8
45	70.8
50	79.2
56	89.3